POLITECNICO
MILANO 1863

SCUOLA DI INGEGNERIA INDUSTRIALE
E DELL'INFORMAZIONE

Modelling of a solid desiccant low regeneration temperature system for providing thermal comfort in a NZEB building in Milan.

TESI DI LAUREA MAGISTRALE IN
ENERGY ENGINEERING
INGEGNERIA ENERGETICA

Authors:
Adrian Felipe Acosta Herrera
Leonardo del Piero Pacheco Cabarcas

Student ID: 963737 - 963858
Advisor: Marcello Aprile
Academic Year: 2022-23

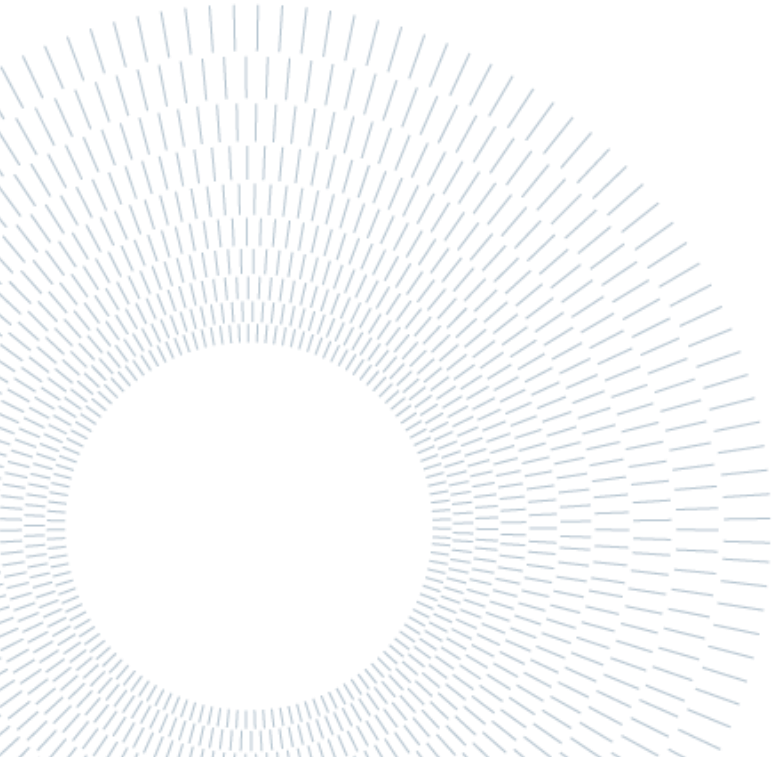

Abstract

The escalating global demand for air conditioning driven by the ambitious energy demand targets, necessitates the development of high-efficiency and environmentally sustainable cooling systems. The present thesis undertakes an in-depth examination of the feasibility of integrating a solid desiccant cooling system model into a residential building located in Milan, Italy, as a prospective alternative to conventional vapor compression cooling systems. The primary objective is to quantitatively assess the system's thermal and electrical efficiency across varying component dimensions and operational conditions in order to delineate its practical applicability. The system's performance is investigated for an air regeneration temperature around 60°C, thereby accommodating low-temperature heat sources such as solar energy and waste heat. The outcomes evidenced a substantial number of thermal comfort conditions in the conditioned period, around 86% with the integration of a control strategy reaffirming that the technology is capable of managing sensible and laten loads.

Key-words: Desiccant, Cooling, regeneration temperature, thermal comfort.

Abstract in italiano

La crescente richiesta globale di condizionamento degli ambienti, guidata dagli ambiziosi obiettivi di domanda energetica, richiede lo sviluppo di sistemi di raffreddamento ad alta efficienza e sostenibili dal punto di vista ambientale. La presente tesi magistrale intraprende una valutazione approfondita della fattibilità dell'integrazione di un modello di sistema di raffreddamento ad adsorbimento solido in un edificio residenziale situato a Milano, in Italia, come potenziale alternativa ai sistemi convenzionali di raffreddamento a compressione di vapore. L'obiettivo primario è valutare quantitativamente l'efficienza termica ed elettrica del sistema attraverso le diverse dimensioni dei componenti e le condizioni operative al fine di delinearne l'applicabilità pratica. Le prestazioni del sistema vengono studiate per una temperatura di rigenerazione di circa 60°C, adattando così fonti di calore a bassa temperatura come l'energia solare e il calore di scarto da altri processi. I risultati hanno evidenziato un numero abbastanza considerevole di condizioni di comfort termico nel periodo condizionato, circa al 86% con l'integrazione di una strategia di controllo, riaffermando che la tecnologia è in grado di gestire carichi sensibili e latenti.

Parole Chiavi: Essiccante, Raffreddamento, temperatura di rigenerazione, comfort termico.

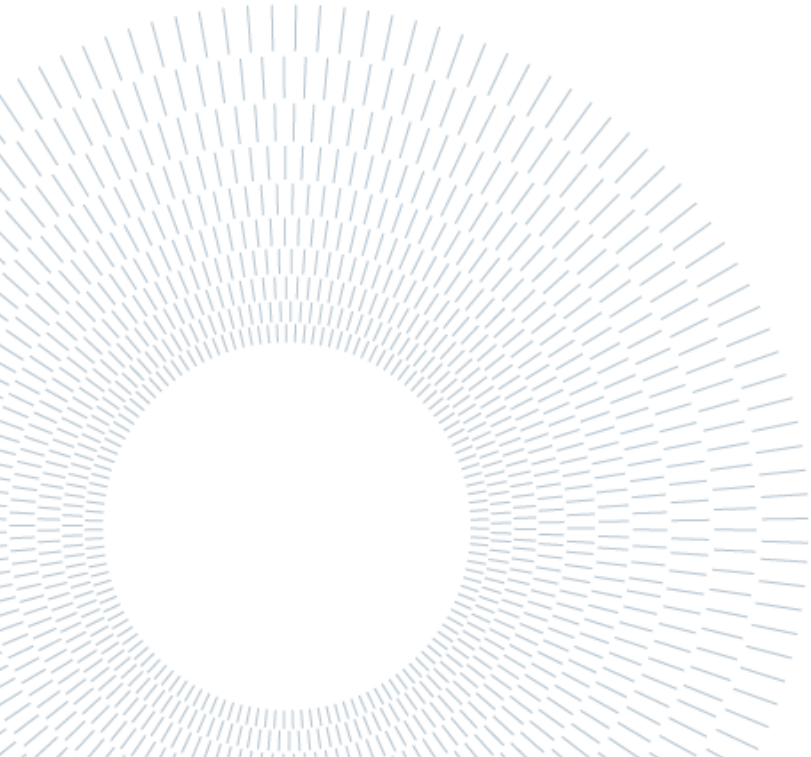

Contents

Introduction

The current global climate crisis due to the increase of CO2 concentration in the atmosphere is irreversible; based on a study, even if emissions are stopped, the atmospheric temperatures will not be drop significantly for at least 1000 years [1]. Considering this fact, the mission of engineers today, of developing new technologies environmental-friendly, to meet the society needs, becomes a duty. Among the needs, it is found a great aspect: the energy sector, which is widely needed in a variety of usage, especially in the building environment. According to the US Energy Information Administration (EIA), the building sector, accounting for operations, construction and materials is responsible for almost 48% consumption of the total energy produced in the United States in 2012 (Figure 0.1) [2]. Additionally, for Europe, the household's energy consumption is nearly 30% of the total consumed (Figure 0.2) [3]. Therefore, the way in which energy is produced and provided to buildings is a key factor in order to reduce the total energy consumption and CO2 emissions of cities.

Focusing on the energy building sector; Building operations/Households is formed by the demand for day-to-day operations, including heating, cooling, lighting, ventilation, appliances, equipment, etc. Based on the US Department of Energy (DEO), a substantial amount of the energy consumed by buildings is attributable to the heating, cooling, and ventilating systems, around 50%, as it is shown in Figure 0.3. [4]

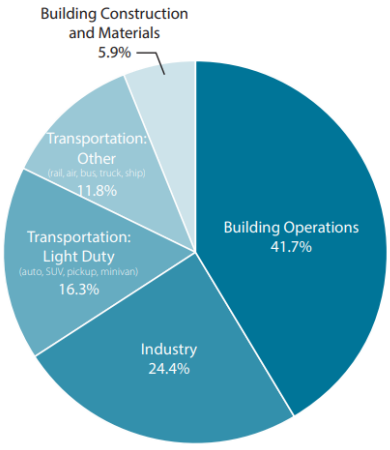

Figure 0.1. Final energy consumption by sector in U.S. in 2012. [2]

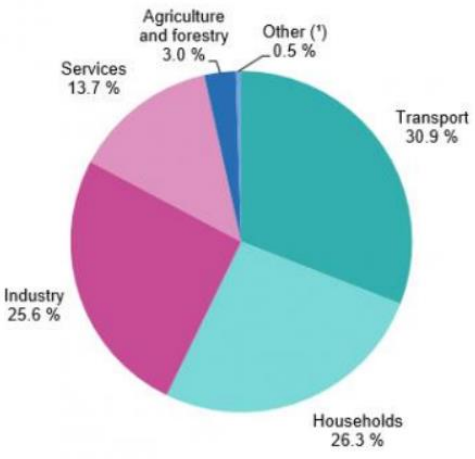

Figure 0.2. Final energy consumption by sector in EU in 2019. [3]

Being aware of the previous arguments, engineers are putting a lot of effort into developing new systems to satisfy the heating and cooling demands in residential buildings and to replace the conventional technologies, such as boilers in order to reduce the CO2 emissions and the use of fossil fuels. Since cooling demands accounts for sensible and latent loads for experiencing indoor thermal comfort, to address this situation, desiccant cooling systems (DCS) are a suitable and cost-effective technology for reaching the mentioned goal in climates with a significant latent load. DCS are an alternative to traditional mechanical vapor compression systems, which only control the sensible loads of the residences by using a larger primary energy consumption and gases with high harmful potential.

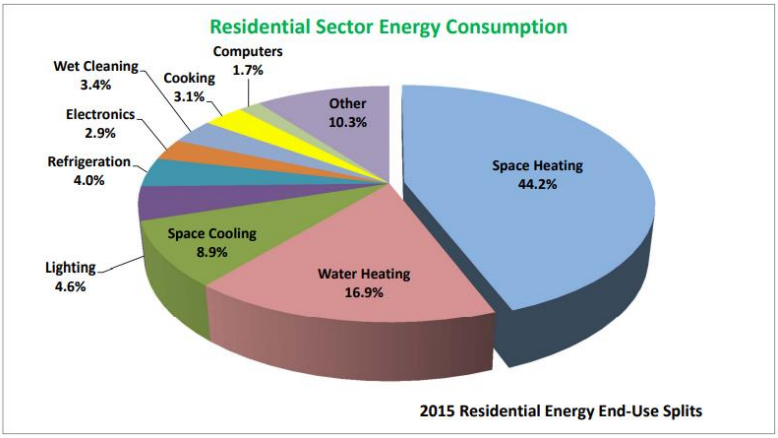

Figure 0.3. Energy consumption in the residential sector. [4]

The main objective of this master thesis work is to verify the possibility of implementing a Desiccant Cooling system, considering as regeneration heat source the low temperature water coming from the 4th generation district heating system, in a residential building to obtain, during high summer temperatures, good thermal comfort in terms of temperature and humidity ratio levels.

In the following chapters are explained the description of the building of interest, the simulation of its sensible and latent loads during the summer season, as well as the desiccant cooling system proposed integrated to a control strategy for achieving high level of thermal comfort for human occupancy.

1 Chapter one: Project overview.

1.1. Background of the project.

The city of Milan is working on the development of a strategic plan for the regeneration of urban spaces, which consists of transforming and recovering seven underused railway areas of the city. Greco-Breda, Farini, San Cristoforo, Porta Romana, Porta Genova, Rogoredo, and Lambrate are the zones where the intervention is intended to take place. In line with this initiative, the project "EX Scalo Greco-Breda - L'Innesto" was developed with the objective to renew and transform part of the currently decommissioned Greco-Breda railway station into a residential zone through the incorporation of green spaces and high-quality services. This intervention is expected to promote sustainability, elevating the overall quality of life for local inhabitants, and facilitating increased community engagement.

L'Innesto project won the first edition of Reinventing Cities, a worldwide competition that promotes sustainable, innovative, and zero-carbon urban regeneration projects. This competition encourages cities to identify under-utilised locations with the potential to be renovated and to invite multidisciplinary teams - including architects, engineers, planners, developers, investors, environmentalists, creative project holders, start-ups, academics, and community associations - to submit innovative proposals that can be taken as global models against climate change and global warming [5].

The challenges that characterize the competition Reinventing Cities are:

- Energy efficiency and clean energy supply
- Sustainable materials and circular economy
- Green mobility
- Resilience and adaptation
- Ecological services for the site and the surrounding environment
- Development of green and intelligent cities
- Sustainable water management
- Biodiversity, urban vegetation, and agriculture
- Inclusive activities and local community benefits
- Innovative architecture and urban design

Considering the challenges that define the Reinventing Cities competition, the project's specific focus on social housing, as well as the constrains imposed by the local context, the project L'Innesto introduces three main objectives that encompass social, technical, constructive, and environmental aspects. These three objectives are

described in the following subsections and objective 2 is included at the end of subsection 1.

1.2. Objective 1: First zero-carbon social housing project in Italy.

To achieve this objective, the project applies all the innovative and sustainable constructive approaches, as well as energetic, monitoring and management strategies necessary to obtain, over a period of 30 years, zero-carbon buildings with a net energy balance close to zero (nZEB).

For the construction of the buildings, prefabricated construction systems with a high percentage of sustainable materials – low environmental impact considering all their life cycle - will be used so that CO2 production can be limited as much as possible. This construction methodology follows the principle of material optimization that involves selecting and utilizing the materials taking into consideration their physical, mechanical, and chemical properties to maximize their performance and efficiency for a specific application. In this way, it is possible to avoid the over-design or excessive use of resources, allowing to minimize waste but also to limit unnecessary energy consumption since most of the materials used in the construction sector are produced by energy intensive processes.

The implementation of dry connection techniques to assemble the prefabricated systems will allow to easily dismantle, and then recycle, the entire structure at the end of its life cycle. By applying this constructive approach, this project can achieve a high level of sustainability by reducing the CO2 emissions during construction stage but also by promoting a sense of circular economy and efficient use of resources.

In addition, excavation land will be threated through bioremediation technique that uses microorganisms to decontaminate soil and subsoil, as well as superficial and ground water, while minimizing the environmental impact. A surface equal to 60% of the project area will be object of urban forestation by planting new trees that will contribute to mitigate CO2 emissions.

The L'Innesto project also proposes innovative interventions regarding building systems that include proposes for the water management, the integration of renewable energies not only for space conditioning and DHW but also for electricity production for self-consumption of the structure. For the water management system, it is proposed the reutilization of the rainwater to avoid the saturation of sewage systems and to minimize the consumption and waste of drinking water. Rainwater is totally collected and treated on site as well as a percentage of the wastewater that is also recycled and reutilized on site.

For space heating and domestic hot water production, it is proposed an innovative 4th generation district heating system (4GDH) where part of the heat is produced by the

integration of a solar thermal plant. It also includes a wastewater heat recovery system to take advantage of the energy content of the wastewater.

A photovoltaic plant has also been planned in this project to cover a portion of the electrical energy demand of the buildings and installations. All these energetic and constructive strategies have been designed to reach the target of zero-carbon and zero-energy buildings. The features of a highly efficient building together with the integration of efficient systems leads to a better use of the available resources but also to an environmentally friendly operation.

The objective 2 is related to the long-term participation in the management of the spaces and community resources in a responsible and reliance way. The project search to manage all the interventions regarding social housing in an innovative and integrated way, over a period of 30 years, combining sustainable strategies in the management of buildings and enhancing the relations between inhabitants involving them in the conservation of shared spaces.

1.3. Objective 3: Creating a collaborative neighbourhood with interest in agriculture and creating a human adaptative zone to regenerate urban areas.

L'Innesto is intended to be a collaborative neighbourhood with interest in agriculture. The creation of flexible and multifunctional spaces has been planned in order to promote the relations between inhabitants and to involve the residents in the care of the shared areas. In these areas there will be equipped green spaces, private and educational gardens, an orchard, greenhouses, and a community garden. In addition, the integration of aquaculture and hydroponic horticulture will significantly reduce the use of fertilizers, insecticides, and fungicides and the waste of products.

The project also includes the construction of places for meetings and socialization. These includes living rooms and a kitchen for common use, laboratories, urban gardens, and services that will be managed in an integrated way by inhabitants, non-profit operators, and local stakeholders. From this interaction, will come to life a Human Adaptative Zone that will offer a network of cutting-edge services such as the community food bub, the circular economy district, the energy showroom, the zero-waste store, and the neighbourhood welfare project. The integration of social, physical, and technological infrastructures will foster the relationship and the development of collaborative projects and will increase the vitality of the neighbourhood and the sense of belonging of families and students.

1.4. Description of the project area.

The area of the project covers a total gross area of 66.700 m2, comprising 5 sub-areas divided as shown in the Figure 1.1. Area A+B are the former railway station (currently decommissioned) and the rail depot, respectively. These two areas represent a total surface area of 30.000 m2, being around 50% of whole project area. Area C is a former orchard with a dimension of 16.000 m2. Area D, delimitated by active tracks and Via Sesto San Giovanni, also accounts for a surface area of 16.000 m2. Finally, area E account for a total surface of 4.700 m2 delimitated by the current Via Breda. All the intervention area considered by the project belongs to the administrative territory of the municipality of Milan.

Figure 1.1. Distribution of the total area considered by the project.

The project plans to construct buildings for both residential and commercial purposes, utilizing 24.000 m2 of the total available area. A portion of 21.000 m2 will be designated for the residential use of social housing, and will be distributed as follows:

- Buildings for sale with special price lower than market prices: 8.324 m2.
- Buildings for rent at agreed rent contract (price usually lower than market price): 10.676 m2.
- Buildings for rental to allocate low-income families: 2000 m2.

According to the project information, approximately 380 apartments will be available, including one-room, two-room (small and big), three-room (small and big) and four-room apartments. They are grouped considering two categories: spaces for sale and spaces for rent. The apartments will be located in separated buildings depending on their category in order to allow an efficient and coherent management of the spaces. The distribution of the building is shown in Figure 1.2.

On the other hand, it is pretended to designate a surface of 3.000 m2 for commercial purposes, distributed as follows:

- Circular Economy District: 1.200 m2
- Zero Waste Food store: 500 m2
- Community Food Hub: 1.200 m2
- Miscellaneous commercial activities: 100 m2

The construction of a university residence is also considered in the project, utilizing an area of approximately 7.000 m2. In this area, four hundred single beds will be available to allocate students from Milano and other regions or countries. In addition, the intervention estimates the creation of public area that corresponds to a share of around 60%, including green areas, pedestrian zones and equipped public areas to provide useful services to the community.

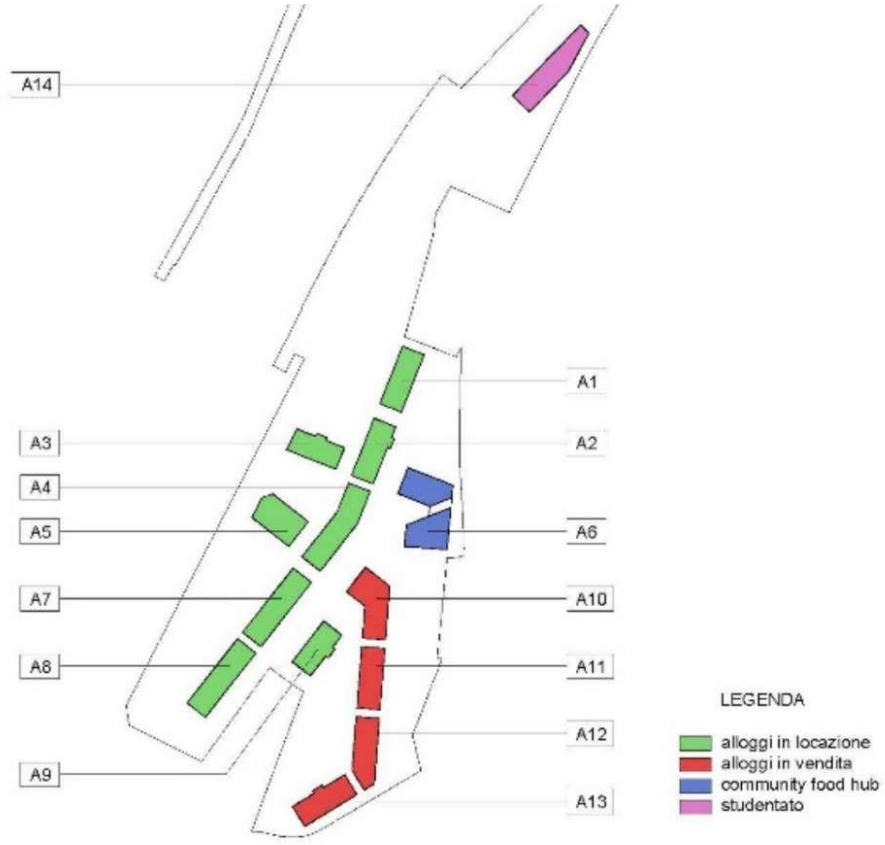

Figure 1.2. Distribution of the buildings depending on their category (building for sell or building for rent).

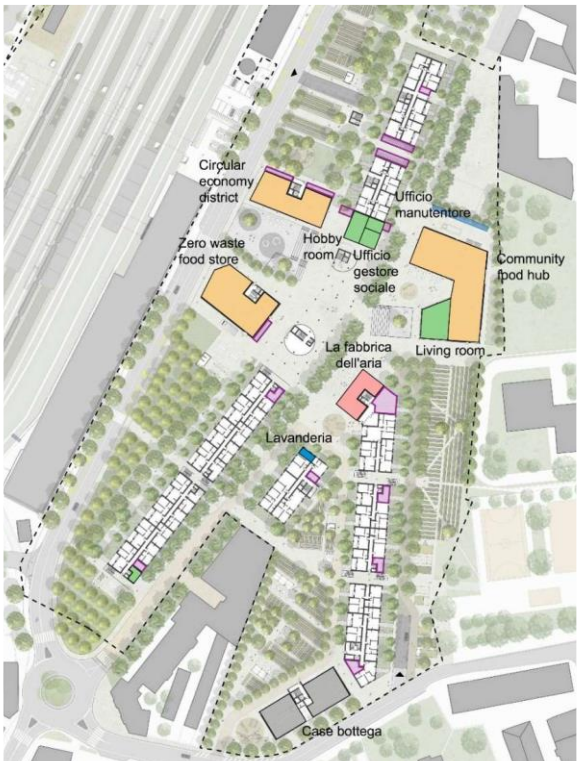

Figure 1.3. Position of the commercial buildings and student residence.

The contribution of this thesis work to this innovative project is related to the implementation of an air conditioning system able to provide cooling during summer by using the low temperature heat produced by the district heating system. Since the system will be used for both air temperature and humidity control, the best option is a desiccant cooling system (DEC) which is capable to provide ventilation while controlling temperature and humidity of the inside air. This system will be tested in one building only and its implementation in other buildings will be considered depending on the results of the DEC system operation. It is in our interest to verify the feasibility of the system to provide not a fixed-point air conditioning but cooling of the spaces. The operation of the DEC system is verified by performing a dynamic simulation, looking for acceptable thermal comfort inside the conditioned rooms considering the residential application.

2 Chapter two: **State of art: Desiccant evaporative cooling systems.**

2.1. Description of the main components.

The main objective of a DEC systems is having temperature and humidity control of an indoor space. In order to achieve this goal, the sensible and latent load are controlled separately by two crucial components: a desiccant dehumidifier and an evaporative cooler. The system takes the outdoor air stream, and it gets dehumidifier by the desiccant material, where humidity is reduced to the desired value; in a second stage, the process air passes through an evaporative cooler which diminish the air temperature until an acceptable value is obtained. Moreover, the continuous operation of the cycle is guaranteed by taking the indoor air and forcing it to pass through a regenerator, which raised the temperature before going into the desiccant material, this air is responsible for absorbing moisture and finally goes into to the environment [6].

2.1.1. Type of Evaporative Coolers.

This component uses the latent heat of water vaporization for cooling the air, this allows to replace convectional compression cycles, avoiding the use of refrigerant, which have a considerable environmental impact. EC can reach high values of electric COP due to the fact that the only power consumption required is for circulation of the air. Nevertheless, the cooling performance is strongly related to the climate conditions, which can limit the applicability. Evaporative cooler can be categorized as shown in Figure 2.1.

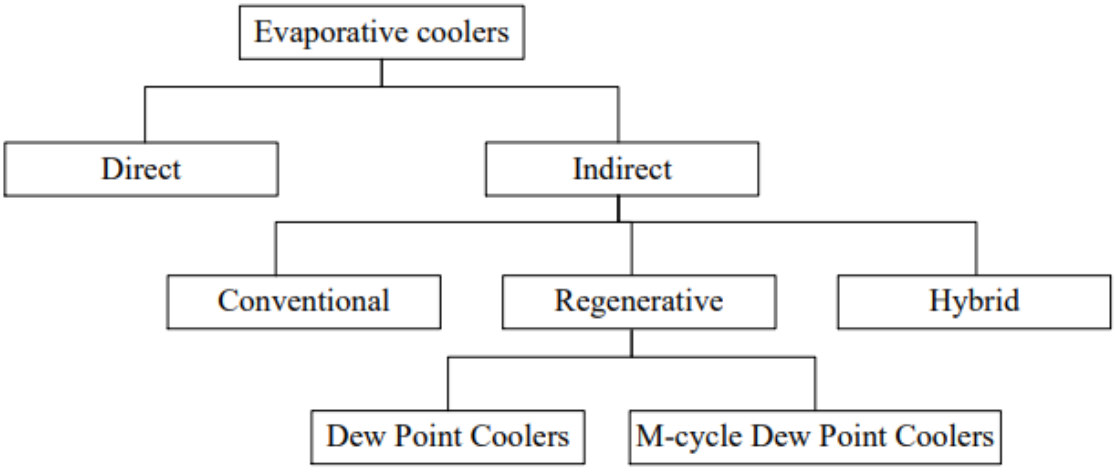

Figure 2.1. Types of evaporative coolers. [7]

2.1.1.1. Direct evaporative coolers.

For Direct Evaporative Coolers (DECs), the primary air stream is subjected to an adiabatic process because the air temperature is reduced due to the high moisture content added in the component. The common procedure consists of passing the air steam and put it in direct contact with the cooling water that can be placed into wet surfaces or membranes, Figure 2.2. shows a schematic representation [8]. For these devices, the wet bulb temperature becomes a crucial parameter because of it is the minimum theoretical supply temperature, a well-design DEC can achieve an effectiveness of 85% approximately [9].

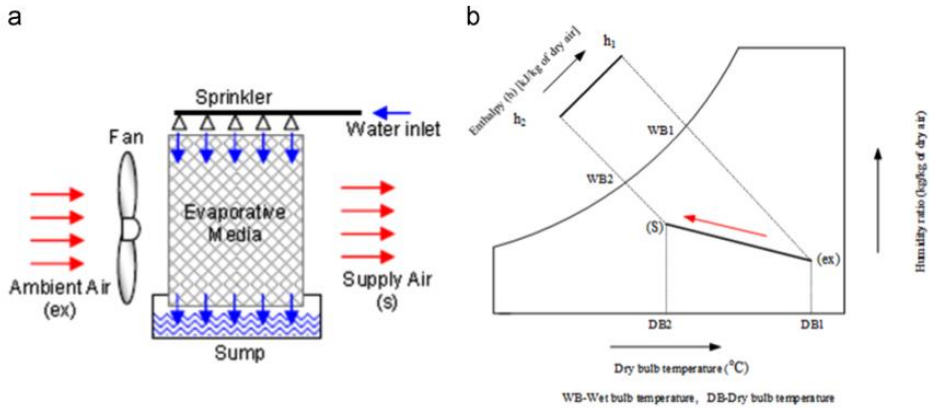

Figure 2.2. Schematic representation for DECs. [8]

2.1.1.2. Indirect evaporative coolers.

Indirect evaporative coolers (IECs) are usually air to air heat exchanger and the majority consist in a flat plate stack configuration [7]. The working principle of this component consist of cooling down the primary air stream by passing through dry channels, while a secondary air stream passes in adjacent wet channels. One important characteristic is the capability of reduce air temperature without adding moisture to primary air, which meant just sensible cooling, this fact makes suitable IECs for hot and humid climates [10]. Moreover, depending on the secondary air stream, IECs can be further classified as shown in Figure 2.3. [7]

Conventional IEC takes the secondary air from any place that can have the same or different conditions of the primary air stream; an example is the counter-flow configuration shown in Figure 2.3.a.

The Dew Point Cooler (DPC) pre-cools the working air (or secondary air) prior to its diversion into the wet channels; this practice can decrease both dry bulb and dew point temperatures of the air within the wet channels, thus achieving 20 and 30% higher cooling efficiency compared to the conventional IECs [11].

Counter-flow M-cycle DPC configuration can cool down the primary air stream to a temperature below the wet bulb and near to the dew point of the secondary air stream. Looking at Figure 2.3.c. the secondary air stream goes into a dry channel, which has

some perforations along the flow path. During the flowing, the air is partially cooled and diverted into the wet channel through the holes. The secondary air in the wet side is able to extract heat from the adjacent sides; One of them is channel for the primary air, which flows in counter flow and gets cold down. Experimental studies carry out by Zhan et all. Shown that the cooling capacity of M-cycle counter-flow DPC is 20% higher in comparison with the cross flow DPC [12]; Moreover, it presents a greater dewpoint and wet-bulb effectiveness under the same sizing and operating conditions. On the other hand, cross-flow M-cycle arrangement presented a 10% higher energy efficiency (COP). [12]

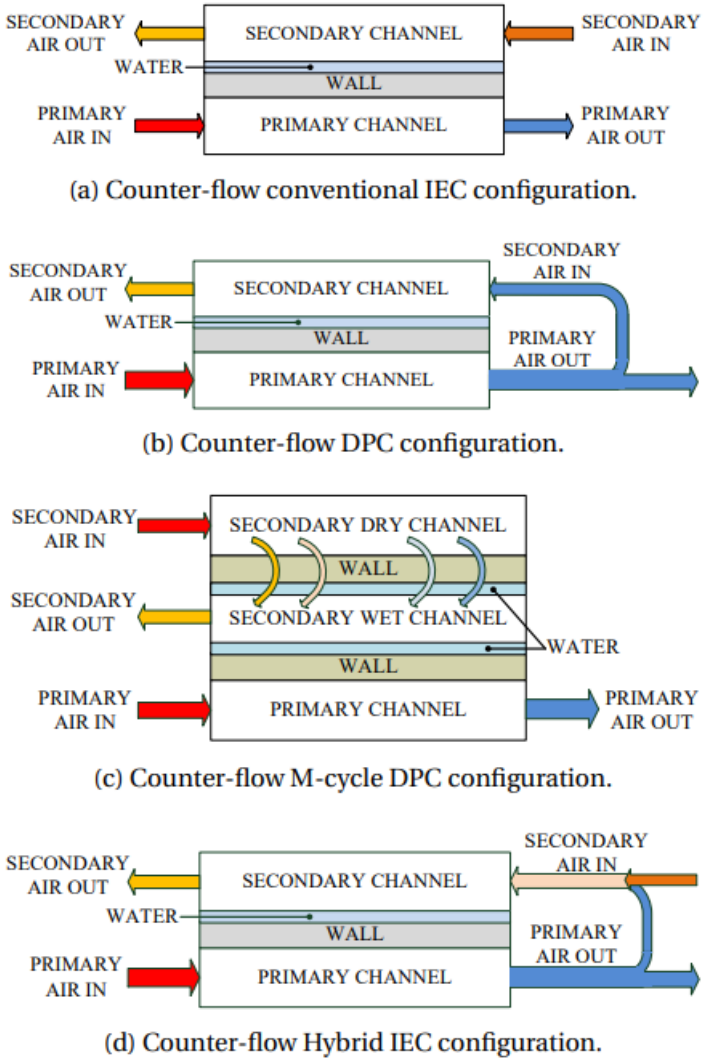

Figure 2.3. Classification of IECs. [7]

In other to reach a higher performance, some studies look for different configuration of ECs. Among them there is the two-stage evaporative cooler, which a schematic description and psychometric process are shown in Figure 2.4. This innovation consists of combining the direct and indirect technologies. All the primary air stream gets into a heat exchanger (considered the IEC), where the air is pre-cooled. Then, the component takes a certain flow rate and goes into a second stage, where moisture is

added to the stream (DEC); while the remaining flow passes through a bypass channel. Finally, the two streams are mixed. Kulkarni and Rajput, theoretically speaking, studied the performance of a two-stage EC for an application in Bhopal, Inda. They found that increasing the primary air flow rate from 0.3 to 1.25 kg/s, the performance of an IEC decreases from 0.95to 0.82. In addition, the cooling capacity ranges from 5.06 to 20.50 kW and an outlet temperature range between 22.5°C and 24.6°C, considering a dry bulb temperature of 39.9°C and relative humidity of 32.8%. [13]

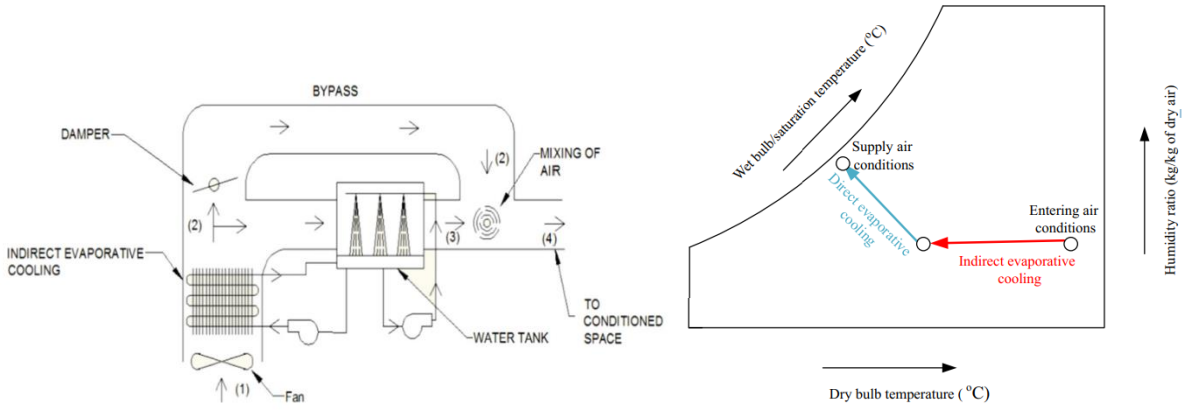

Figure 2.4. Schematic representation of the two-stage evaporative cooler. [14]

2.1.2. Desiccant dehumidifier.

Depending on the type of desiccant used, this material can be classified as liquid desiccant systems, Solid desiccant systems and Hybrid desiccant systems as shown in Figure 2.5.

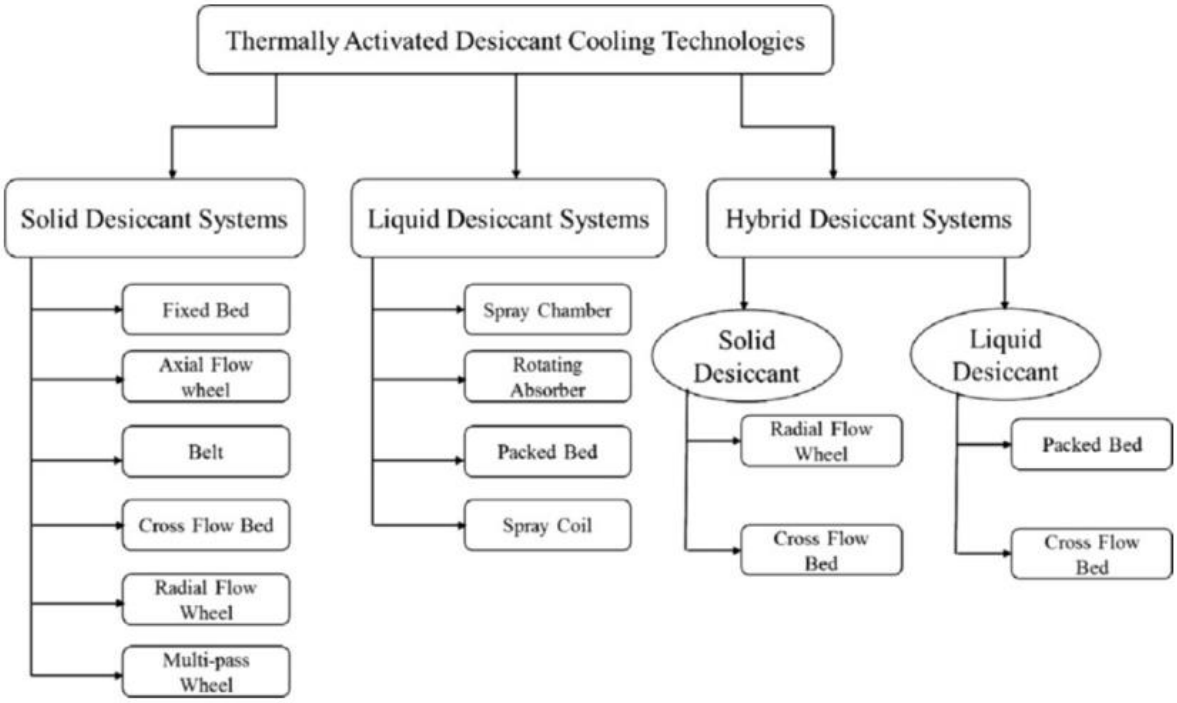

Figure 2.5. Classification of Desiccant technologies. [15]

2.1.2.1. Solid desiccant systems.

The theory of water vapor adsorption is the working principle of the solid desiccant cooling process. Thanks to the water vapor pressure difference between the process air and the desiccant material surface, the moisture content can be removed from the primary air stream. However, the dehumidification efficiency of desiccant components decreases due to the saturation, meaning that it is necessary to regenerate the material by using a low humidity content and high temperature air flow. Moreover, this procedure required the adsorption of heat, leading to an increase in the process air temperature. This consequence requires a further sensible heat exchanger or cooling coil to get the desired room conditions. [16]

Starting from the fixed bed technology; this component is made of a stationary bed with desiccant granules packed tightly. The regeneration and dehumidification process can be done by alternating the air flow that passes through the bed. The main advantage of the configuration is simplicity of the structure and manufacturing. Nevertheless, the low mass and heat transfer efficiency, because of the weak contact between desiccant material and air flow, is the main disadvantage that affects its usage. Additionally, it is required an elevated power consumption for moving the process air due to pressure drop suffered in the device [17]. The packed bed can be further categorized into convectional axial flow bed (Figure 2.6.a) and an alternative for reducing the pressure drop in the component, which is named the radial flow bed (Figure 2.6.b). Awad et al. (2008) theoretically and experimentally investigated the radial flow fixed bed dehumidification system and the results shown that compared to the vertical bed, the hollow cylindrical bed presented an important reduction in the pressure drop, meaning that air blowing energy required is minimum in comparison with the axial flow bed as presented in Figure 2.6.c. [18]

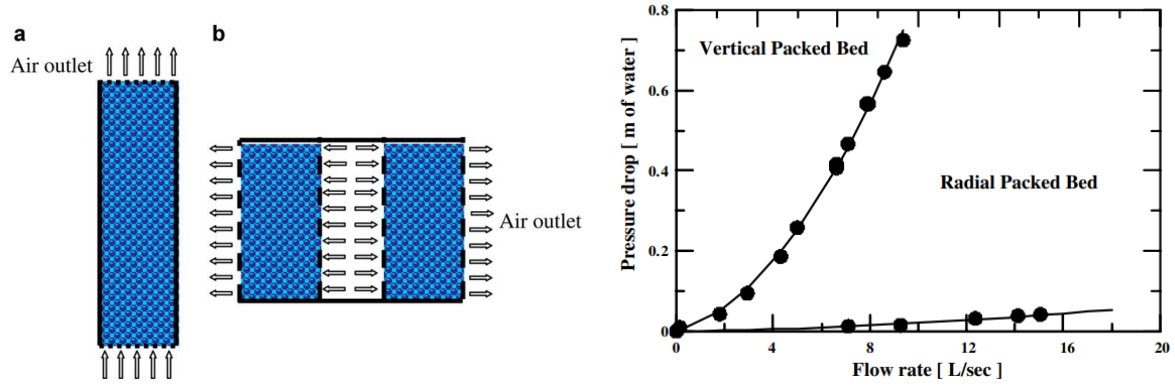

Figure 2.6. a - Convectional axial packed bed; b – Radial flow bed; c – pressure drop for axial and radial flow component. [18]

Moving forward into solid systems, one of the most relevant components is the rotating desiccant wheel (DW), which compared with other dehumidifying configurations, provide more benefits such as higher efficiency and compactness; moreover, desiccant wheel allows to configure a continuous working cycle that can be regenerated from low-grade heat sources like solar energy or wasted heat [16]. As it is represented in Figure 2.7. the operating principle consists of diving the wheel structure into the process and regeneration air sides by a clapboard. While the wheel rotates constantly passing through the two sections, in one side the process air gets dehumidified due to the adsorption material; and the same time in the other section, the desorbing process takes place thanks to the hot regeneration air stream which removes water content from the desiccant [19]. For optimizing the performance of DW, Ahmed et al. (2005) did a theoretical and experimental study in order to evaluate the influence of several design parameters [20]. They tried to get the optimum ranges for the thickness, the ratio between the regeneration and adsorption section and wheel speed according to different operating conditions. The findings evidenced that for desorption temperature between 60 to 90°C, acceptable values for the thickness were about 18 - 26 cm, the rotational speed ranges from 15 to 60 rph and the recommended wheel area ratio was 0.8 for 60°C and 0.3 for 90°C. [20]

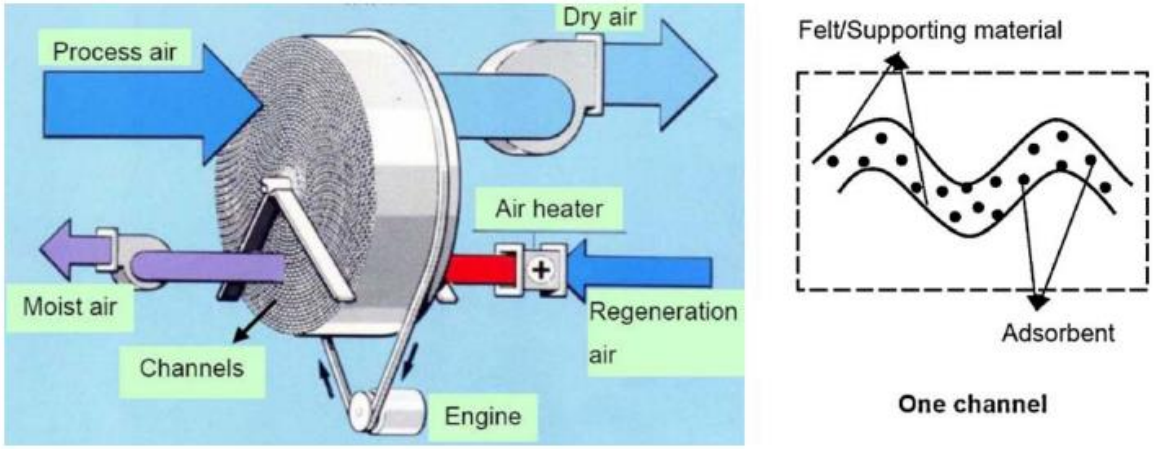

Figure 2.7. Schematic diagram of axial rotary desiccant dehumidifier. [19]

One drawback of the convectional desiccant wheel is the overheating of the intake air and the desiccant particles due to the dehumidification process. The way in which the heat is released plays an important role at moment of the wheel performance calculation. Kodama et al. (2005) launched a non-adiabatic multi-pass honeycomb rotating desiccant wheel (Figure 2.8) that simultaneously to the heating in the regeneration section, in the adsorption area, a counter flow air stream cools down the desiccant. The study found that the modification enhances by a 30% the dehumidification performance in comparison with traditional DW, the dimension is 40% less and the optimal rotational speed is 3 times slower than conventional rotor. [21]

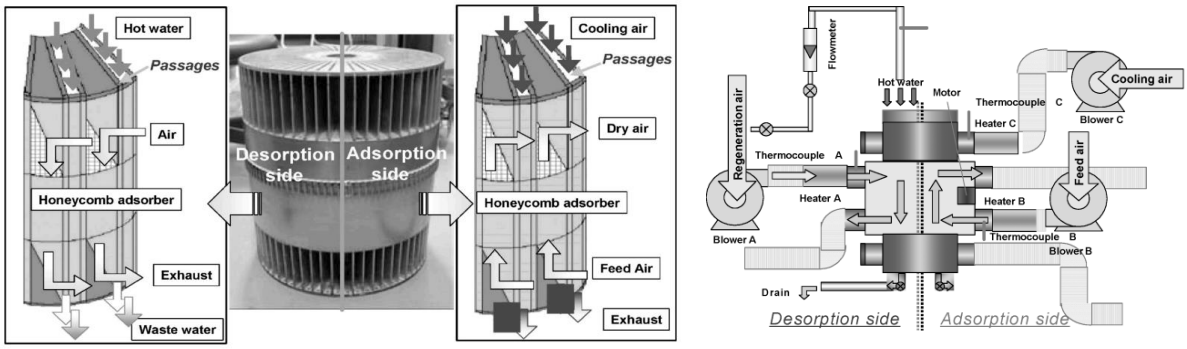

Figure 2.8. Diagram of the multi-pass honeycomb rotating desiccant wheel. [21]

2.1.2.2. Liquid desiccant system.

Considering all the properties that a desiccant material must have, the most usual liquid desiccants are glycol and solutions of halide salts. The triethylene glycol presents the advantage of having a low toxicity and compatibility with the majority of metals; but it is a volatile fluid because of the low surface vapor pressure and sometimes it evaporates and goes into the conditioned space. Additionally, it has a high viscosity which causes unstable system operation. On the other hand, LiCl and LiBr, are salts of Halides, that work well at ambient conditions and have low viscosity, reducing the pumping power. However, the principal drawbacks are the high cost, they are naturally corrosive and mixing with supply air must be avoided. [22]

The packed bed is the most common configuration in liquid desiccant dehumidifier/regeneration. The liquid fluid is distributed on the top of the packed and flows through it getting in direct contact with the air flow. This component can be arranged in adiabatic form (Figure 2.9.a.) where the desiccant solution temperature changes during the process because of the heat and mass transfer; An alternative in order to enhance the mass transfer is the internally cooled/heated (Figure 2.9.b.), or isothermal, in which a third fluid keeps constant the temperature [23]. An experimental study carried out by Bansal et al. (2010), compared the two systems, they found that the effectiveness of the internally cooled packed bed was 28 - 45% higher than the adiabatic one; but they noticed that part of the advantage is obtained because of the condensation on the chilled coil surface. [24]

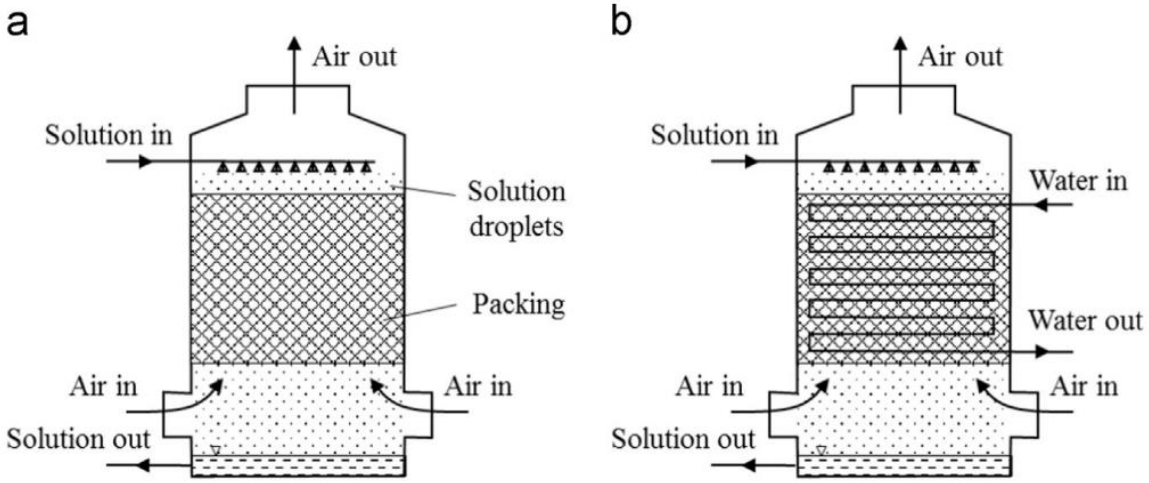

Figure 2.9. Schematic diagram of a) Adiabatic and b) Internally cooled packed beds. [23]

An alternative to stationary packed bed, it can be used a rotating absorber configuration for optimizing the moisture removal. Gu et al. (2019) performed an investigation with a rotating packed bed (RPB) for liquid desiccant regeneration, the experiment set up is shown in Figure 2.10. the outcomes evidenced a mass transfer coefficient of between 12.5 – 35.6 kg/m³s, which means 6 times greater than traditional regenerators [25]. Additionally, they conclude that moisture removal rate increases as the high gravity factor, air flux air inlet temperature, solution flux and solution inlet temperature also growth. [25]

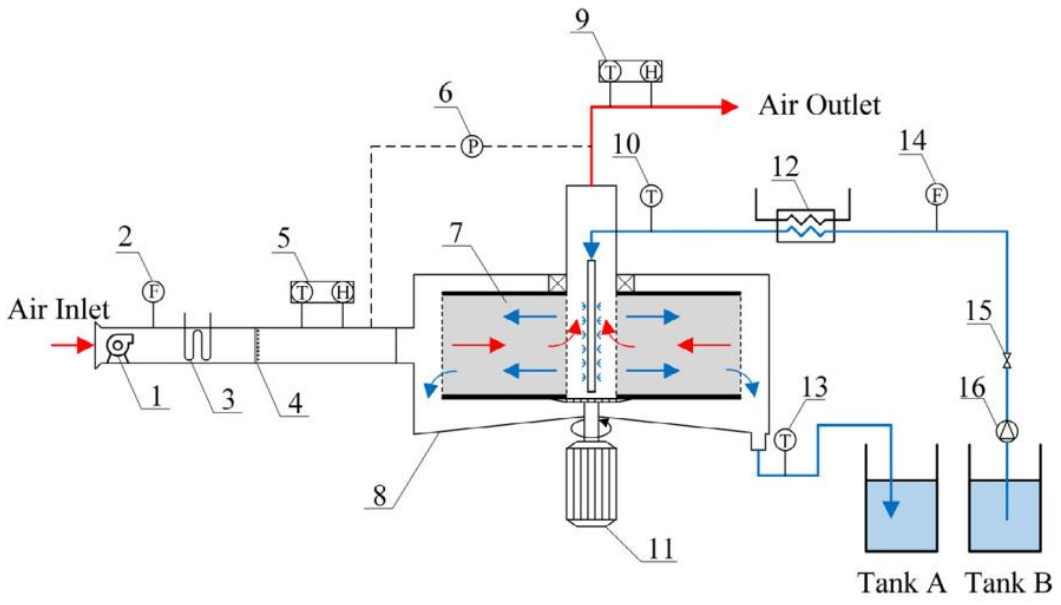

Components: (1) Fan; (2) Air flow meter; (3) Heat Exchanger; (4) Humidifier; (5) Integrated temperature and humidity sensor; (6) Differential pressure gauge; (7) RPB; (8) RPB shell; (9) Integrated temperature and humidity sensor; (10) PT100; (11) Motor; (12) Heat Exchanger; (13) PT100; (14) Liquid flow meter; (15) Valve; (16) Pump.

Figure 2.10. Liquid desiccant regeneration using rotating packed bed. [25]

Another liquid dehumidifier is the Spray tower, in which the desiccant solution is sprayed at the top of the tower in small droplets. In counter flow, the air stream gets in contact with the droplets allowing the heat and mass transfer at drop surface [23].In advantage to the packed bed, this arrangement can operate at lower flow rates, and it presents smaller pressure drop [26]. In contrast, the droplet carryover effect is higher. As for packed bed, the use of a cooling coil helps to increase by 20% the effectiveness of the spray configuration. Figure 2.11. presents the two alternatives.

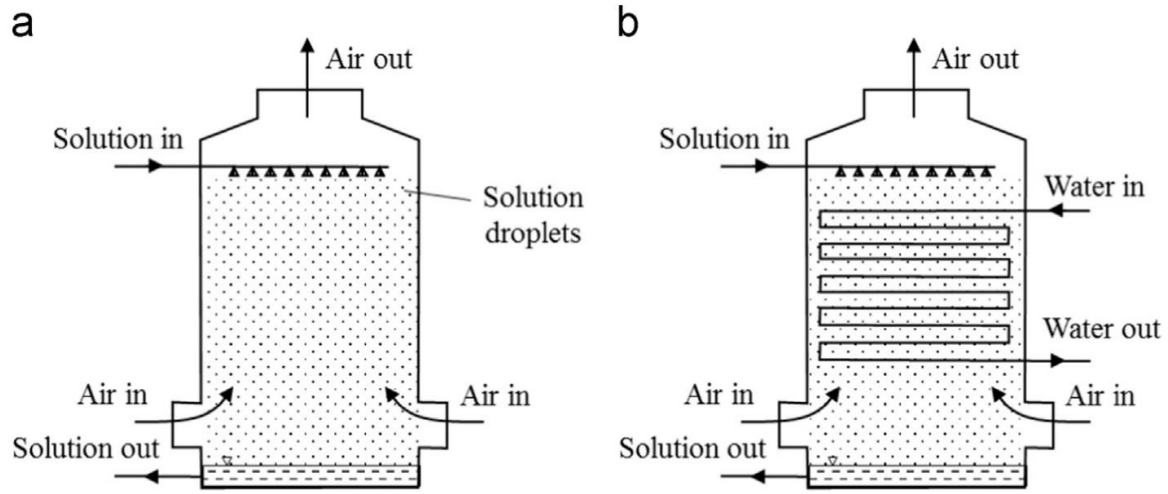

Figure 2.11. Schematic diagram of a) Adiabatic and b) Internally cooled Spray tower. [23]

2.2. Solid DEC Configurations.

For the purpose of this thesis, the radial flow wheel solid desiccant system will be the focus of the study. The most common rotating solid-desiccant configurations are the ventilation mode, the recirculation mode and the Dunkle cycle. [27]

For the ventilation cycle, the indoor room air is used to regenerate the desiccant wheel. The process description consists of taking room air and forcing it to pass firstly through an evaporative cooler, then it goes into a heat exchanger to pre-cool the primary air stream. Moreover, before entering in the desiccant wheel, the secondary air stream is subjected to a regeneration process, where heat from an external source, raises the air temperature in order to perform the desiccant drying and finally released into the atmosphere. Considering the supply air flow, it is taken from the outside environment and gets dehumidified by crossing the desiccant wheel in a first stage, secondly it is precooled by the sensible heat exchanger and finally the process air is further cold down by evaporative cooling component [27]. The block diagram and psychometric representation for the ventilation mode is shown in Figure 2.12.a. and Figure 2.12.b. respectively.

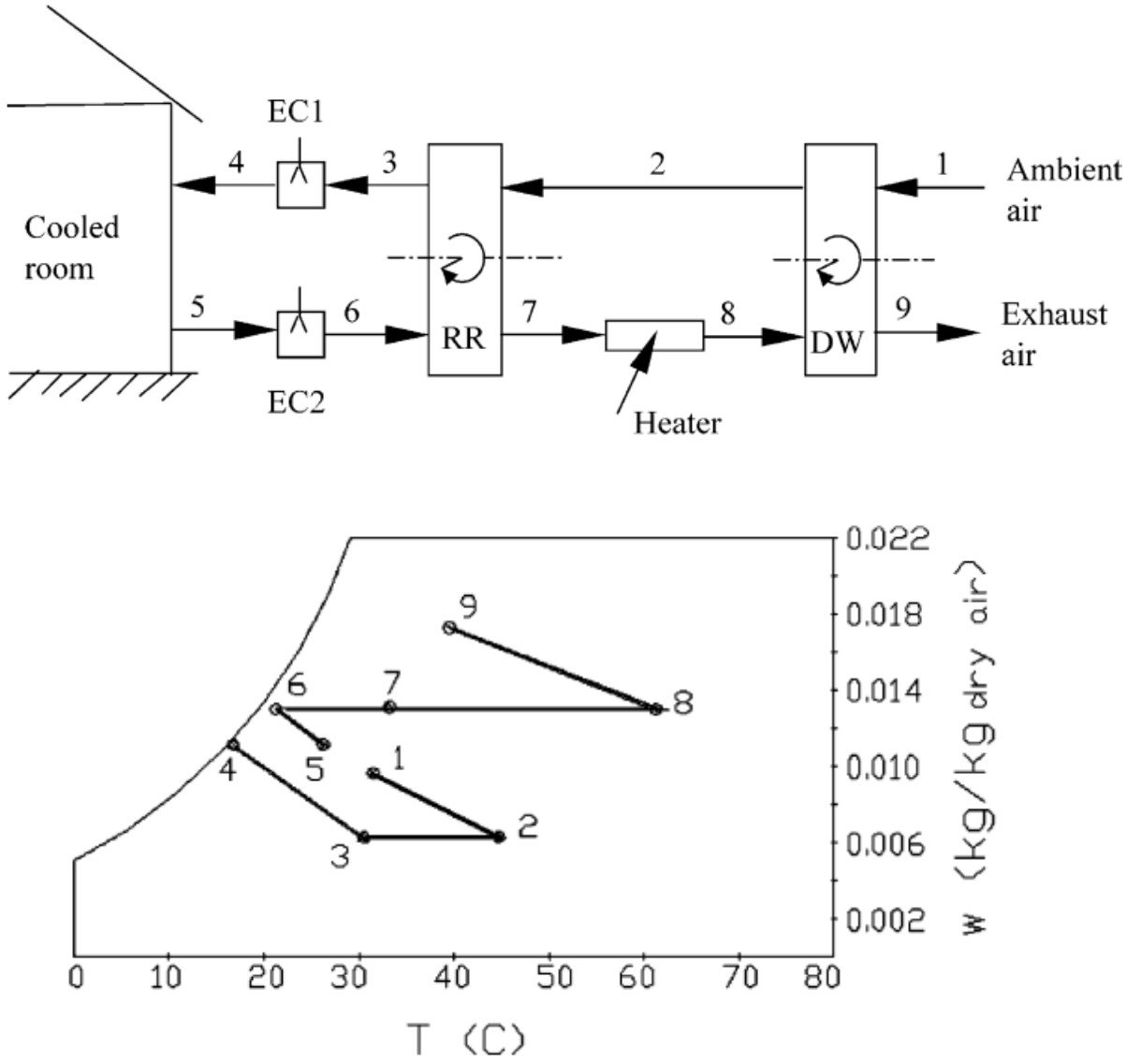

Figure 2.12. Schematic representation of a solid desiccant wheel evaporative cooling system in ventilation mode. [28]

In practice, the recirculation mode is formed by the same components of the ventilation arrangement; with the difference that the room air is continuously reconditioned in a close loop using the environmental air just for the regeneration process as presented in Figure 2.13. A thermodynamic advantage for the cycle is the higher availability for cooling. However, having a cold sink-temperature can reduce the performance of the cycle. Additionally, for this case there is not a direct fresh air supply, the only way is by the introduction due to normal infiltration such us for conventional vapor compression cycle, whereas for ventilation mode, all the supply air to the conditioned space is fresh. It means that for application with requirements of indoor air quality, the recirculation mode is not suitable. [29].

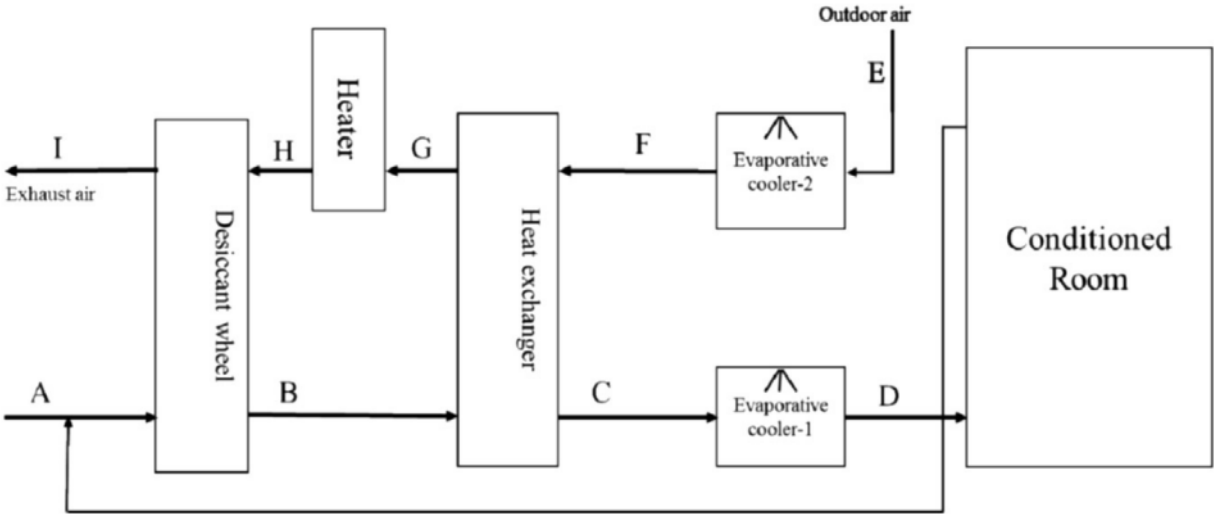

Figure 2.13. Schematic representation of a solid desiccant wheel evaporative cooling system in recirculation mode. [29]

Finally, regarding the Dunkle cycle, it tries to combine the ventilation and recirculation configuration in order to take the thermodynamic advantages of both cycles [30]. It uses the higher cooling availability room air as in the recirculation mode and the lower cold-sink temperature of the ventilation mode [27]. However, one disadvantage of the cycle is the non-control of the fresh air supplied to the building.

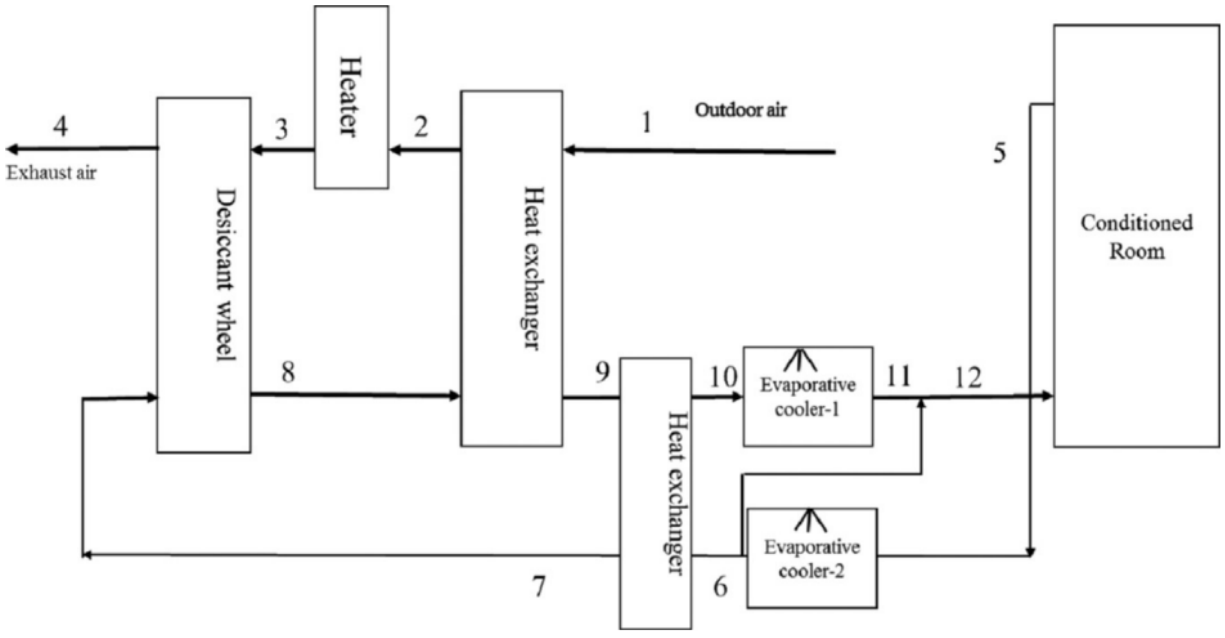

Figure 2.14. Schematic representation of a solid desiccant wheel evaporative cooling system – Dunkle Cycle. [30]

2.3. Case studies.

Moving forward to specific studies similar to the purpose of this thesis work. It is found the simulation carried out by Narayanan et al. (2018), in which they evaluate the applicability of DEC system in the residential sector, considering the weather conditions of Brisbane, Queensland, Australia. It is used a solid DEC in the ventilation mode arrangement as evidenced in Figure 2.12. The main components are the desiccant wheel, a direct evaporative cooler, and a regeneration temperature of 75°C (an electrical resistance is assumed). The TRNSYS modelling package is used for the simulation, taking into account that the conditioned spaces were just the living room and bedrooms. The results shown that regarding the cooling demand, the proposed DEC configuration can technically cover about 50% of the required hours. Additionally, they pointed out that heat source for regeneration must be provided by a cheap or waste-heat resource to make the system economically viable. [31]

Regarding cheap heat sources, Katejanekar and Kumar (2007) proposed a solar regenerated liquid desiccant ventilation system. The configuration, as shown in Figure 2.15. is formed by two air and liquid loops. Air loops take care about the dehumidified and regenerating air loop, while liquid loops are the liquid desiccant and the cooling tower loop. The process air goes into the dehumidifier (Packed bed), where it gets in contact with the strong desiccant solution (Lithium chloride) in counter flow for absorbing moisture; them it is sensible cooled by heat exchanger in which passes the cooling tower loop. For reconcentrating the desiccant solution, it is used the solar energy and regeneration air stream. The experimental results evidenced that a humidity control can reduce the relative humidity from 60% until 30% if it is necessary, additionally, the study determined that the most influential parameters were the solar radiation, the ventilation rate and the desiccant solution concentration. [32]

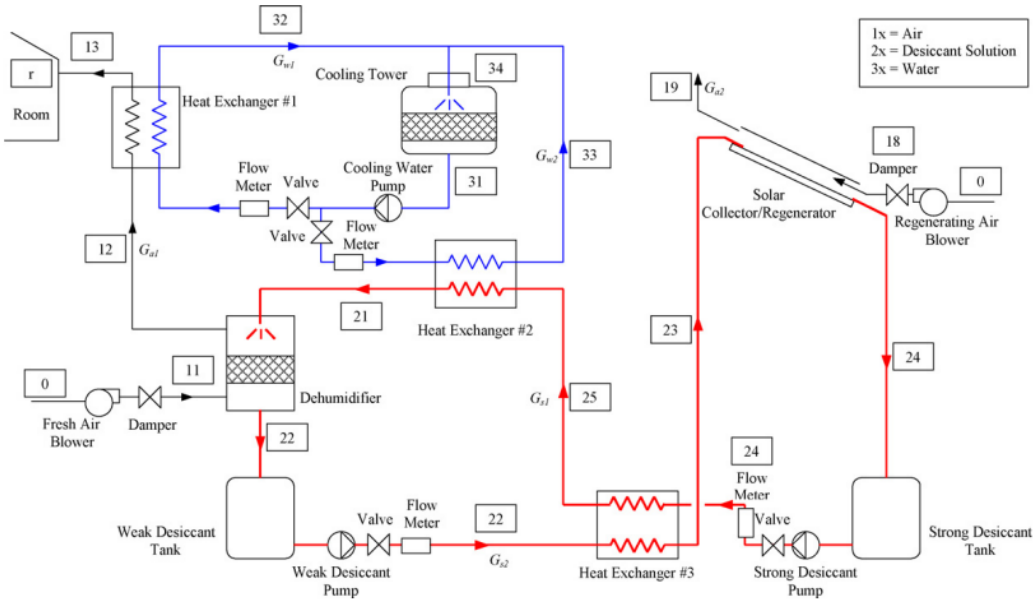

Figure 2.15. Representation of the solar-regenerated liquid desiccant system. [32]

Another interesting prototype of DEC system is presented by Ouazia et al. (2019). They assessed experimentally and theoretically the configuration in diverse region of Canada. Concerning the experimental results, for a set point of 24°C and 50%RH, the tested DEC system was not able to maintain the average indoor temperature. However, measuring the relative humidity, the desiccant evaporative cooling evidenced a better humidity control and comfort than the convectional HVAC system. They suggested that potential application areas for this type of technology are those with a low sensible heat ratio, meaning considerable latent load. Moreover, they concluded that in order to enhance the performance of the system is necessary to consider components with high electrical efficiency and to install the system outside building envelope. [33]

3 Chapter three: Dehumidification and cooling demands simulation.

3.1. Building thermal characteristics and modelling

The definition of the cooling and dehumidification demand is a critical step in the design of a desiccant cooling system because they cannot be satisfied if the system is undersized, on the other hand, resources and materials are not optimized if the system is oversized. For this reason, a reference point is required to properly size and select all the components that will provide the thermal and humidity comfort inside the conditioned spaces.

Firstly, we need to define what a conditioned space is. It is an area inside a building where temperature and humidity are controlled. This conditioned space is separated from the external environment by the building envelope. The temperature and moisture content of the air inside the conditioned spaces are modified by internal heat and mass transfer processes. The appliances inside the spaces generate heat when they are used, and this heat is transferred to the surrounding air increasing the air temperature. Also, people that occupy the space produce not only heat but also increase the water content inside the air. These are called internal loads and their effects need to be balance by the conditioning system in order to maintain the desired indoor air conditions.

There are external factors that also modify the thermal environment inside conditioned spaces. The external air temperature and humidity, solar radiation and wind velocity

have a direct effect in the temperature and humidity of the conditioned spaces. Their impact on the internal thermal environment is limited by the building envelope and their effects need also to be balanced by the air conditioning system. All these processes must be taken into account when we want to calculate the cooling and dehumidification demand of the conditioned spaces.

In this thesis work, cooling and dehumidification demand are estimated by performing a dynamic simulation using TRNSYS software. The simulation needs as input the weather data of the site where the building is placed. Weather data is obtained through the software METEONORM that provides climatological information for multiple sites around the world, using measured data from meteorological stations and sophisticated extrapolation techniques. It is also required a detailed model for the building that must include the characteristics of the building envelope, internal gains (illumination, appliances and heat produced by people), occupation profile, shading devices as well as the building distribution and orientation of the spaces.

In order to model the building, the component TRNBuild of TRNSYS software is used. As a first step, the building envelope is created considering the distribution of the apartments and the materials that constitute all the structure of the building. The building studied in this thesis is composed by 4 floors and the basement. Each floor is divided into six apartments, all with different area and orientation. The distribution of the apartments is the same for each floor and it is shown in Figure 3.1.

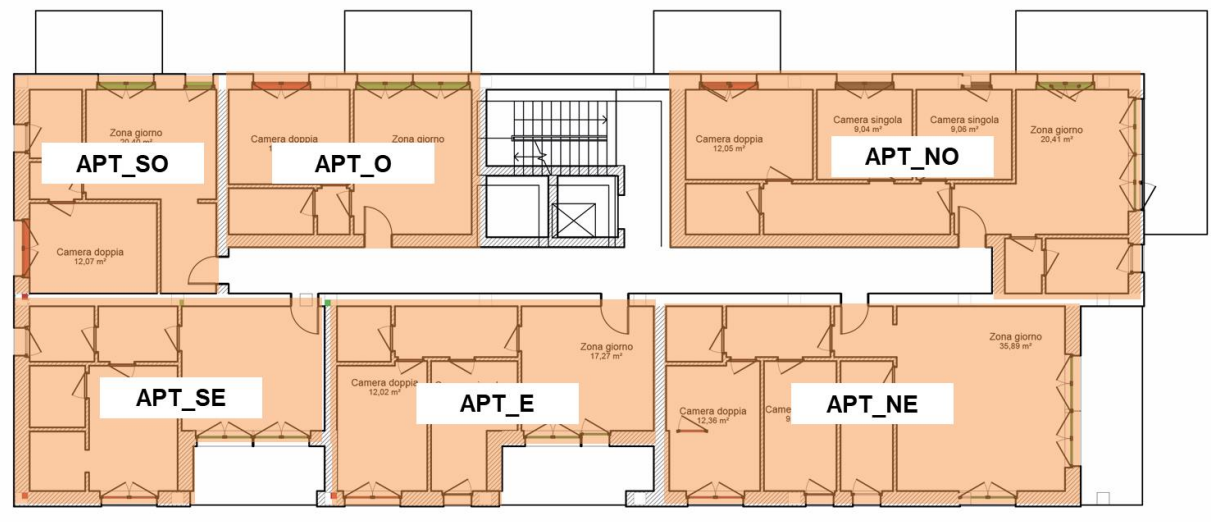

Figure 3.1. Distribution and orientation of the apartments in a floor.

The building shell is composed by the internal and external walls, fenestration, ceilings, internal and external floors, and external roof. The material composition of the structures and its average transmittance value inserted into the TRNSYS model are reported in the Table 3.1.

Table 3.1. Materials and average transmittance for the structures the building consists of.

Type of Structure	Average Transmittance [W/(m2*K)]	Materials
External wall	0.214	plasterboard, cavity, glass wool, block (poroton 600), expanded polystyrene, plaster
Internal wall	0.238	plasterboard, cavity, external glass wool, cavity, internal glass wool
Ground floor	1.923	tile, mortar, screed, gravel
Basement ceiling	0.197	tile, radiant screed, expanded polystyrene, premixed subfloor, vapor barrier, screed, predalles slab, plaster
Adjacent ceiling	0.373	tile, radiant screed, expanded polystyrene, footfall noise insulation, premixed subfloor, screed, latero-cement floor, cavity, plasterboard
External floor	0.224	TEPP, ESTR, MIWO, BET, DAEMA
External roof	0.152	plasterboard, cavity, latero-cement floor, screed, premixed subfloor, footfall noise insulation, vapor barrier, stiferite, bituminous membrane, tile
Windows	1.36	GU SunGuard HP 41/33_#2_Ar90: 2 glazing with argon gap

This information must be included in the model because the thermal behavior of the building respect to the external environment depends on the materials used for its construction. A well-insulated building allows to have a better control of the internal spaces with lower energy consumption of the air conditioning systems. For this reason, designing properly the building envelope by selecting the right materials considering the project context, may lead to energy savings due to improvements in building efficiency.

Italian government has stablished, through DM-Requisiti Minimi, the minimum values of transmittance required to obtain a near zero energy building (NZEB) that change according to the zone where the building is constructed. According to D.P.R. n. 412 del 26 agosto 1993, The city of Milan corresponds to a climate zone E, thus the minimum requirements for a nZEB building are the corresponding to this climate zone [34]. In Table 3.2, are reported the minimum values of transmittance and the values obtained for the building studied.

Table 3.2 . Comparison between building transmittance and minimum values required by Italian government for a nZEB building [35].

Type of Structure	**Average Transmittance [W/(m2*K)]**	**Minimum transmittance [W/(m2*K)]**
External wall	0.214	0.260
Internal wall	0.238	0.800
Ground floor	1.923	0.220
Basement ceiling	0.197	0.800
Adjacent ceiling	0.373	0.800
External floor	0.224	0.260
External roof	0.152	0.220
Windows	1.360	1.400

According to Table 3.2, it is possible to observe that transmittance values for all the structures of the building are lower than the values required by Italian normative for a nZEB building. Therefore, we can consider this building as a nZEB building with high performance and low energy consumption.

In our case study, which is focused on cooling season, these building thermal characteristics allows to reduce the heat gain from the external environment, thus the heat that the desiccant cooling has to remove to maintain temperature and humidity of the inside air will be lower than for a building with higher values of transmittance.

To simulate the internal gains, it is necessary to determine the amount of heat generated by people inside the rooms as well as the amount of heat generated by the appliances. The values set as input for the simulation are reported in Table 3.3.

Table 3.3. Parameters for the internal heat generated by people, lighting, and appliances.

People	Density	0.04 pers/m2	8 W/m^2
	Sensible heat	80 W/pers	
	Latent heat	38 W/pers	
Lighting and appliances	Sensible heat	4.92 W/m2	

The instantaneous heat generated by the combination of the two sources is calculated as 8 W/m2, as reported in Table 3.3.

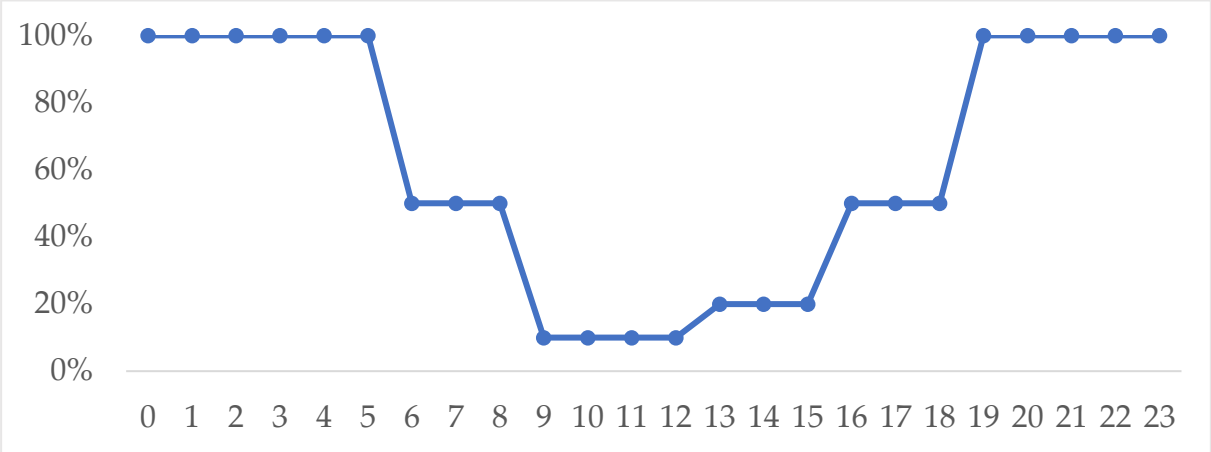

Figure 3.2. Occupation profile during weekdays.

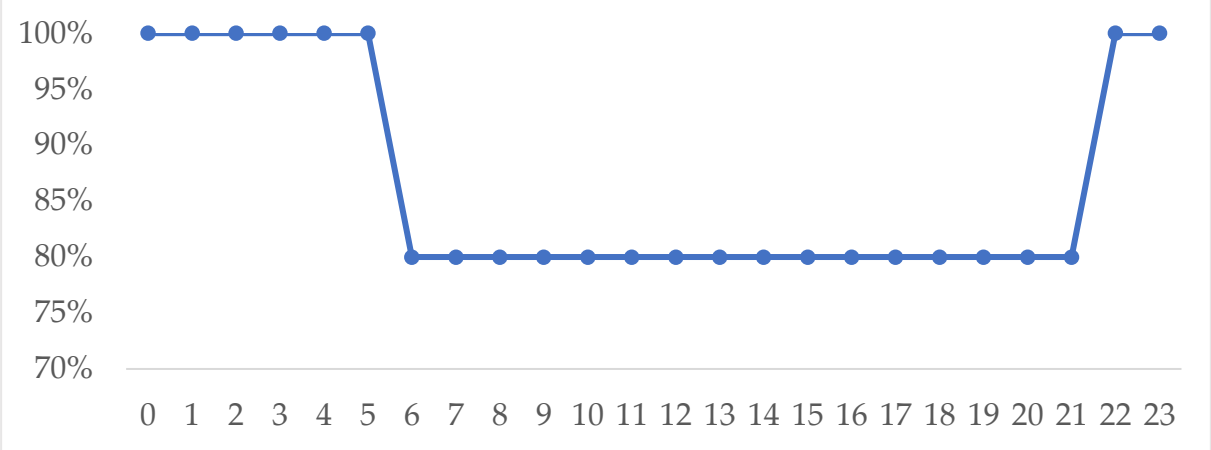

Figure 3.3. Occupation profile during weekend.

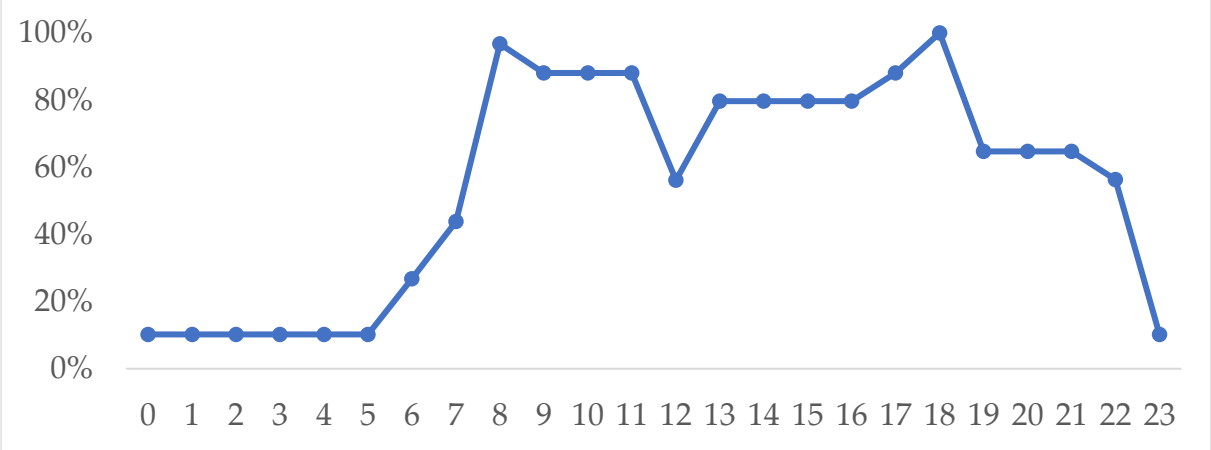

Figure 3.4. Schedule for lighting and appliances use.

Internal gains have been modeled by introducing an occupation profile of the building that changes between weekday and weekend, and a schedule for the lighting and appliances. Considering Figure 3.2, the occupancy of the building falls during morning until afternoon at 18 because people exit from home to perform their daily activities like working or going to school. During weekend the occupancy is always higher than 80% as shown in Figure 3.3, because people usually stay at home.

Shading devices are also part of the building envelope, and they allow to control the heat gain generated by the solar radiation by controlling the shading factor which varies between 0 (totally open) and 1 (totally closed). This building is provided with two types of shading devices: awning and shutter sunblind. Also for shading devices are defined schedules that change between weekdays and weekend. The schedule profile of shutters during weekdays and weekend are shown in Figure 3.5 and Figure 3.6, respectively. Figure 3.7 and Figure 3.8 show the schedule profile for awnings during weekdays and weekend, respectively.

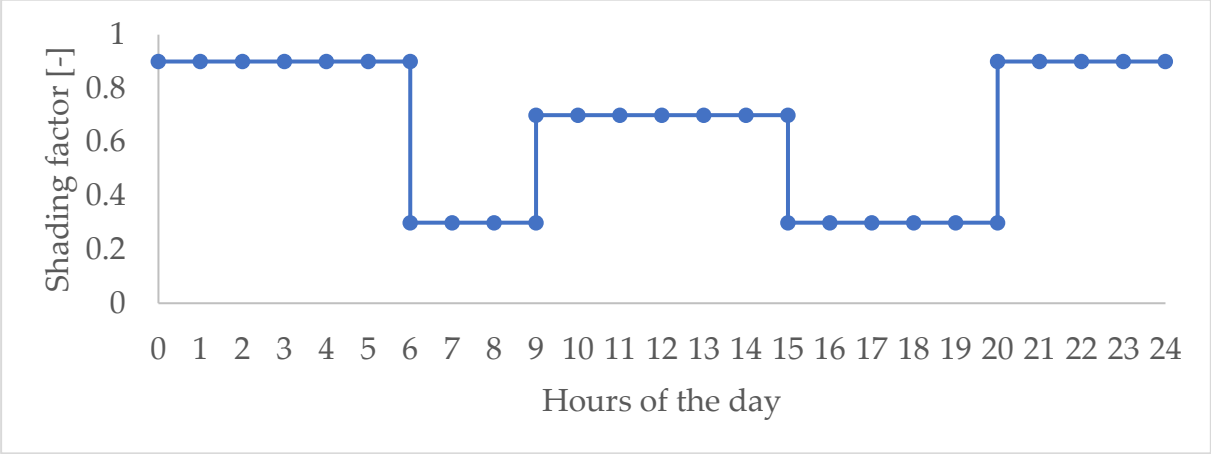

Figure 3.5. Schedule profile for shutters during weekdays.

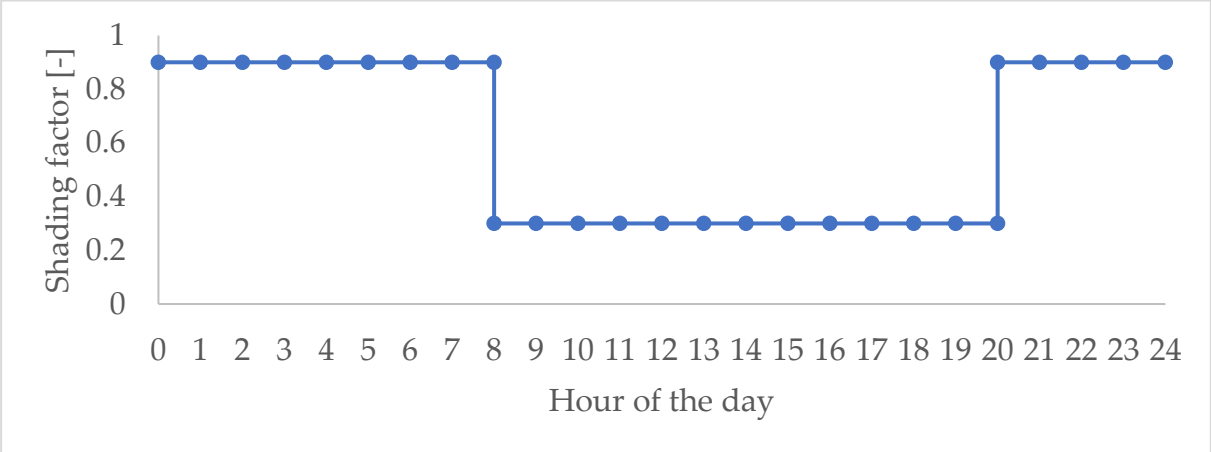

Figure 3.6. Schedule profile for shutters during weekend.

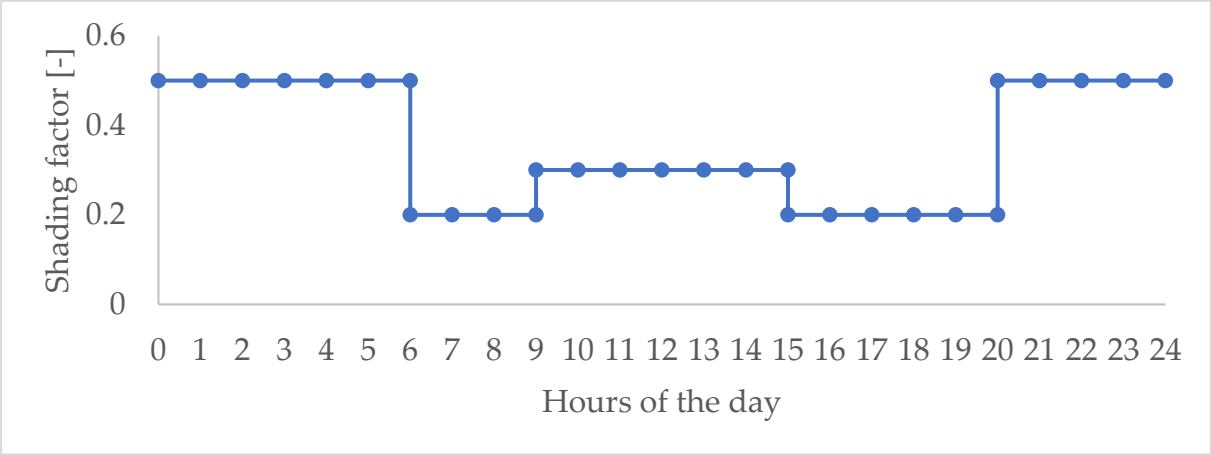

Figure 3.7. Schedule profile for awnings during weekdays.

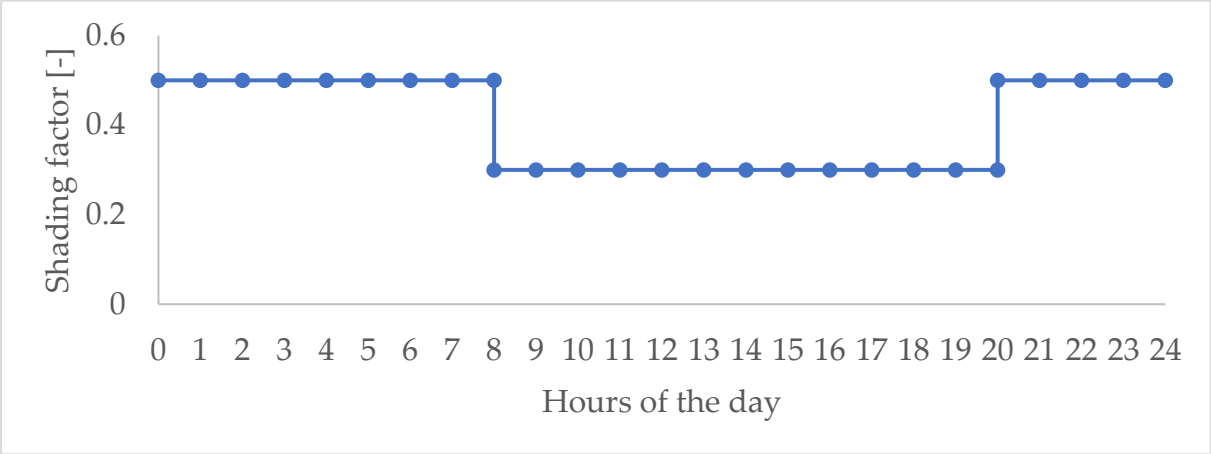

Figure 3.8. Schedule profile for awnings during weekend.

Finally, inserting all the information of the building in the TRNBuild type, we obtain the building model necessary to perform the dynamic simulation to estimate the cooling and dehumidification demand of all the apartments. The model of the building generated by TRNBuild is shown in Figure 3.9, and it includes all the building envelopes and shading devices involved in the heat transfer process.

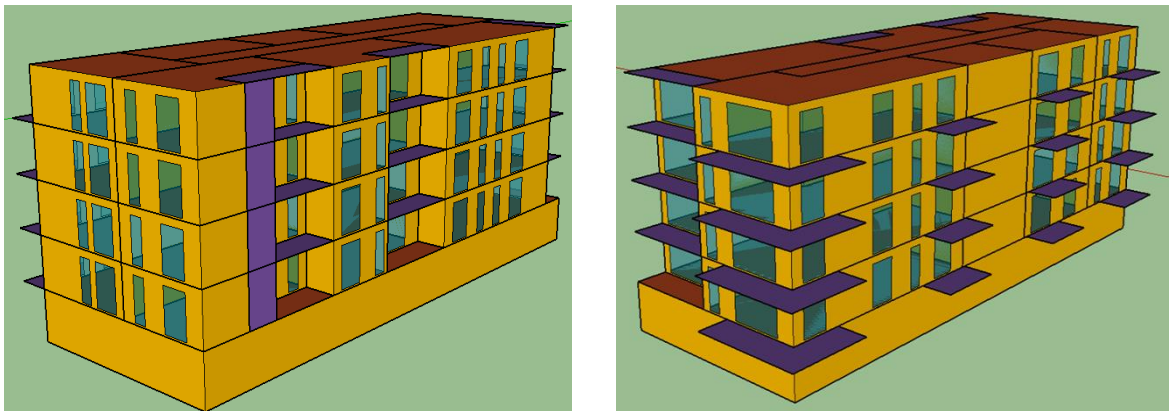

Figure 3.9. Model of the building created by using TRNBuild type of TRNSYS.

3.2. Weather conditions of Milan

Considering the weather data conditions provided by the TRNSYS software, Milan presents an annual maximum temperature of 35°C; those temperature ranges are expected during the summer season months, which are June, July, August, and September. Regarding the winter, spring, and autumn months from October to May, cooling demand is less required, even it is necessary to use a heating system. From Figure 3.10 to Figure 3.12 are shown the dry bulb temperature, the humidity ratio and relative humidity profiles by month for the Milan climate during the year, respectively. Keeping in mind the information presented in those figures, we can say, that the Milan weather is relatively humid and hot, during the summer period, signifying that dehumidification will be required on the season.

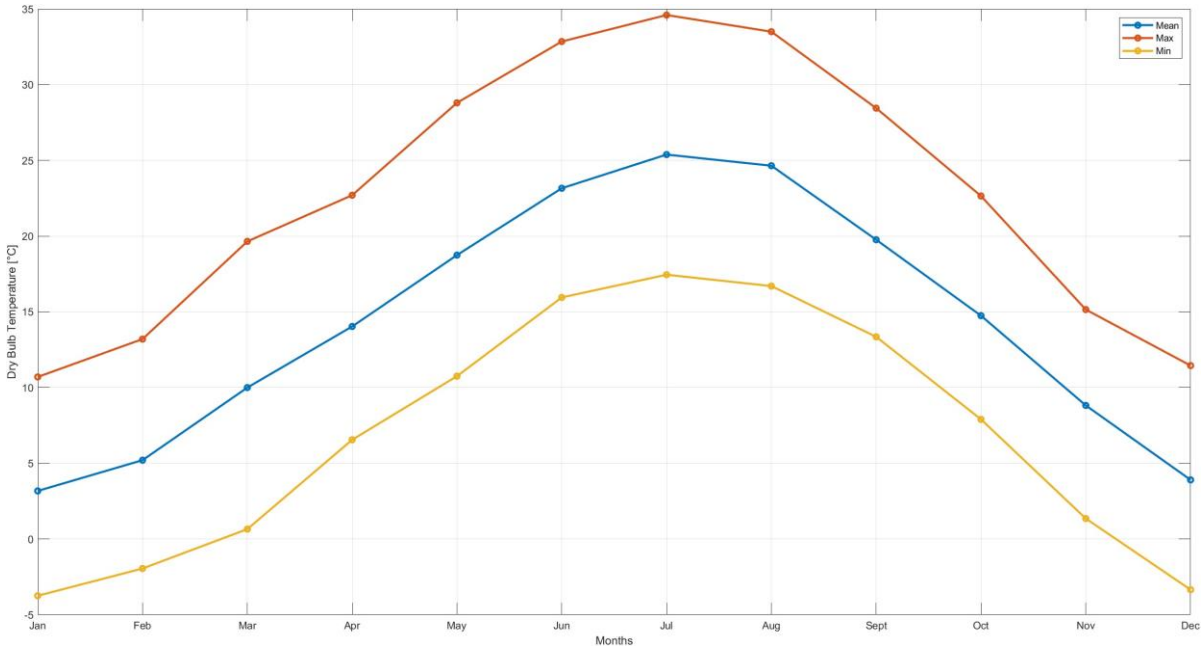

Figure 3.10. Monthly dry bulb temperature profile of Milan.

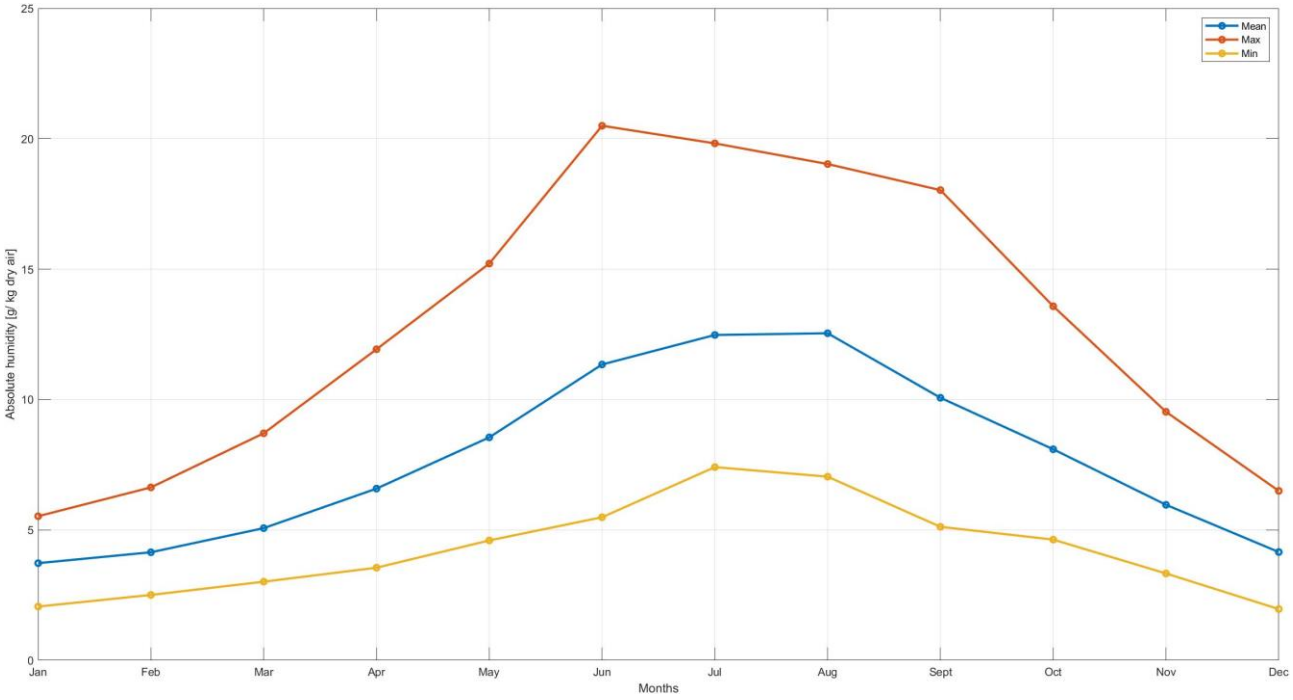

Figure 3.11. Monthly humidity ratio profile of Milan.

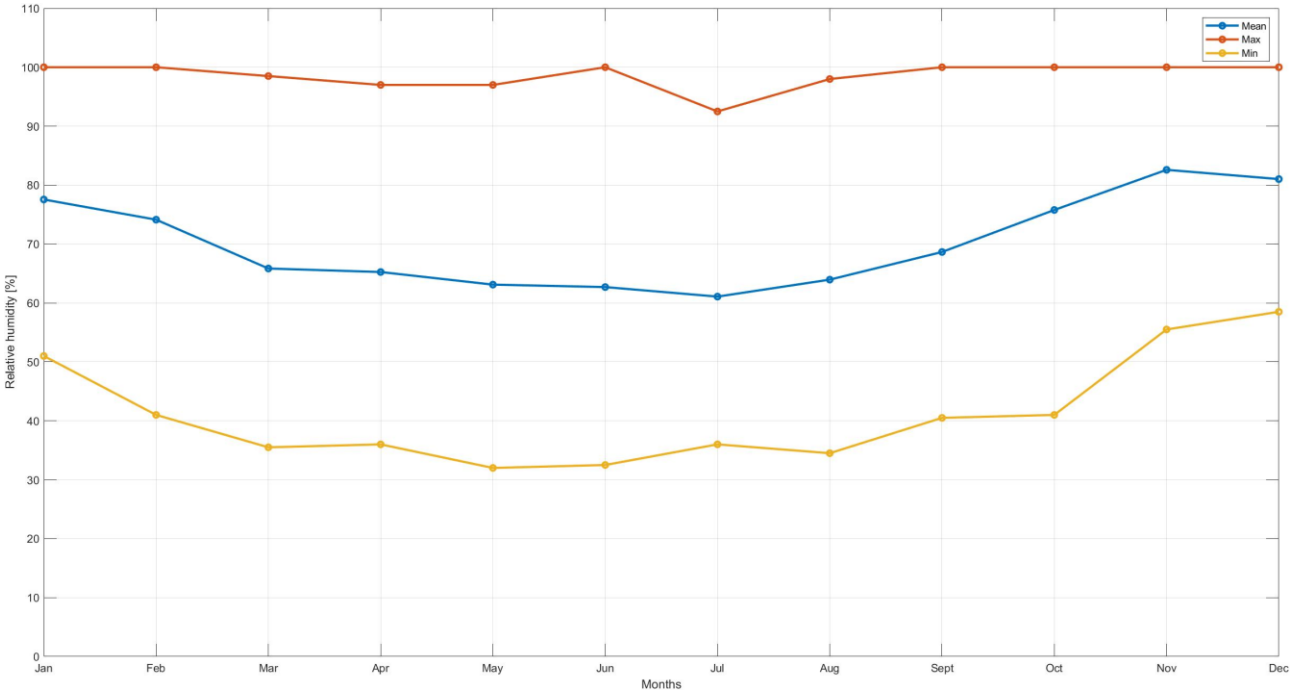

Figure 3.12. Monthly relative humidity profile of Milan.

3.3. Cooling and dehumidification demand.

Considering that the cooling requirements will be comprised between the period of June 1st to September 30th; and taking into account the requirements for indoor space conditions defined by the normative UNI-TS 11300. The limiting state for a conditioned space should have at least a temperature of 26 °C and 60% relative

humidity (12.6 g /kg of dry air for absolute humidity) in normal cooling operating system [36]. Keeping in mind this target point, the TRNSYS building simulation estimate a base case, where it calculates the sensible and latent demand for each apartment in the building, hypothesizing that there would always be an ideal system available for reaching the stablished condition. The results are presented in Table 3.4 and Figure 3.13, where it is depicted in a graphic way the findings obtained and can be easier identified the dwellings north-west and north-east oriented at the 3rd and 4th floor as the conditioned spaces with the highest sensible and latent load.

Furthermore, looking at Table 3.4, it can be observed that for the same orientation of an apartment, the ones at the fourth floor present always the higher sensible load and more or less the same dehumidification load. In the next, for the seek of simplicity, the results will be focused on those dwellings at flat 4th, particularly for north-west and north-east oriented.

Table 3.4. Total cooling and dehumidification energy demand by apartment during the summer period.

Apartments	Cooling Load [kWh]	Dehumidification Load [kWh]
Ap 01_NE	1442.3886	494.1153
Ap 01_E	1152.2236	334.3749
Ap 01_SE	998.0455	285.9413
Ap 01_SO	841.1856	265.0709
Ap 01_O	832.4216	246.1598
Ap 01_NO	1668.3770	508.4154
Ap 03_NE	**1768.9586**	**493.7964**
Ap 03_E	1400.7064	334.2349
Ap 03_SE	1176.8124	285.7400
Ap 03_SO	999.6477	264.9074
Ap 03_O	1039.2023	246.0136
Ap 03_NO	**2018.1911**	**508.0675**
Ap 04_NE	**1794.9002**	**494.1767**
Ap 04_E	1408.0817	334.3877
Ap 04_SE	1192.2538	286.0936
Ap 04_SO	1010.6676	265.1815
Ap 04_O	1045.0437	246.1457
Ap 04_NO	**2055.5415**	**508.4879**

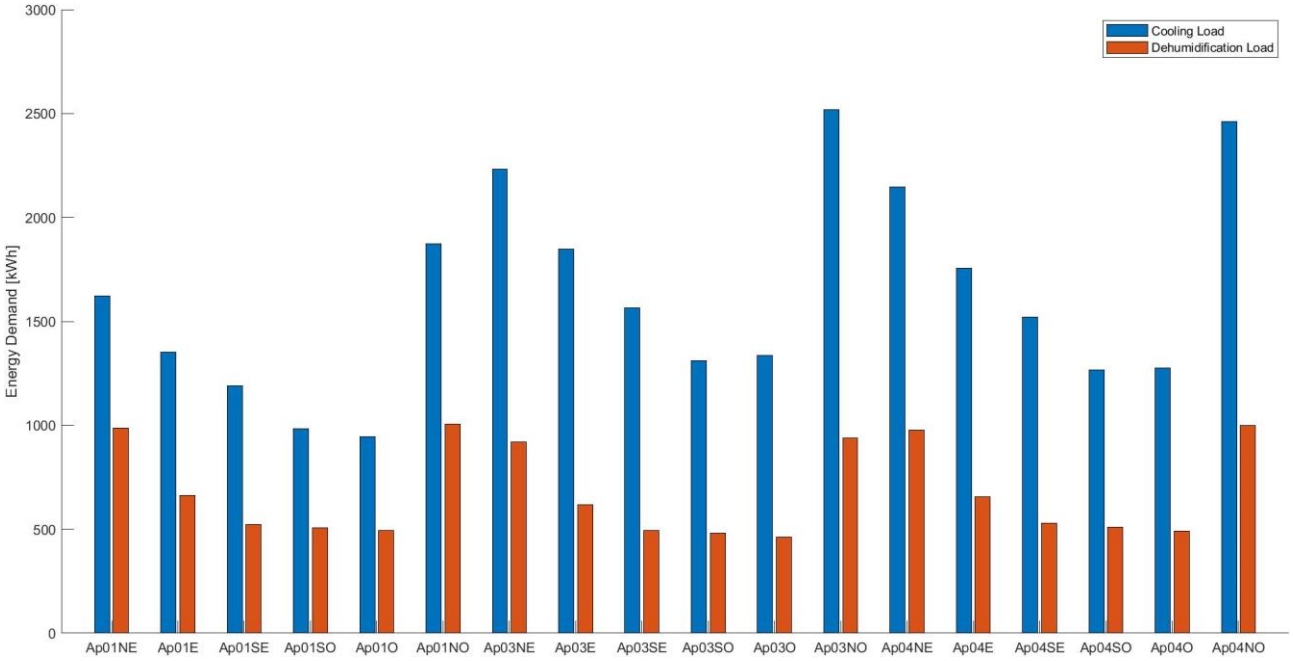

Figure 3.13. Cooling load (sensible) and dehumidification load (latent) in the base case simulation for all the apartments.

Since, it is essential to consider cooling needs as the combination of temperature (Sensible cooling) and humidity (latent cooling) to ensure comfort. Another important aspect that can be pointed out from the data in Table 3.4 is that the latent load represents more or less 22% of the total conditioning demand, a significant portion of the energy required and pointing out a good omen for the performance of the DEC system that will be implemented. Table 3.5 presents the sensible heat ratio (SHR) for each apartment, which is a measurement that characterizes these the cooling aspects. SHR is defined as the ratio of sensible heat gain to the combined sensible and latent heat gain in the conditioned space [33]. A low SHR indicates that the primary cooling load predominantly consists of the latent load. This indicator is employed by researchers when evaluating the applicability of a desiccant system in the considered location; values over 90% makes little sense to implement this kind of technology [33].

Table 3.5. Sensible heat ratio by apartment.

Apartments	**Ap 01_NE**	**Ap 01_E**	**Ap 01_SE**	**Ap 01_SO**	**Ap 01_O**	**Ap 01_NO**
SHR [%]	74.48%	77.51%	77.73%	76.04%	77.18%	76.64%

Apartments	**Ap 03_NE**	**Ap 03_E**	**Ap 03_SE**	**Ap 03_SO**	**Ap 03_O**	**Ap 03_NO**
SHR [%]	78.18%	80.74%	80.46%	79.05%	80.86%	79.89%

Apartments	**Ap 04_NE**	**Ap 04_E**	**Ap 04_SE**	**Ap 04_SO**	**Ap 04_O**	**Ap 04_NO**
SHR [%]	78.41%	80.81%	80.65%	79.22%	80.94%	80.17%

3.4. Base case – Natural ventilation.

Initially, before starting to introduce the model of the desiccant system. It is necessary to look for a reference case in order to compare how much is the improvement of the purposed system respect to not doing any intervention in the building; for the aim of this thesis work, the natural ventilation of the building is taken as the reference. Meaning that for the simulation it is not considered any cooling system, just the natural ventilation in the building, that is traduced into opening the windows of the different apartments and leaving the outdoor air, without any treatment, flows into the spaces for conditioning them.

The TRNSYS model performs a calculation of how much is the volumetric air flow rate that enters into each apartment using equation (1), and considering the weather conditions of Milan. The used expression, that takes into account the Bernoulli equation for estimating the air velocity, is the following one:

$$\mathrm{Q}_i = C_d * C_{d0_i} * A_{d\,i} * \left(\frac{2 * |\Delta P|}{\rho}\right)^{0.5} * L_T \qquad (1)$$

In the following subsections are exposed the results of the simulation focusing on the temperature and humidity ratio profile for the apartments 04_NE and 04_NO which were the ones with the higher loads. Then there is presented an evaluation of the indoor space conditions during the summer period for all the dwellings at the fourth flat.

3.4.1. Dry bulb temperature profile.

In Figure 3.14 and Figure 3.15 is shown the temperature profile of the apartments 04-NE and 04-NO as a result of the natural ventilation simulation. It can be observed that for the beginning of the conditioning period, more or less until the hour 4000 that corresponds to June 15th, the temperature in both apartments is mostly under the 26°C, which is an acceptable value according to the ASHARE limit. Likewise, the same behavior of the indoor temperature is presented in the hours before the end of the summer period, from September 8th. It can be said that for those regions, the natural ventilation allows to have a sensible comfort condition, meaning that it is no necessary a cooling system in these two-time intervals.

On the contrary, in the middle time interval from June 16th to September 7th, roughly 2000 hours, the temperature behavior goes to values over the 26°C, even reaching values above the 30°C. In this period, that represents approximately the 69% of the conditioning period, people will need the presence of a cooling system.

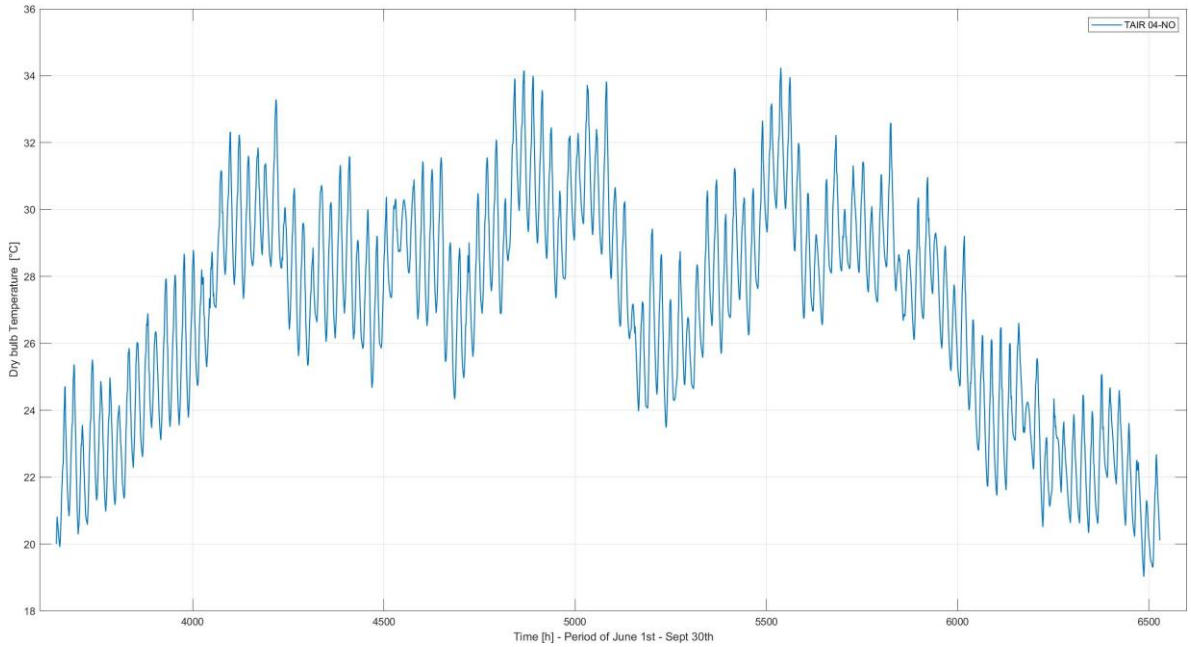

Figure 3.14. Dry bulb temperature profile of apartment 04_NO - Natural ventilation results.

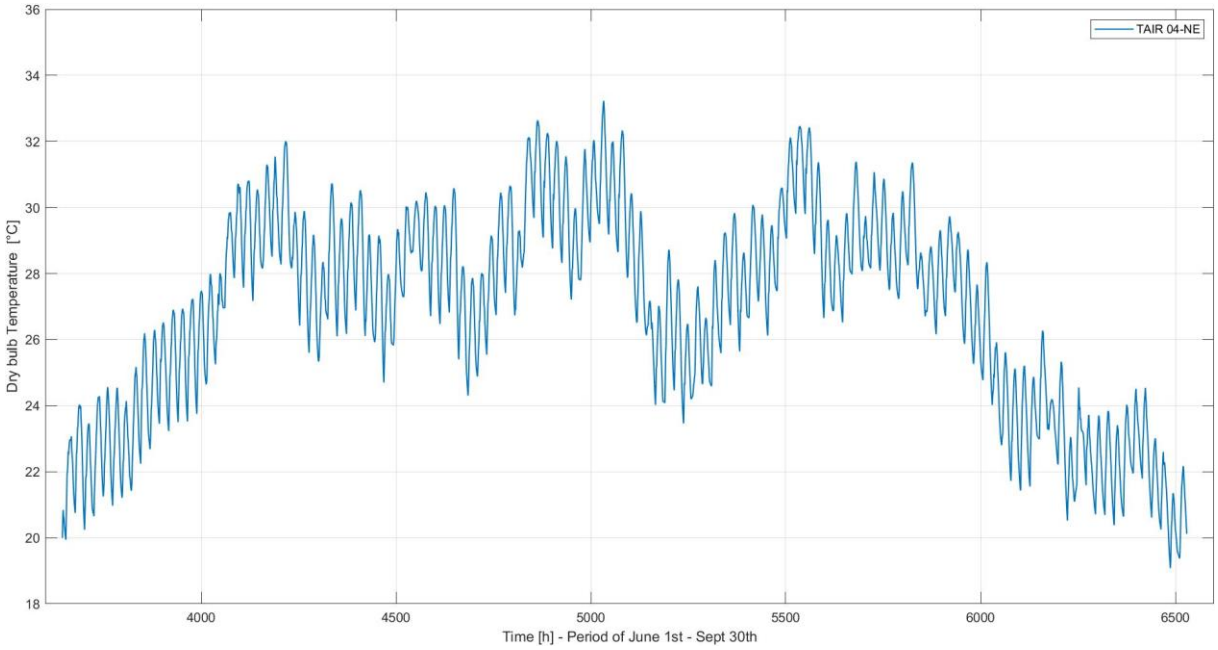

Figure 3.15. Dry bulb temperature profile of apartment 04_NE - Natural ventilation results.

3.4.2. Humidity ratio.

For a humidity comfort condition, corresponding to a dry bulb temperature of 26°C and a relative humidity of 60%, it is necessary to have a humidity ratio around 12.6 g/kg of dry air inside the spaces. Observing Figure 3.16 and Figure 3.17, where it is evidenced the absolute humidity results for the natural ventilation simulation, it can be appreciated that along the whole summer period, there is the presence of humidity

ratios above the reference value; confirming the necessity of having a system capable for reducing the air moisture content.

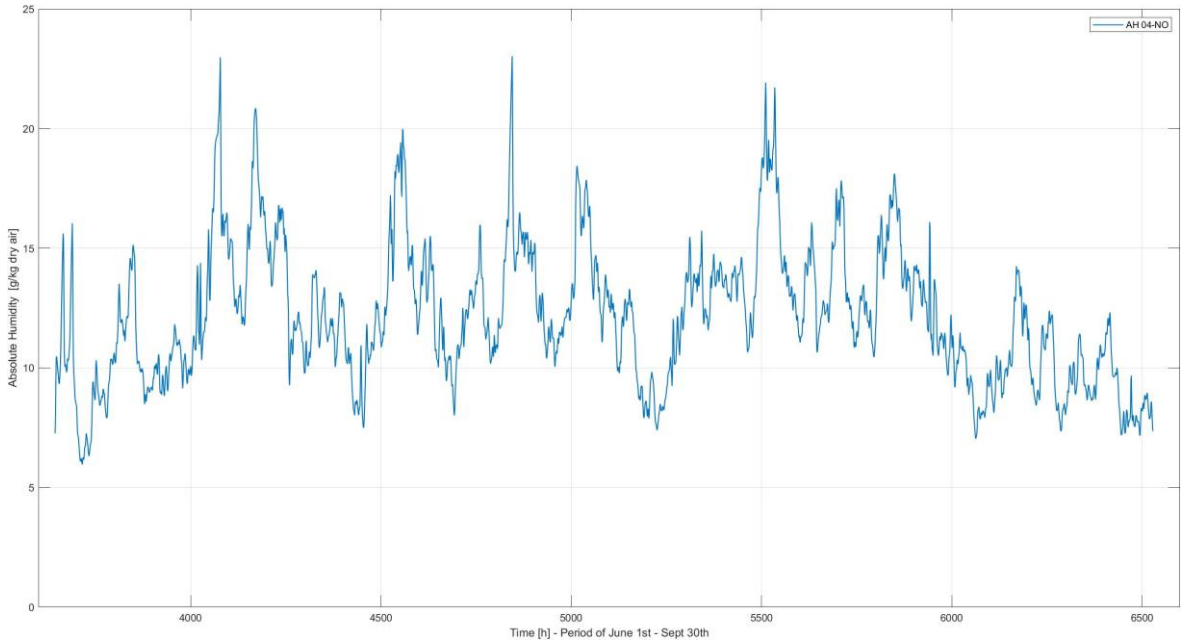

Figure 3.16. Humidity ratio profile of apartment 04_NO - Natural ventilation results.

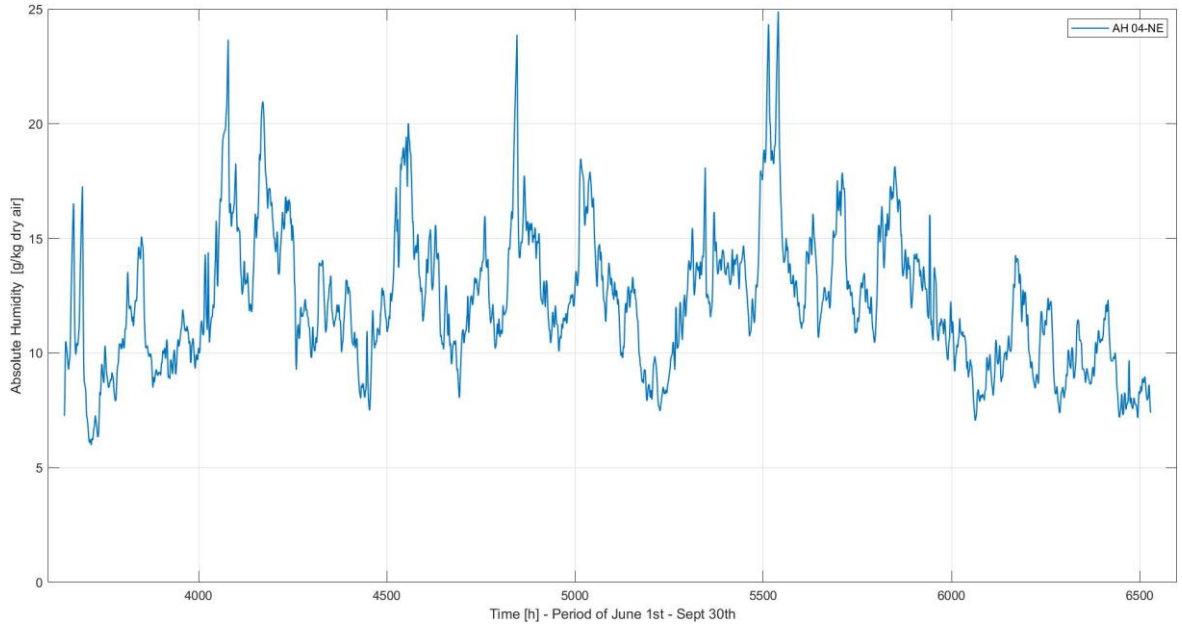

Figure 3.17. Humidity ratio profile of apartment 04_NE - Natural ventilation results.

3.4.3. Comfort conditions.

In order to evaluate whether a certain environmental condition at a specific time is considered as thermal comfort, which is defined as the feeling of satisfaction with the thermal environment in which a person is located [37], it is necessary to determine a range of thermal environmental conditions that are required to achieve acceptance by

a certain percentage of occupants in a considered space. The ASHRAE standard 55-2004 collected a large amount of experimental and field data that gives statistics about conditions in which occupants will find thermally comfortable [37].

The standard considers six main parameters when establishing criteria for thermal comfort. These factors can change over time and the specifications given by the study can be valid for stable conditions [37]. Consequently, individuals entering a space conforming to this standard might not instantly perceive the conditions as comfortable if they have recently encountered different environmental conditions; meaning that there is an influence of prior exposure or activity in the comfort perception for around one hour [37]. The factors are:

1. Metabolic rate
2. Clothing insulation
3. Air temperature
4. Radiant temperature
5. Air speed
6. Humidity

The standard evidenced two comfort zones due to the fact that during the winter and the summer season, people typically wear different clothes. The two regions shown in Figure 3.18 are referred to 0.9 (for winter) and 0.5 (for summer) clo of thermal resistance. Additionally, the comfort condition zones delimited establish that 80% of occupancy will perceive the environment condition as thermally acceptable. [38]

For the purpose of this thesis work, only the summer comfort zone will be considered. Temperature limits are stablished by the constant effective temperature line between 23 and 26 °C. Moreover, humidity ratio limits will be related to the relative humidity curves between 30% and 60%, since values below this range correspond to a possible cause of dryness of the skin and mucous surface; and above it can be annoying, and people may experience a damp sensation on their skin. [38]

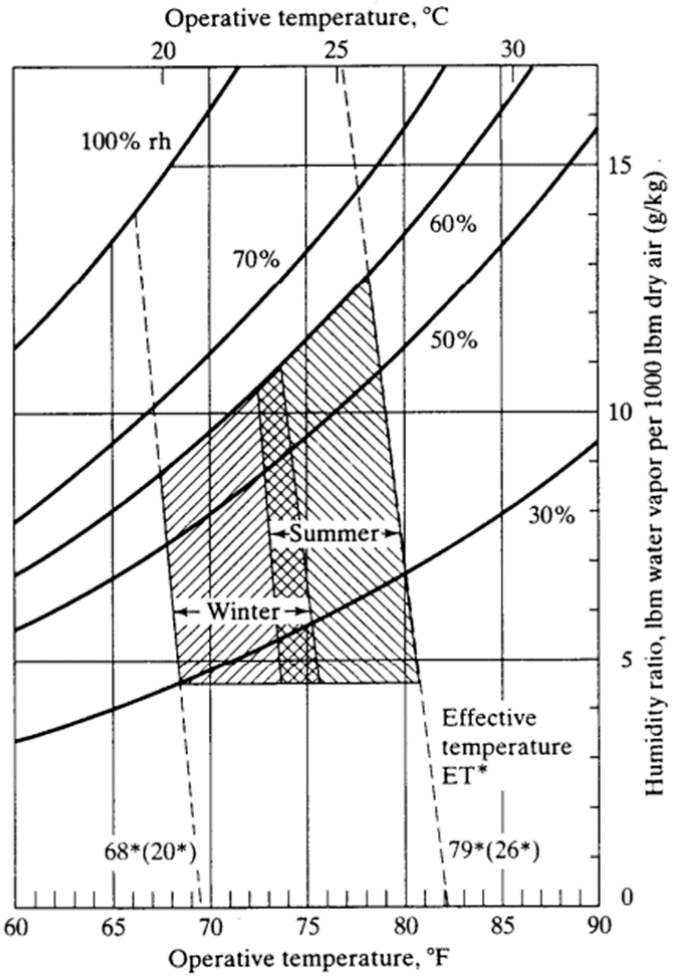

Figure 3.18. ASHRAE Summer and Winter Comfort Zones. [39]

In the context of the outcomes derived from simulations conducted on natural ventilation, an in-depth analysis was carried out to assess various conditions; these conditions were plotted on the psychometric chart, which is a tool for representing the air conditions considering its moisture content, evidencing the comfort thermal zone defined by the ASHRAE. This kind of representation allows to have a compressive understanding of the hours that are considered as comfort conditions if there is only used the natural ventilation as the source for satisfying the latent and sensible demand in the conditioned period. The results are illustrated in Figure 3.19 where all the conditions for the six apartments at the fourth floor are shown; The analysis of these results reveals that, while some data points fall within the thermal comfort zone, a majority of them lie outside this range. Notably, many data points are situated on the right side of the comfort zone, signifying a substantial number of hours during which occupants are exposed to elevated temperatures within the dwellings.

It may be tempting to assume that the relative humidity range is met, implying humidity comfort within the space. However, it is crucial to acknowledge that relative humidity is a variable dependent on both temperature and humidity ratio. A closer

examination of the graphs reveals a significant portion of data points with a humidity ratio exceeding 12.6 g/kg dry air, indicating a substantial moisture content in the indoor air.

Moreover, Table 3.6 supplements these findings by presenting a breakdown of hours with distinct requirements. This table outlines the hours necessitating dehumidification or cooling, along with the hours in which a comfort condition is achieved across various apartments within the building.

During the annual period spanning from June 1st to September 30th, approximately 23% of the hours exhibit an acceptable thermal condition as defined by ASHRAE's Thermal Environmental Conditions for Human Occupancy. Notably, this percentage remains relatively stable across apartments, irrespective of their orientation.

Furthermore, it is observed that, on average, around 55% of the hours necessitate additional cooling despite the presence of fresh air circulation. This percentage tends to increase notably for dwellings situated on the third and fourth floors, primarily due to the elevated outdoor temperatures during these hours.

Another important aspect is the necessity to reduce the humidity in the air, approximately 27% of the considered time interval presents a higher moisture content that exceeds the stablished limits. Interestingly, the requirement for dehumidification is more pronounced for residences on the first floor. This phenomenon can be attributed to the lower temperature profile in these housing units, leading to higher relative humidity levels for the same absolute humidity content.

Table 3.6. Comfort hours for the natural ventilation simulations.

Apartments	01_NE	01_E	01_SE	01_SO	01_O	01_NO	03_NE	03_E	03_SE
Deh. Required	989	839	955	943	829	915	767	579	778
Cooling Required	1438	1615	1391	1458	1604	1486	1617	1769	1521
Comfort hours	692	695	728	699	683	686	655	664	700
No Comfort	2194	2191	2158	2187	2203	2200	2231	2222	2186

Apartments	03_SO	03_O	03_NO	04_NE	04_E	04_SE	04_SO	04_O	04_NO
Deh. Required	749	592	713	800	630	805	792	631	748
Cooling Required	1610	1773	1633	1596	1754	1519	1591	1754	1602
Comfort hours	671	635	648	666	672	686	660	652	672
No Comfort	2215	2251	2238	2220	2214	2200	2226	2234	2214

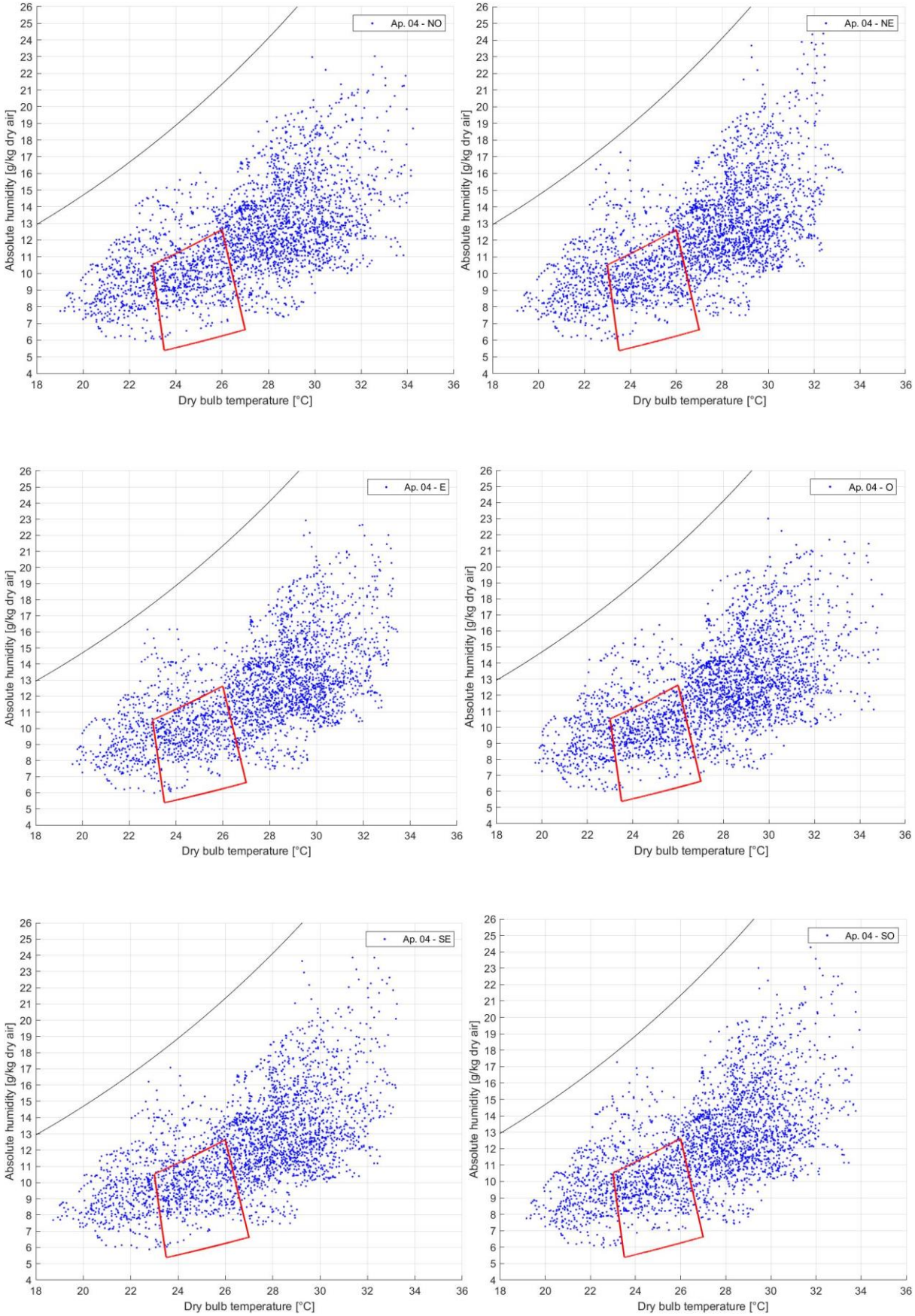

Figure 3.19. Natural ventilation results presented in the psychometric chat.

4 Chapter four: Desiccant Evaporative Cooling Model.

The current chapter will be dedicated to evidence the different assumptions, equations, conditions, operation mode and other aspect related to the modelling of the desiccant cooling system proposed for satisfying the total energy demand of the building studied.

The system consists of a ventilation mode DEC configuration composed by one silica gel desiccant wheel, a sensible rotary heat recovery, an air to water cooling coil, a air to water heating coil for regeneration, and a humidifier.

In principle, the system takes the outdoor air (process air) and force it to pass through the desiccant wheel, that reduce the moisture content of the fluid until a desired value. Them a pre-cooling stage for the process air takes place in the sensible rotary heat recovery, taking advantage of the return air temperature (secondary fluid). Before going into the indoor spaces, a further cooling step is carried out in the cooling coil for achieving a desired supply temperature.

Furthermore, in order to operate cyclically the system, after exchanging heat and mass with the different spaces, the indoor air is taken as a return air, which first goes into the humidifier for performing an evaporative cooling, them it passes through the rotary heat recovery for a pre-heating of and before entering in the desiccant wheel for removing moisture from the desiccant structure, it is regenerated in the heating coil, where temperature is increased. The previous process steps are reported in Figure 4.2 over the psychometric char.

Moreover, it can be said, that the study considers a whole system for supplying the entire building. So, the supply stream, after being treated in the desiccant system, is divided in different air mass flow rate for each apartment. Additionally, the model of the system is developed in a MATLAB code that will be interconnected with the TRNSYS file. In Figure 4.1, there is a schematic representation of the system with the different components evidencing the different state point before and after.

All the variable meaning involved in the system that are reported in Figure 4.1 and Figure 4.2 can be found in the symbols table at the end of the document.

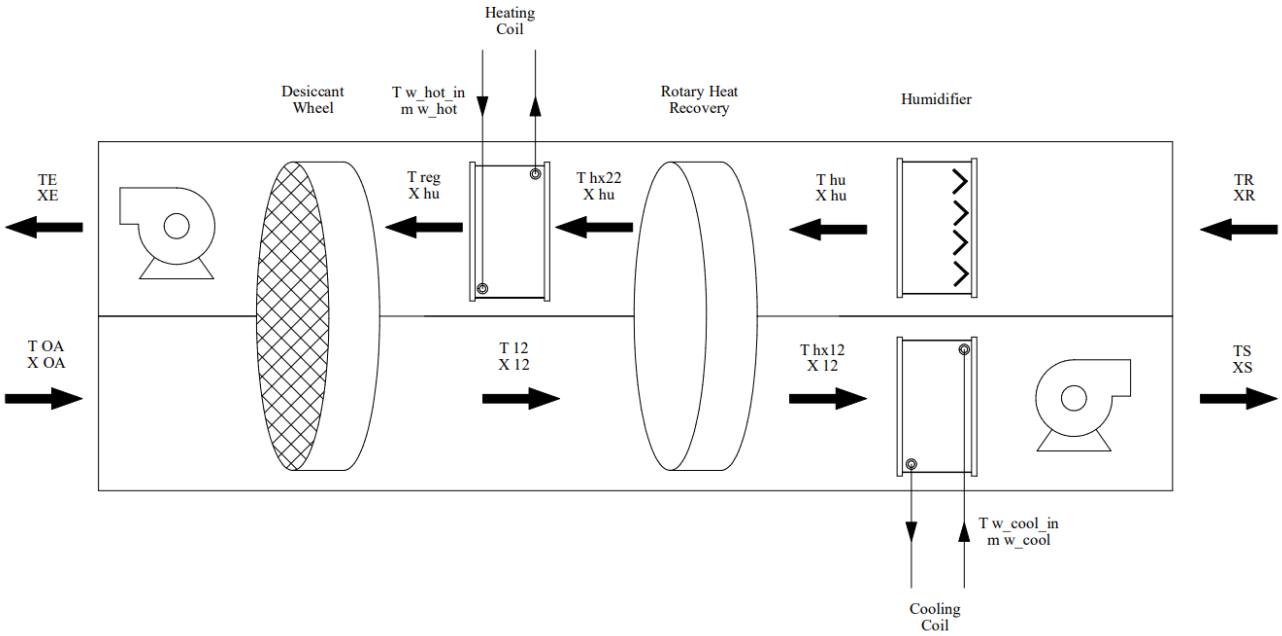

Figure 4.1. Desiccant system proposed.

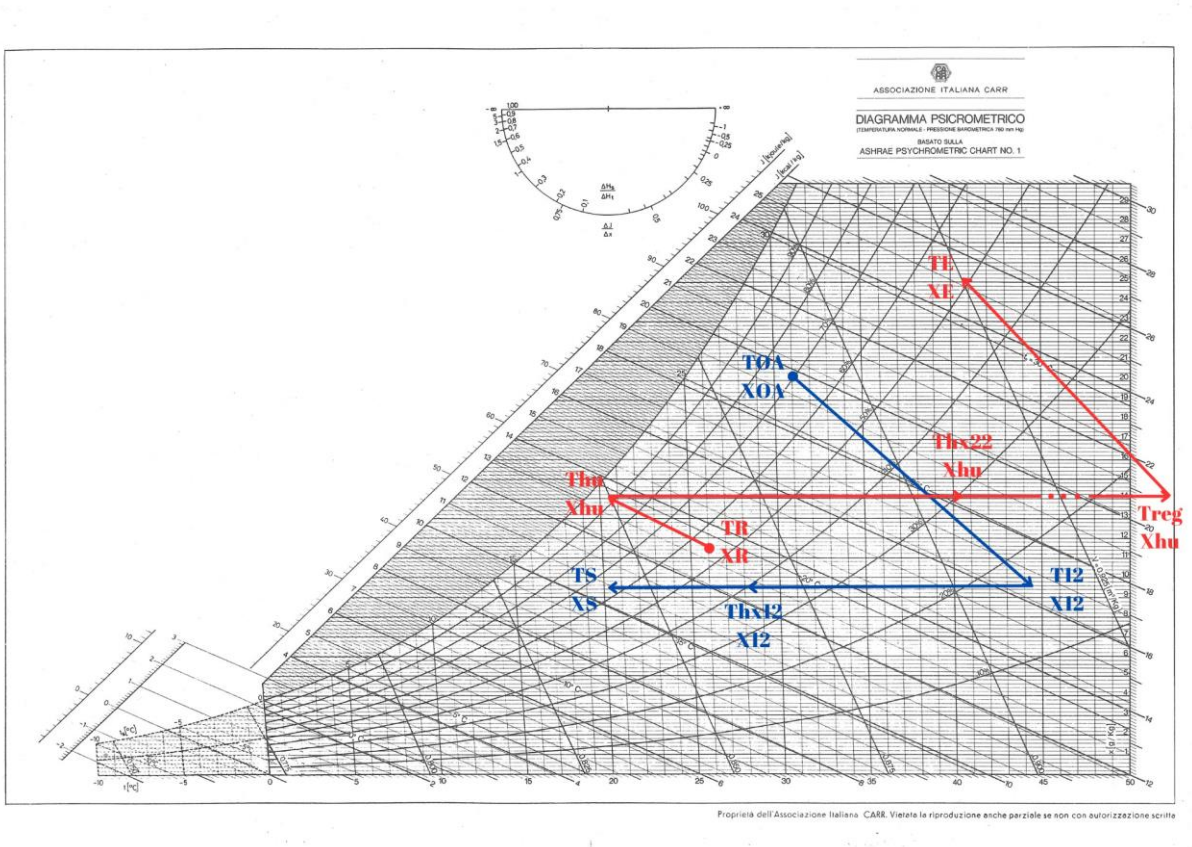

Figure 4.2. Representation of the process steps in the psychrometric chart.

4.1. Desiccant Wheel.

For the modeling of the desiccant wheel, it is considered a mathematical model, developed by Stabat and Marchio, that simplifies the heat and mass transfer partial differential equations with a good accuracy and giving the possibility of characterizing the equipment under all the operating conditions with low computational time. The model was compared with experimental and manufactures data providing good results. [40]. The model presents the following assumptions:

1. The axial heat conduction and water vapor diffusion in the air are neglected.

2. The diffusion and capillarity in the desiccant matrix are assumed to be negligible in the axial direction (z);

3. The temperature and humidity ratio gradients in the radial direction (r) are neglected, otherwise T = T (z, a) and w = w (z, a) are independent of the wheel radius;

4. The sorption is supposed without hysteresis.

5. The pressure drop in the wheel is neglected.

6. The inlet air temperature and humidity ratio are uniform.

7. The channels have all the same geometry.

8. The thermos physical properties of the matrix, the air and water vapor are constant in all the operating conditions.

9. The conditions are in steady state.

They present the dimensionless mass and heat transfer balance equations in a small volume element of the wheel, the equations employed goes from (2) to (5):

- Dimensionless variables:

$$\tau = \frac{\dot{m}_a t}{Md} \quad (2)$$

$$X = \frac{z}{L} \quad (3)$$

- Mass transfer equation

$$\frac{\partial W}{\partial \tau} = \frac{h_m A}{\dot{m}_a} * (w_a - w_{eq}) \quad (4)$$

- Energy conservation equations:

$$\frac{\partial H}{\partial \tau} = \frac{h_m A}{\dot{m}_a} * (w_a - w_{eq}) * (h_{fg} - C_{pa} T_a) + \frac{h_c A}{\dot{m}_a} * (T_a - T_m) \quad (5)$$

Taking into account that the previous equations are hyperbolic expressions, the characteristic method is used as the technique for solving them and obtaining similar equations to those of a rotary heat transfer equation. They transform the expressions to a set of uncouple wave equations by introducing the potential functions [40]. Then, an analogy for adapting the model for building simulation tools is introduced by choosing the following potential functions, expressed in equations (6) and (7), that are suitable for silica gel rotors:

$$F_1 = h \tag{6}$$

$$F_2 = \frac{(273.15 + T)^{1.5}}{6360} - 1.1w^{0.08} \tag{7}$$

At the end, the two effectiveness, considering the points of Figure 4.1, are defined in terms of the potential function as presented in equations (8) and (9):

$$\varepsilon_1 = \frac{F_{1,OA} - F_{1,12}}{F_{1,OA} - F_{1,reg}} \tag{8}$$

$$\varepsilon_2 = \frac{F_{2,OA} - F_{2,12}}{F_{2,OA} - F_{1,reg}} \tag{9}$$

The MATLAB code find the solution for point "12", that satisfy the expressions (8) and (9) by knowing the conditions of "OA" (outdoor air), "reg" (regeneration point) and keeping constant the effectiveness ε_1 and ε_2. As stablished in the study, the first effectiveness should be close to 0.1, while the second effectiveness around 0.8 [40]. For the purpose of this thesis, it will be considered ε_1= 0.126 and $\varepsilon_2 = 0.737$.

4.2. Cooling coil.

For the cooling coil, it is considered an air to water heat exchanger and equations are referred to the ε-NTU method. The effectiveness of cooling coil is calculated by using equation (10) and for the preliminary simulation it is decided to be 0.52153 and constant.

$$\varepsilon = \frac{\dot{m}_a C_{pa}(Thx_{12} - TS)}{\min[\dot{m}_a C_{pa}; \dot{m}_w C_{pw}] * (Thx_{12} - Tw\ cool_{in})} \tag{10}$$

Groundwater is considered to provide the cooling effect in the cooling coil. The temperature of the water depends on the heat transfer phenomena that occurs underground, so it depends on the temperature variation of the ground.

In order to obtain the vertical variation of the soil temperature, Trnsys TYPE77 (Simple Ground Temperarure Model) was used. This type is based on the Kusuda model which

is an analytical model that allows to calculate with good accuracy the vertical variation of the soil temperature as a function of the site weather, time of the year, soil thermal properties and depth [41]. The correlation developed by Kusuda is reported in equation (11):

$$T_{z,t} = T_{mean} - T_{amp} * exp\left(-z * \left(\frac{\pi}{365 * \alpha_s}\right)^{0.5}\right) * cos\left(\frac{2\pi}{365} * \left(t_{now} - t_{shift} - \frac{z}{2} * \left(\frac{365}{\pi * \alpha_s}\right)^{0.5}\right)\right) \quad (11)$$

Kusuda found that T_{mean} can be approximated to the average annual air temperature for the given location, which in our case corresponds to the city of Milan. Tamp is calculated as suggested by Trnsys type documentation as half the difference between the maximum and minimum monthly average temperatures over the year [42].

Soil thermal diffusivity is calculated considering the soil as a continuous medium with uniform thermal properties, according to equation (12):

$$\alpha_s = \frac{k_s}{\rho_s * Cp_s} \quad (12)$$

Where k, ϱ y Cp are the soil thermal conductivity, soil density and soil specific heat, respectively. These values depend on soil characteristics like moisture, composition of underground layers, surface conditions (ex. Vegetation) and others. Soil properties must be determined by means of soil analysis; however, this procedure is out the scope of this thesis. All the properties considered for the soil modelling were provided to us within the project information and are reported in Table 4.1.

Table 4.1. Soil thermal properties for thermal diffusivity calculation.

Thermal conductivity [W/mK]	Density [kg/m3]	Specific heat capacity [kJ/kgK]
2.42	3200	0.84

A comparison was done as an additional verification considering the values of soil thermal conductivity and soil specific heat reported in ASHRAE handbook. According to ASHRAE, a thermal conductivity equal to 2.16 W/(m*K) must be used for chilled-water systems in the absence of any-site specific soil data. For the specific heat, it is possible to consider the specific heat of dry soil which is nearly constant for all types of soils, and it may be taken as 0.73 kJ/(kg*K) [43]. At this point, it is possible to consider the information provided by the project as an acceptable input for the ground temperature model.

The mean annual air temperature, the amplitude of the surface temperature of the ground and the time shift have been set as 13.35°C, 11.10°C and 13, respectively, according to the weather file for the city of Milan.

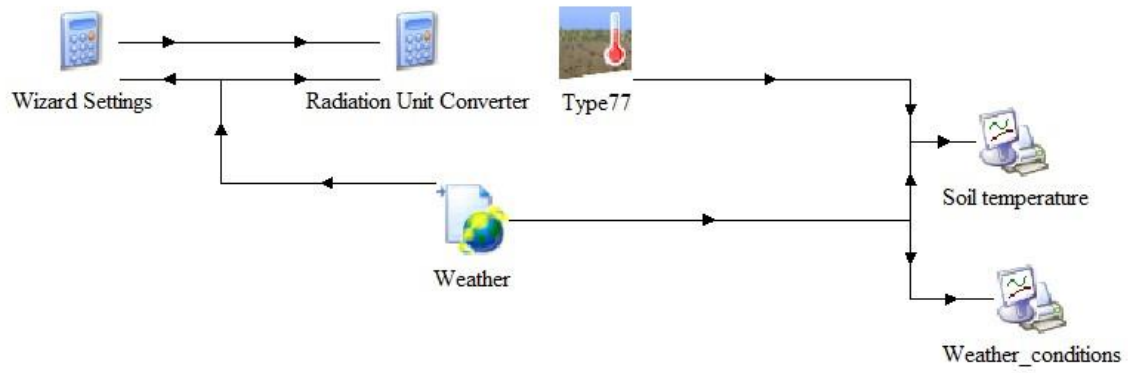

Figure 4.3. TRNSYS model for the simulation of ground thermal behavior.

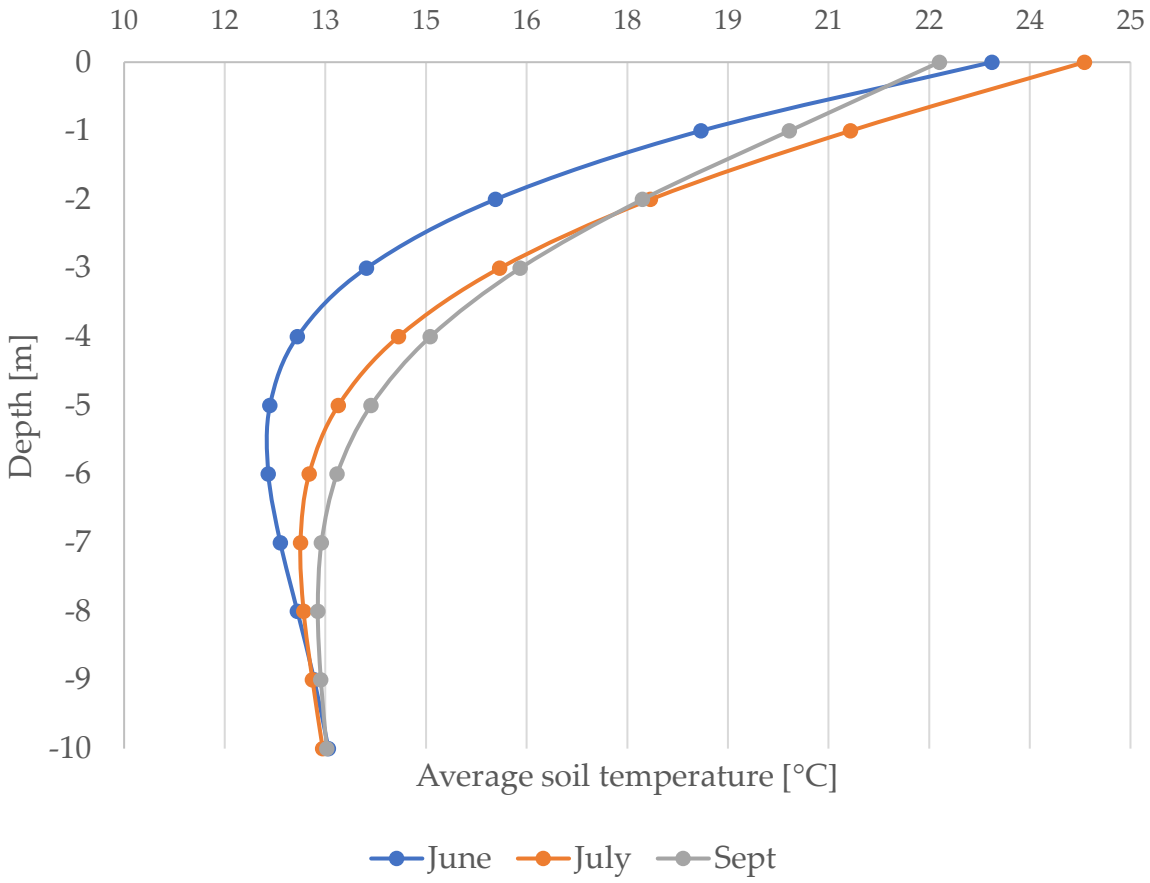

Figure 4.4. Monthly average soil temperature at different depths.

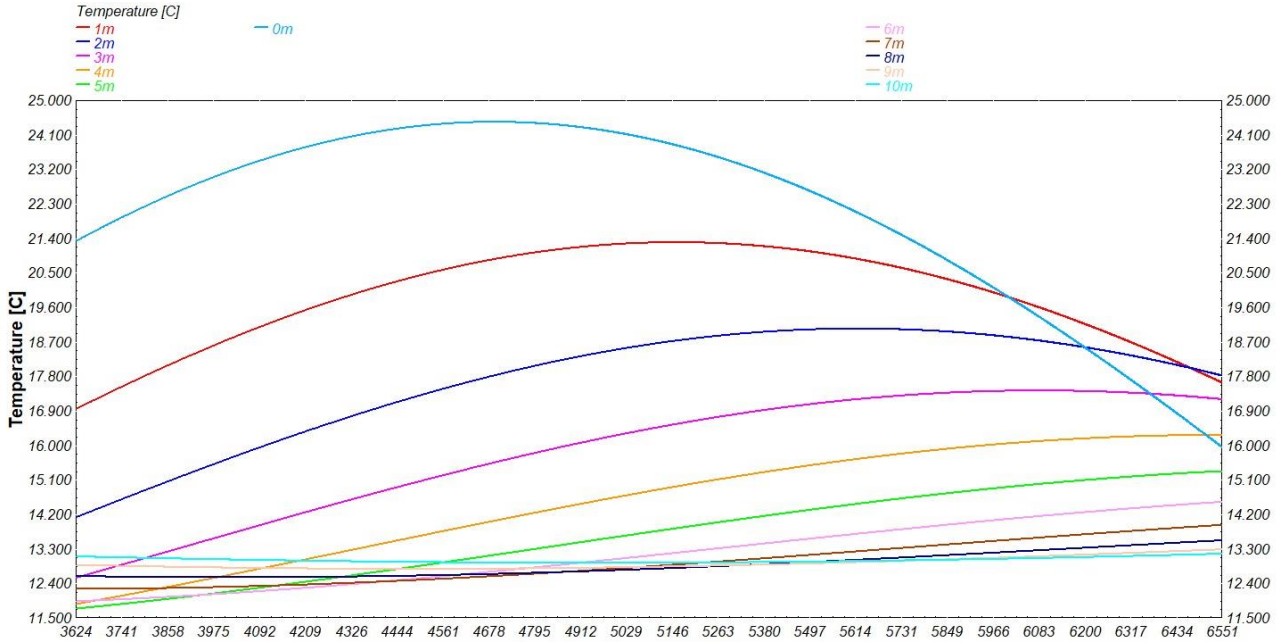

Figure 4.5. Soil temperature variation at different depths between 1st June and 30th September.

The variation of soil temperature respect to air temperature is more significant near the surface, as shown in Figure 4.4 and Figure 4.5. For higher depths, it is possible to observe a reduction in the soil temperature variation. The soil temperature keeps almost constant for depths values higher than 6 meters.

Assuming that groundwater is taken from a 7 meters depth well, we can consider the water temperature equal to soil temperature at the same depth. This is supported by the fact that soil temperature is almost invariable, and its value does not change considerably during the simulation time range. Considering this assumption, to perform the simulation of the DEC system, the input temperature of the groundwater entering the cooling coil is assumed to be 13°C during the cooling period.

4.3. Regeneration coil.

For the heating coil, it is considered an air to water heat exchanger and equations are referred to the ε-NTU method. The effectiveness of the cooling coil is calculated by using equation (10).

$$\varepsilon = \frac{\dot{m}_a C_{pa}(T_{reg} - Thx_{12})}{\min\left[\dot{m}_a C_{pa}; \dot{m}_w C_{pw}\right] * (Tw\ hot_{in} - Thx_{22})} \quad (13)$$

The definition of the inlet water temperature is provided by a district heating based on renewable energy sources ("Teleriscaldamento" in Italian), which provides water at 65 °C, that will be used for the regeneration of the return air stream before entering into the desiccant wheel. This water flow comes from a wasted heat from other process,

but for the desiccant system performs an important role in the regeneration of the desiccant material; In the base case configuration, it is assumed to operate the heating coil with a constant regeneration temperature equals to 58.8 °C in the preliminary case simulation, meaning that the effectiveness and water mass flow rate changes during the operation.

4.4. Humidifier.

For the humidifier device, it is decided to use a direct evaporative cooler for reducing the return air temperature before entering into the heat recovery. Here the main correlations of the components are:

$$Thu = TR - \varepsilon_{hu}(TR - T_{sat}) \quad (14)$$

$$Xhu = XR - \varepsilon_{hu}(XR - X_{sat}) \quad (15)$$

It is pointed out that T_{sat} and X_{sat} in equations (14) and (15) are calculated by means of the psychometric chart expressions considering the enthalpy of the return air stream, which is function of temperature and absolute humidity. The effectiveness of the device is stablished to be 0.8 and constant during operation.

4.5. Heat recovery.

For this component it is considered a sensible rotary heat exchanger with a constant effectiveness of 0.8 during operation. The main expressions of the components are reported in equations (16) and (17):

$$Thx_{12} = T_{12} - \varepsilon_{HR}(T_{12} - Thu) \quad (16)$$

$$Thx_{22} = Thu + \varepsilon_{HR}(T_{12} - Thu) \quad (17)$$

The working principle of the device is based on an indirect heat exchange; during the rotation of the thermal conductive structure, the process air flow rate heats up the half side of component and then thanks to the rotational movement, the hot part is cooled down when it passes through the regeneration air stream.

This component performs an important role in the operation of the system, since it accounts for two positive effects; the first one related to the pre-heating of the regeneration air flow rate, reducing the size of the cooling coil, which means less hot water and electricity consumption. The other one is corelated to the pre-cooling of the process air stream, which help significantly in reducing the cooling coil dimension.

5 Chapter five: Base case - Preliminary simulation results.

In this section, we proceed with the implementation of the previously established desiccant cooling system model, developed within the MATLAB programming language, integrating it with the broader building model in the TRNSYS software.

The principal aim in the current chapter is to conduct a series of simulations, encompassing a range of volumetric air changes per hour (ACH), in order to assess the system's capacity to effectively address both dehumidification and cooling demands throughout the conditioned period. The primary objective for performing this study is to identify a narrow band of air mass flow rates that the system must handle in order to achieve a higher number of comfort thermal conditions in comparison with the natural ventilation reference scenario.

Additionally, establishing an optimal volumetric flow rate will be helpful for the sizing of the main components of the system and setting up the nominal and partial working condition for each device. Table 5.1 delineates the four simulation cases carried out for various air changes per hour; starting from a minimum air change hourly stipulated by the normative UNI 10339 for residential building, considering living rooms and bedrooms, equals to 0.5. The analysis extends to an upper limit equal to 2.0 ACH for avoiding the over-dimension of the system. It is imperative to note that increasing the ACH means increasing the dimension of all the component involved in the proposed system; thereby giving rise to an increment of the maintenance expenses, the initial investment costs, and the energy consumption during system operation such as electricity consumption for operating the pumps, fans, and other electrical devices.

Hence, it becomes evident the needs for finding a compromise between optimizing thermal performance to ensure indoor thermal comfort and preserving the economic viability of the system. This chapter is particularly dedicated to find the minimum air flow rate range required to obtain a substantial number of thermal comfort hours in order to avoid oversizing of the components that could increment the cost of the proposed system.

Table 5.1. Air flow rates for the different Air changes per hour.

Air changes per hour	ACH= 0.5	ACH= 1.2	ACH= 1.6	ACH= 2.0
Air flow per floor [m3/h]	473.44	1136.25	1515.00	1893.75
Total air flow [m3/h]	1893.75	4545.00	6060.01	7575.01

Table 5.2. Air flow share for the different apartments.

Apartment	Volume [m3]	Volume share [-]	Total air flow share [-]	Total Volume [m3]
E	148.4	0.1567	0.0392	593.6
SO	117.6	0.1242	0.0310	470.4
O	109.228	0.1154	0.0288	436.912
NO	225.568	0.2382	0.0596	902.272
NE	219.24	0.2315	0.0579	876.96
SE	126.84	0.1340	0.0335	507.36
Total	946.876	1.0000	0.2500	3787.504

Before entering into the discussion of the results, a series of relevant aspects, that were considered for the operation of the system, are reported below.

As mentioned in the previous chapter, the system supplies the entire building, hence it is necessary to determine the amount of air flow rate that correspond for each residence. In Table 5.2 there are the air flow rate shares corresponding to the diverse typology of apartments since they have the same dimensions over all the floors. This indicator allows to stablish the quantity of supply air that enters into each apartment according to its volume portion of the entire structure.

Another important aspect is the calculation of the return air temperature and humidity ratio. It is known that the orientation of the apartments is different, and as a consequence the thermal demand varies from apartment to apartment. Although, the supply condition of the process air is equal for all the residence, because of its orientation and internal gains, the return air conditions will not be same. Energy and mass balance, bases on proportionality constants, as reported in equation (18) and (19), enable to calculate the right condition arriving on the desiccant system.

$$TR = \sum_{i=1}^{19} \frac{flow\ rate_i}{Total\ flow\ rate} * TR_i \quad (18)$$

$$XR = \sum_{i=1}^{19} \frac{flow\ rate_i}{Total\ flow\ rate} * XR_i \quad (19)$$

Where the subscript "i" accounts for the value of the indicated variable in the reference apartment "i" of the building.

Furthermore, in this group of simulation, all the components are always working at the nominal conditions described in the chapter 4 meaning that they are always in the ON state regardless the external or internal conditions. Summarizing: The Desiccant wheel operates with the nominal regeneration temperature of 58.8 °C; the heating coil works at constant air outlet temperature indicating that the water mass flow rate varies

to obtain this temperature in function of the inlet air temperature (Thx22). Moreover, the cooling coil, the heat recovery and the humidifier operate at constant effectiveness signifying that the outlet temperature depends on the inlet condition.

Unlike the reference scenario of natural ventilation studied in section 3.4, where the windows were open during the summer period; in this case the windows are assumed to be always closed denoting the desiccant cooling system as the only source for performing the indoor air exchange that must overcome the sensible and latent load, in addition to guaranteeing the indoor air quality.

Beginning with the temperature results, Figure 5.1 illustrates the profiles over the entire conditioned time interval. In general terms, the four profiles follow the same waveforms but with different temperatures levels due to the variation in the amount of treated air. For the case of 0.5 ACH, it can be observed that even if it is supplied fresh air with a temperature around 18-20°C, the mass air flow rate is not enough for dealing with the cooling demand. In fact, from June 19th to September 7th, the residence indoor temperature is above the 30°C, a value completely outside the comfort range previously defined in section 3.4.3. This result may give an indication that the air flow rate necessary to ensure indoor air quality, according to the UNI 10339 standard, can be enough for avoiding the air pollution, but it is insufficient to manage the sensible thermal load.

As expected, once the ACH begins to increase, the return temperature condition decreases reaching values within the comfort zone ranges. For ACH values greater than 1.2, the condition arriving on the system starts to decrease below the 26 °C, which is a more favorable condition for being inside the thermal comfort zone.

Additionally, it can be also appreciated from Figure 5.1, that for the case whit the higher ACH, the internal condition rarely exceeds 24°C during the conditioned period, which means that choosing this condition as the optimal one, can lead to an oversizing of the cooling coil because larger values of the internal temperature can be accepted. In fact, for ACH equals to 2.0, the average summer return temperature is around 22°C, a condition that is below the lower temperature limit of the ASHARE comfort zone.

It seems to be that from the sensible point of view, the cases with ACH between 1.2 and 1.6 present the best operating temperature points. On average, the temperature conditions are in the range of 23.5 and 25°C when ACH is equal to 1.6 and 1.2, respectively. These preliminary results give insight that, during nominal operation, choosing an ACH between this range provides significant indoor temperatures that are reasonable with the thermal comfort requirements.

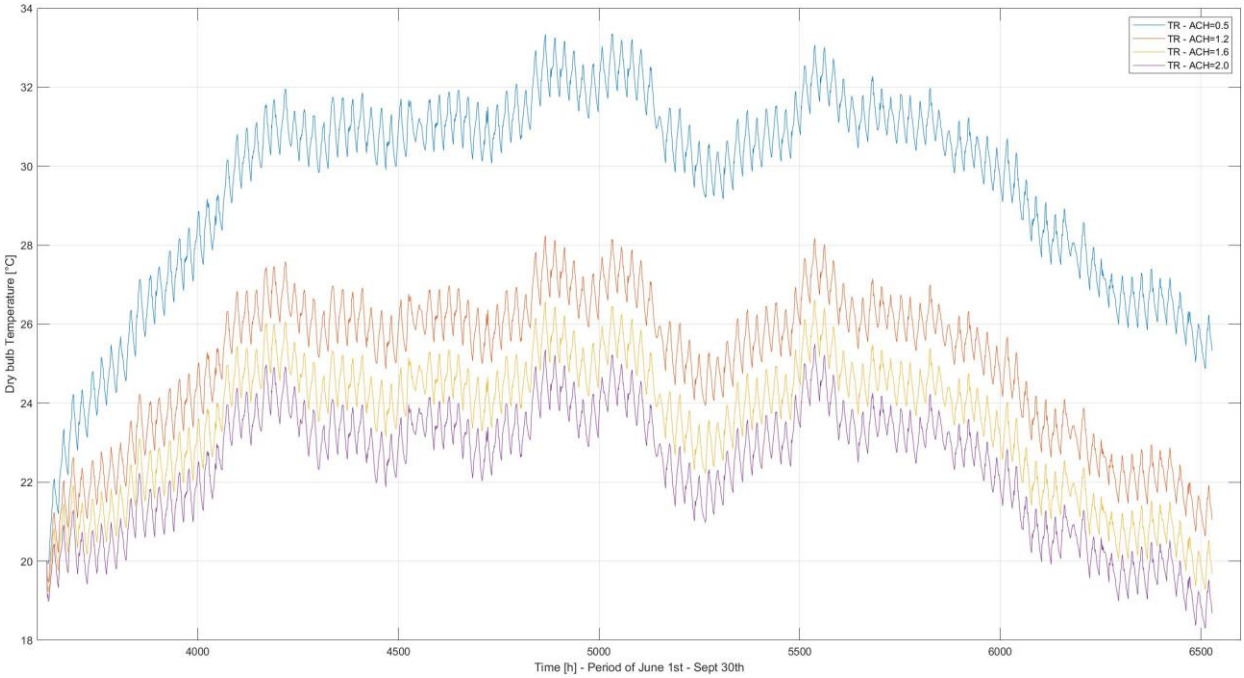

Figure 5.1. Return air temperature profiles for the different ACH in the preliminary results simulation of the model.

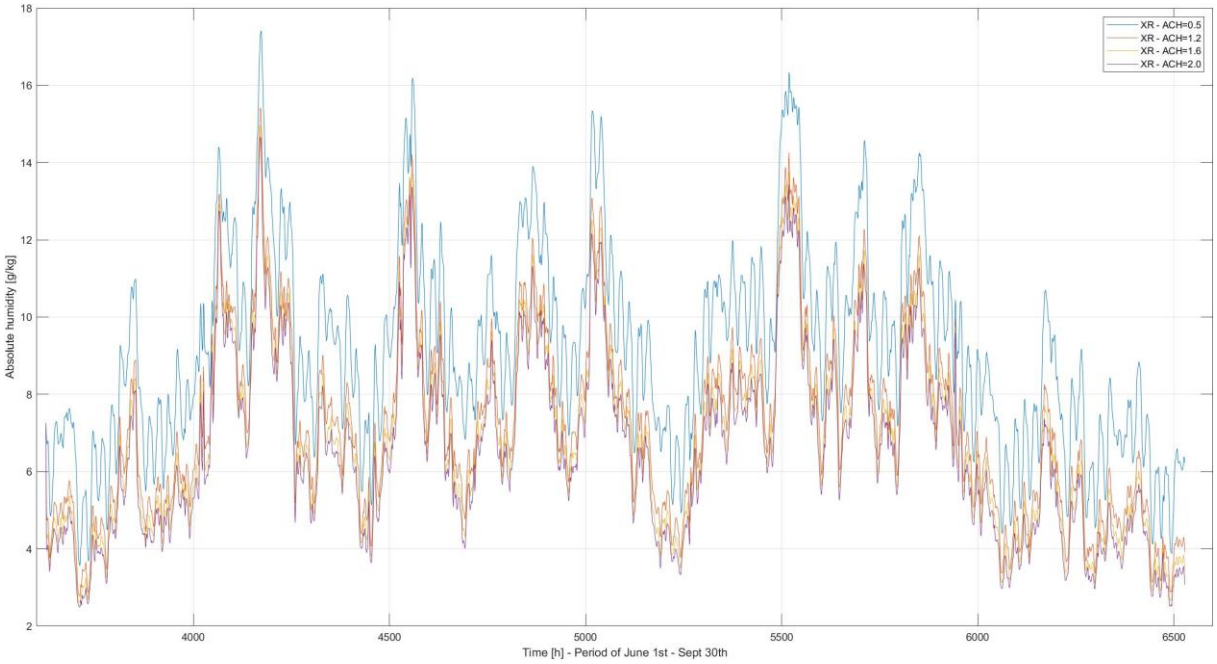

Figure 5.2. Return air absolute humidity profiles for the different ACH in the preliminary results simulation of the model.

Moving forward in the analysis, the comfort condition is not only dependent of the temperature value, but it is also necessary to consider the return humidity ratio profiles, that are presented in the Figure 5.2. In this graph can be observed that for lower values of ACH, the return absolute humidity is higher, which is an expected result because the air is exchanging mass with the latent load in the residences, since the system is supplying less quantity of air, the moisture content in the air will be

higher; On the contrary when the air mass flow rate increases, the same latent demand will be contained in more air, so the humidity ratio will decrease.

If it is taken as a reference the limiting comfort condition defined by the UNI-TS 11300 of 26°C in temperature and 60 % of relative humidity, this condition corresponds to a humidity ratio of 12.6 g/kg of dry air. Having in mind the previous threshold and looking at the Figure 5.2, it is noted that rarely the humidity goes over this value, the points exceeding the limit may correspond to rainy days during the summer period, where the moisture content in air is extremely higher and not even at nominal operation of the desiccant wheel can reduce the humidity until a value below the limited stablished. But, in general, for cases of ACH over 1.2, the humidity ratio does not exceed the 15 g/kg of dry air, which is a value not so far from the minimum required value.

On the order hand, in some regions during the conditioned period, the return air humidity profiles present values lower than 6 g/kg of dry air, meaning that the indoor conditions are located below the lower humidity limit of the ASHRAE thermal comfort zone. In those points the operation of the desiccant wheel must be regulated for avoiding the feeling of dryness in the individuals inside the building.

Trying to represent both profiles in the same graph, it can be used the psychrometric chart, for evaluating the different simulation cases in terms of how many hours of the indoor condition, are inside the thermal comfort zone. From Figure 5.3 to Figure 5.6, it can be visually appreciated the outcome conditions for the diverse ACH considered and how they are distributed in the psychrometric chart.

In the context where the Air Changes per Hour (ACH) equals 0.5, observations reveal a predominant concentration of data points within the right-hand portion of the thermal comfort zone (Figure 5.3); this signifies that indoor temperatures generally exceed the prescribed acceptable range. On the other hand, the humidity level is in a significant portion maintained below 13 g/kg, indicating an effective performance in terms of dehumidifying the outdoor air stream. Additionally, as can be read from Table 5.3, only a limited number of hours fall within the comfort zone across the apartment units. On average, just 11.39% of the total conditioned time interval aligns with the comfort criteria. As a consequence, even if the 0.5 ACH case presents remarkable humidity results, this simulation is discarded because of the incapacity of the to meet the sensible cooling demand, since it was already working at its nominal condition.

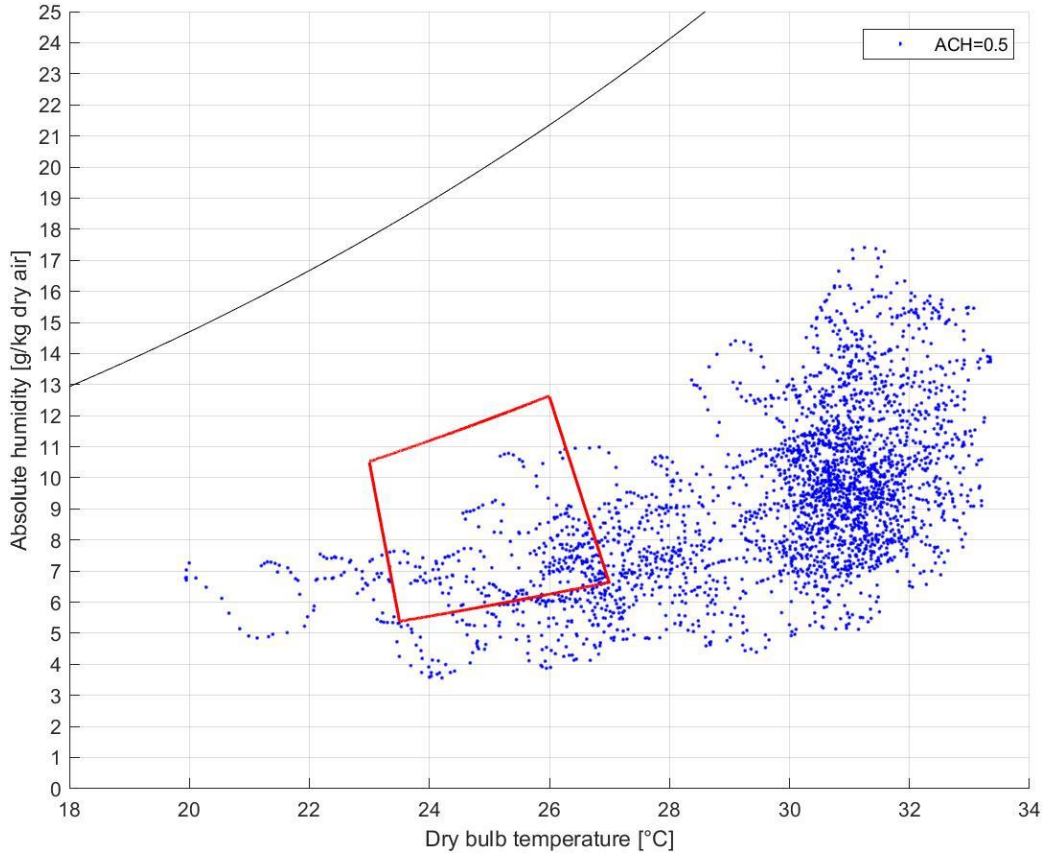

Figure 5.3. Indoor residence conditions for the preliminary results simulation. Case ACH 0.5

For the case of 2.0 ACH, the system presents an excess of sensible cooling, since the indoor conditions are located in the left side of thermal comfort zone (Figure 5.6); and a good performance in terms of managing the dehumidification load. Table 5.3 evidences, in general, that the comfort conditions are above the 1000 hours; and on average, this simulation gives a percentage of 37.26% of interior comfort states, this fraction can be increased by improving the control strategy of the system for working in partial load conditions, but it would mean that most of the time, the system would be working at partial load; hence choosing this ACH value will lead to an oversizing of the components that will raise the exercise costs.

Analyzing the intermediate cases, ACH of 1.2 and 1.6, illustrated in Figure 5.4 and Figure 5.5 respectively, it can be observed a considerably greater concentration of indoor conditions inside the ASHRAE thermal comfort zone. In fact, on average terms, they provide comfort for the internal ambient conditions by 51.84% (1.2 ACH) and 55.68% (1.6 ACH) of the period of the year between June 1st and September 30th. Both cases represent an optimal range for defining the mass flow rate of the system since they are able to deal with the sensible and latent demand of the building and avoiding the indoor air pollution and overestimation of the mechanical components involved. It will be a decision of designer to choose the most suitable value based on a slightly higher thermal performance or a moderately lower operating cost, depending on the needs.

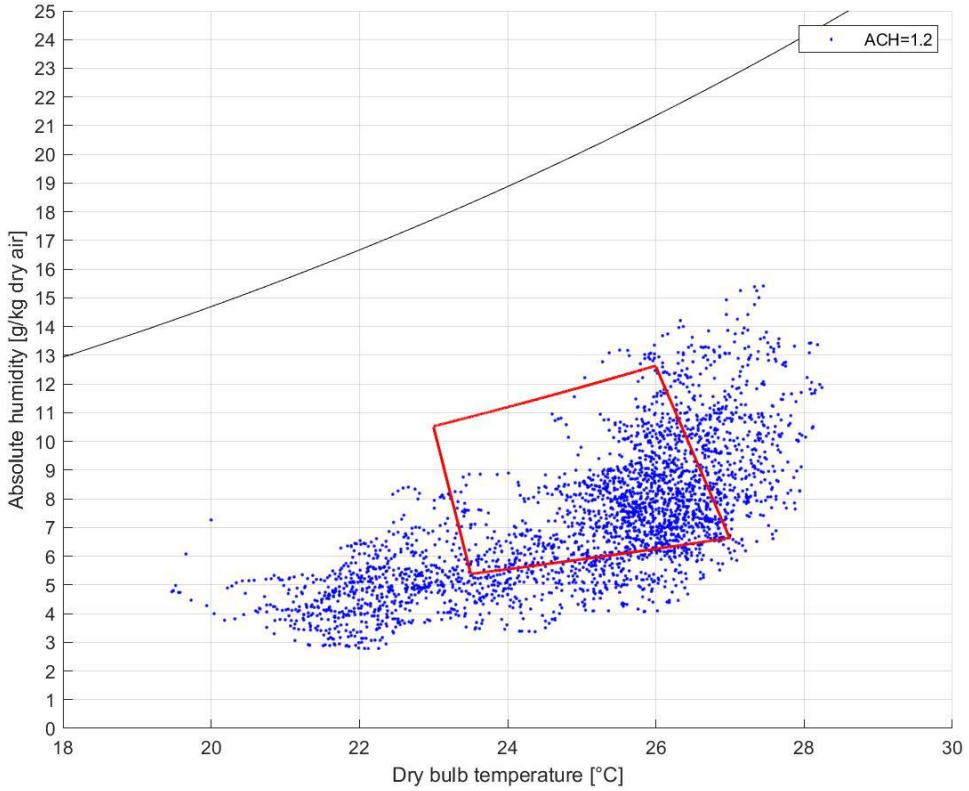

Figure 5.4. Indoor residence conditions for the preliminary results simulation. Case ACH 1.2

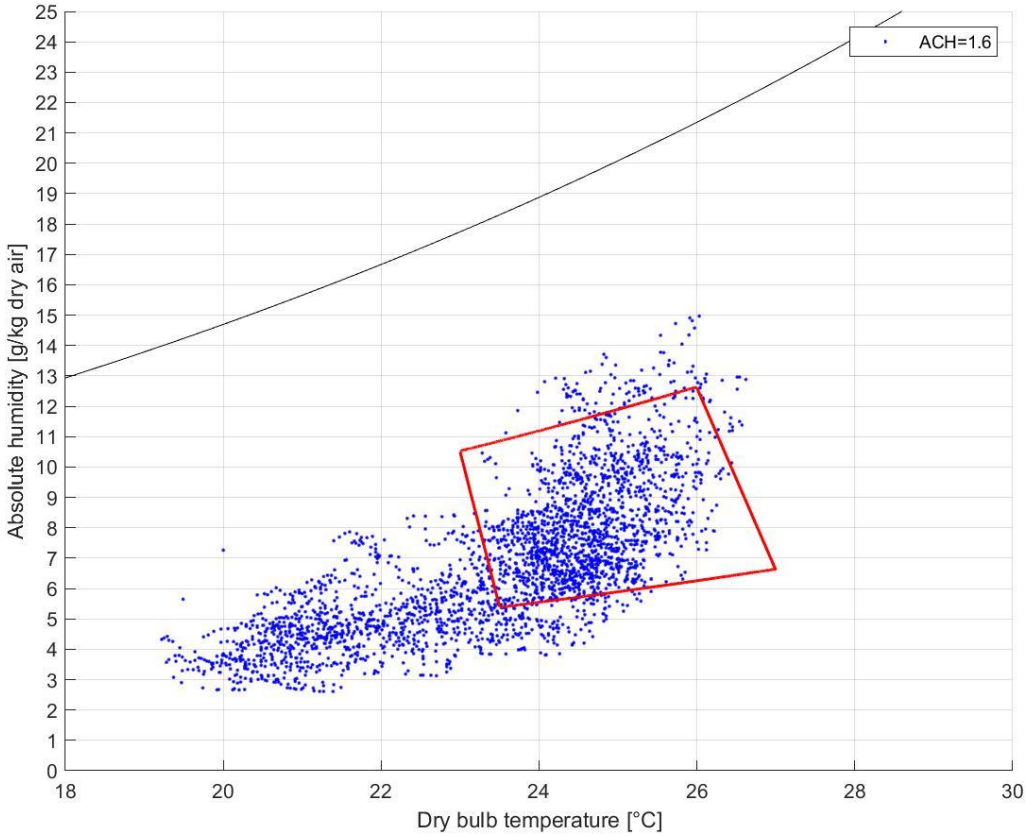

Figure 5.5. Indoor residence conditions for the preliminary results simulation. Case ACH 1.6.

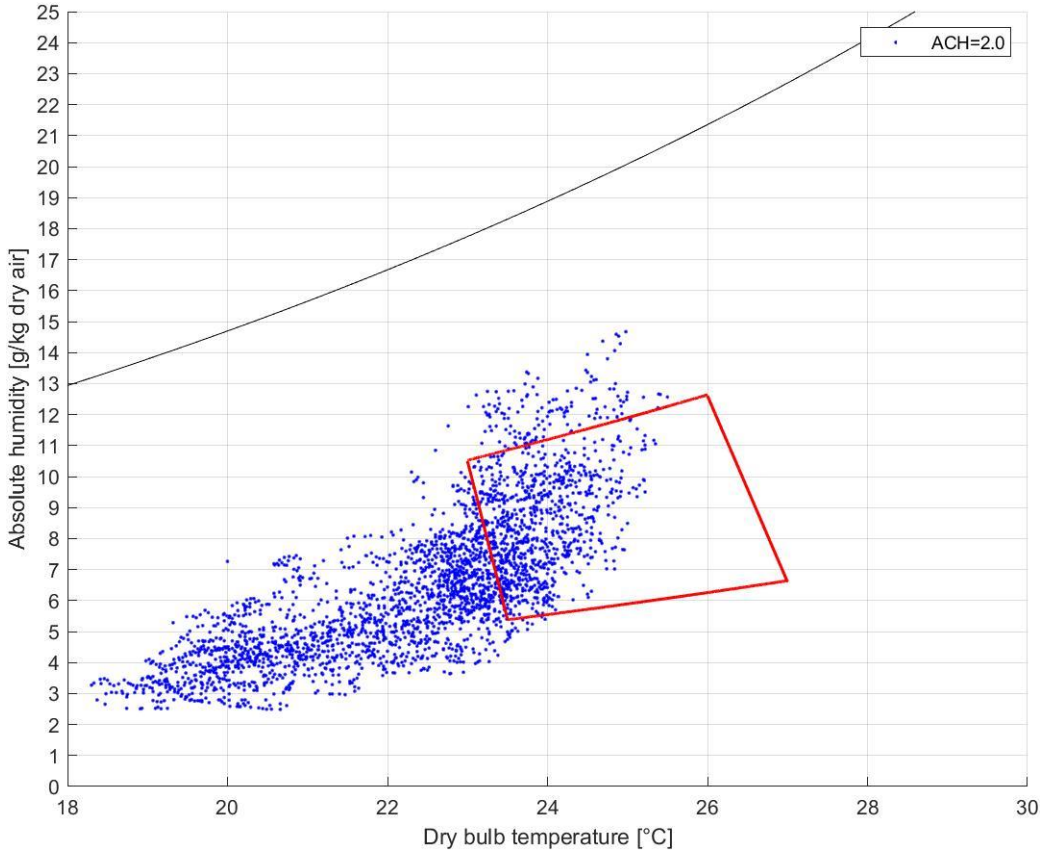

Figure 5.6. Indoor residence conditions for the preliminary results simulation. Case ACH 2.0.

Table 5.3. Comfort hours for the different ACH cases in the conditioned period.

Apartments	01_NE	01_E	01_SE	01_SO	01_O	01_NO	03_NE	03_E	03_SE
ACH = 0.5	546	381	448	519	451	502	270	123	195
ACH = 1.2	1794	1716	1679	1754	1711	1735	1694	1392	1358
ACH = 1.6	1450	1589	1637	1564	1618	1602	1596	1690	1691
ACH = 2.0	484	890	1114	870	947	870	809	1234	1351

Apartments	03_SO	03_O	03_NO	04_NE	04_E	04_SE	04_SO	04_O	04_NO
ACH = 0.5	312	184	253	330	217	276	362	275	316
ACH = 1.2	1532	1233	1413	1603	1306	1254	1407	1219	1308
ACH = 1.6	1659	1670	1676	1600	1635	1646	1617	1575	1600
ACH = 2.0	1149	1329	1187	974	1249	1344	1180	1294	1207

In the following sections of this thesis project the analysis will be focused on the cases of ACH equal to 1.2 and 1.6, since they were the simulations with the better thermal performance; and as previously mentioned, the number of comfort conditions in the residences can be improved by considering a partial load or not operation of some components in the system. This operation mode will limit the amount of moisture that

is removed when the humidity levels are low or constrain the sensible heat remotion from the process air stream when the temperature is low.

6 Chapter Six: Control strategy and final results.

In the current chapter, the operation of the desiccant cooling system will not be any more nominal always. A series of criteria will be described in order to decide separately the behavior mode of each component in the system, in order to improve the thermal operation of the previous simulation groups. The strategy control will be only implemented for the cases of ACH equal to 1.2 and 1.6 because of it was the optimal range defined in the previous section for the air mass flow rate. The results are going to be analyzed in depth.

6.1. Control strategy

The objective of formulating a control strategy resides in the optimization of the desiccant cooling system's performance through the adjustment of operational parameters of its constituent components, being aware of the internal condition of the air-conditioned spaces. This will allow to sustain the building conditions with values suitable for human thermal comfort, thus taking care of both temperature and humidity.

According to the thermal comfort zone evidenced in figures 5.3 to 5.6, it can be identified nine regions that represent different required operational modes by the system if the indoor conditions fall in one of them. These modes are:

1. If the return dry bulb temperature and humidity ratio are between the acceptable ranges outlined by the ASHRAE, the system operation can be kept constant.
2. If the return temperature and humidity ratio are both above the upper limits, it is required to increase the dehumidification in the desiccant wheel and the cooling effect of the cooling coil, humidifier, and rotary heat recovery.
3. If the return humidity ratio is above the upper limit, but temperature is in the admissible range, the dehumidification must be maximized while the cooling capacity of the cooling coil, humidifier, and rotary heat recovery can be maintained.

4. If the return humidity ratio is above the upper limit, but temperature is below the lower boundary; the dehumidification must be maximized while the cooling capacity must be reduced by regulating the cooling effect of the cooling coil, humidifier, and rotary heat recovery.
5. If the return temperature is below the boundary, but humidity ratio is in the admissible range, the dehumidification rate is kept constant while the cooling effect of the cooling coil, humidifier, and rotary heat recovery must be diminished.
6. If the return temperature and humidity ratio are both under minimum accepted boundaries, the system must regulate the dehumidification rate in order to diminish the moisture absorption, and concurrently reduces the cooling effect of the cooling coil, the humidifier, and rotary heat recovery.
7. If the return temperature is within the admissible range, but humidity ratio is under the lower limit, the system needs to regulate the dehumidification rate for diminishing the moisture absorption, and the cooling effect of the cooling coil, the humidifier, and rotary heat recovery can be maintained.
8. If the return temperature is above the accepted range, but humidity ratio is under the lower limit, the system will require to regulate the dehumidification rate for diminishing the moisture absorption, while the cooling effect of the cooling coil, the humidifier, and rotary heat recovery must be maximized.
9. If the return temperature is above the upper limit, but humidity ratio is within the admissible range, the system will require to maintain the dehumidification rate, while the cooling effect of the cooling coil, the humidifier, and rotary heat recovery must be maximized.

Depending on where is located the interior conditions of the apartments in the psychrometric diagram, the control system must select the corresponding operating mode to act on each component. In order to simplify the control strategy, it was selected a central set point in the thermal comfort zone, corresponding to 24.5°C in dry bulb temperature and 9.6 g/kg of dry air for the humidity ratio (50% of relative humidity). During operation, the controller will take decisions by comparing the current indoor conditions with the stablished set point in order to regulate separately the different components in the desiccant cooling mode.

This kind of control is defined as a predictive strategy, or better known as model predictive control (MPC), which operates on a predictive mathematical model of the system being controlled to optimize the future system behaviour. This kind of methodology is receiving significant attention for managing energy requirements in buildings, especially because of its ability to consider constraints, prediction of disturbances and multiple conflicting objectives, such as indoor thermal comfort and building energy demand. [44]

In the next subsections, will be described the different constraints and operation mode for the control of each controller.

6.1.1. Heating coil.

For controlling the heating coil, it is necessary to first determine the limiting variables of the heat exchanger. It is assumed that the nominal effectiveness of the device is equal to 0.8 and it is known that the inlet water temperature provided by the district heating is 65 °C and it is assumed an outlet temperature of 50°C. For estimating the maximum regenerating temperature at the nominal condition, it is considered the inlet air temperature profile at the heating coil of the preliminary simulation results for the cases of ACH 1.2 and 1.6, which are shown in Figure 6.1. Since it is being defined the nominal condition, it is decided to calculate the regeneration temperature with the average value of Thx22, which is equal to 36.85 °C and employing the effectiveness equation defined in section 4.3, it gives a resulting air regeneration temperature of 59.37 °C. This value is valid for both air mass flow rate since the profiles in Figure 6.1 are following the same path.

Then it is verified that for the worst conditions of the inlet air temperature (Thx22), the effectiveness does not exceed the acceptable range for a heat exchanger; for the minimum Thx22, which is 28°C, the effectiveness of the regeneration coil is around 84.78%, which is still a valid value. Additionally, with this condition, it is calculated the maximum power, water flow rate and the water velocity of the device, with the following equations:

$$\dot{Q}_{\max hot} = \dot{m}_{air} C_{p\,air} (T_{reg} - Thx22_{min}) \quad (20)$$

$$\dot{m}_{w\,hot\,max} = \frac{\dot{m}_{air} C_{p\,air} \left(T_{reg} - Thx22_{min}\right)}{C_{p\,w} (T_{w\,hot\,in} - T_{w\,hot\,out})} \quad (21)$$

$$\dot{V}_{w\,hot\,max} = \frac{\dot{m}_{w\,hot\,max}}{\rho_w} \quad (22)$$

$$v_w = \frac{\dot{V}_{w\,hot\,max}}{\frac{\pi}{4} d^2} \quad (23)$$

In the case of 1.2 ACH, the maximum power of the heating coil would be 49.73 kW and the water flow rate is 0.7919 kg/s, corresponding to a maximum volumetric flow rate of 2.851 m³/h; for an air to water heat exchanger, the water pipe could have a diameter of 1 ¼" (internal diameter of 36.6 mm), resulting in a water velocity of 0.7527 m/s, which is in the range of 0.4 -1.5 m/s for avoiding turbulent flow.

Regarding the case of the 1.6 ACH, following the same analysis, the maximum power is 66.305 kW, and the water flow rate is 1.05598 kg/s, corresponding to a maximum volumetric flow rate of 3.802 m³/h; considering the same dimension of the water pipe, the water velocity is 1.004 m/s, still in the reference range.

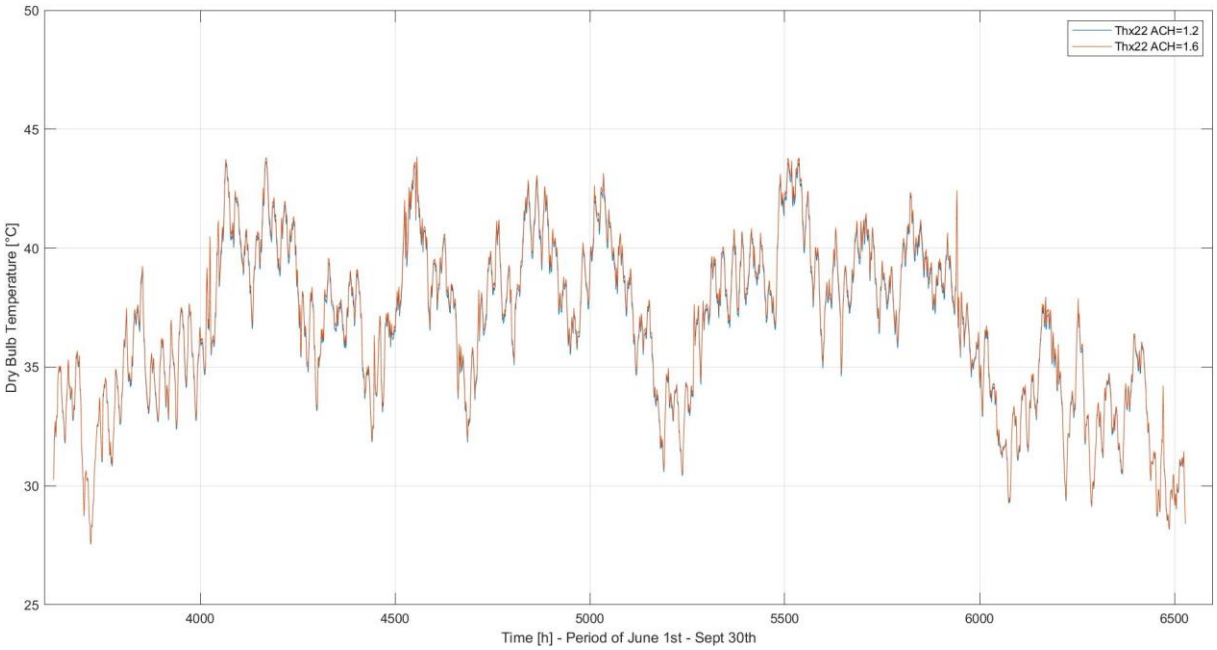

Figure 6.1. Inlet air temperature of the heating coil for the preliminary results. Thx22.

The control strategy for this component will be based on the necessities of the desiccant wheel; In essence, it involves making decisions based on the required regeneration temperature for the desiccant wheel and the incoming air temperature. These decisions can be summarized as follows:

- **Turn off** the regeneration heat exchanger when one of the following two scenarios occurs:
  1. The desiccant wheel is by-passed.
  2. The dehumidification is needed, but the inlet air temperature is greater than or equal to the required regeneration temperature.

  In both cases there is no water flow rate flowing.
- **Turn on** the heating coil when dehumidification is required, adjusting the volumetric water flow rate for obtaining the desired regeneration temperature, which will vary in the regeneration temperature range, taking into account the inlet condition of the return air stream temperature.

6.1.2. Desiccant wheel.

As evidenced in the chapter 5, for the cases of ACH 1.2 and 1.6, the outcomes presented some indoor conditions in which the humidity ratio were below the limits established by ASHRAE, which is 5.2 g/kg of dry air corresponding to 23°C and 30% of relative humidity. Since the operation of the desiccant wheel was at the nominal regeneration temperature, the objective here is to control the moisture absorption by regulating a control variable.

According to the parametrization of the desiccant model explained in section 4.1, the model does not allow to modify the effectiveness in terms of the rotational speed of the desiccant wheel and as argument by Panaras et all., the influence of rotational speed in the humidity control of the component is not effective, hence the desiccant wheel will be operating at its rated rotational speed. [45]

Then, the idea of the control strategy is to regulate the regeneration temperature of air entering in the DW, according to a defined interval, in order to limit the amount of moisture that is removed from the outdoor air stream. The maximum regeneration temperature is assumed to be the maximum achievable at the outlet of the heating coil, which is 59.37 °C and as the minimum, to avoid inconsistencies with the mathematical model, is set to be 40°C, for lower values the desiccant wheel is not operating.

For a better understating of the control in the desiccant wheel, it is illustrated in Figure 6.2 the scheme of control decisions for operating the component. Based on the return absolute humidity condition, the controller operates in the following ways:

1. If the return humidity ratio (XR) is lower than or equal to the set point of 9.6 g/kg of dry air. The desiccant wheel is deactivated, meaning that the system allows to pass the outdoor air without extracting any moisture. Concurrently, the heating coil is also turned off by closing completely valve regulating the water flow rate.

2. On the contrary case, the dehumidification is needed, and the system estimates the required regeneration temperature for obtaining the target humidity ratio (9.6 g/kg of dry air) and depending on its value, the controller can:
   2.1. If the inlet air temperature of the heating coil (Thx22) is equal to or higher than the required regeneration temperature and is within the range of regeneration temperature; the system turns off the heating coil and leaves to enter into the desiccant wheel, the return air with the Thx22 condition.

   2.2. If the inlet air temperature of the heating coil (Thx22) is lower than required regeneration temperature, it is necessary the intervention of the heating coil. according to required regeneration temperature, that can vary between the minimum and the maximum values previously defined, the control strategy calculates the hot water flow rate for reaching the regeneration temperature, based on the equation (21).

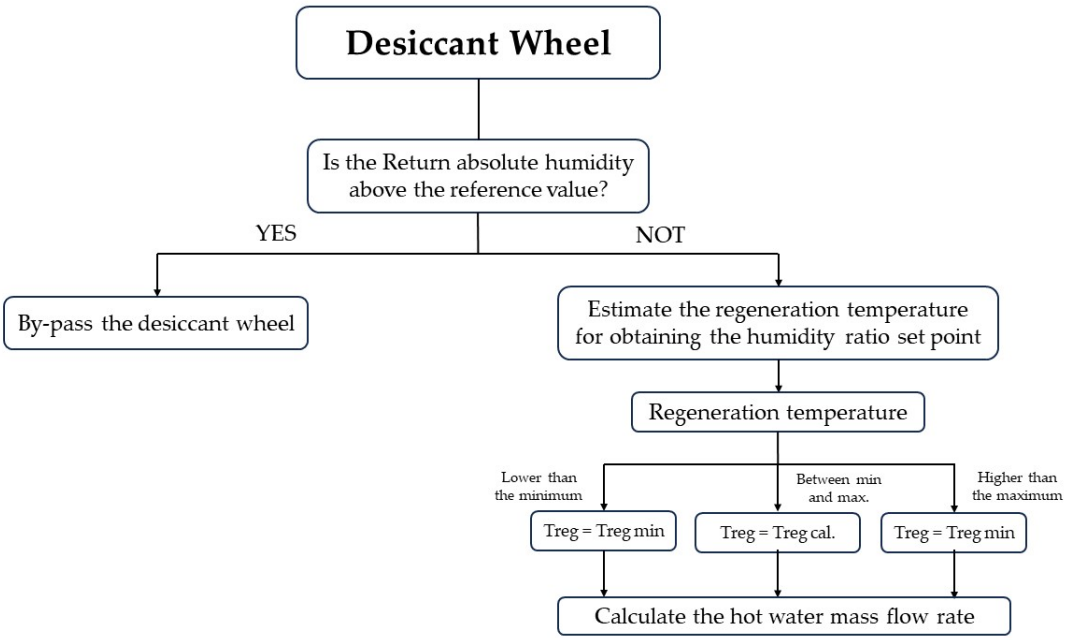

Figure 6.2 . Control scheme for the desiccant wheel.

6.1.3. Cooling Coil.

For the specifications of the cooling coil, a similar analysis as for the heating coil was carried out in order to determine the design variables of the heat exchanger. The nominal effectiveness of the device is equal to 0.52153 and it is known that the inlet water temperature provided by the groundwater system is 13 °C and it is assumed a delta temperature of 4°C, corresponding to an outlet temperature of 17°C.

Since, it is wanted to keep constant the effectiveness of the cooling coil, the maximum power exchanged by the heat exchanger will be estimated with equation (24) considering the maximum incoming process air temperature, which is selected by looking at the profile of the inlet air temperature to the cooling coil (Thx12) in the preliminary results; Figure 6.3 allows to stablish a maximum temperature of 28°C for both cases. With these parameters, the maximum power exchanged is 12.4 kW and 16.535 kW for the case of ACH of 1.2 and 1.6, respectively.

$$\dot{Q}_{\max cool} = \varepsilon_{nominal} * [\dot{m}_{air} C_{p\,air} (Thx_{12\,max} - T_{w\,cool\,in})] \quad (24)$$

$$TS = Thx_{12} - \frac{\dot{Q}_{\max cool}}{\dot{m}_{air} C_{p\,air}} \quad (25)$$

$$\dot{m}_{w\,cool\,max} = \frac{\dot{m}_{air} C_{p\,air} (Thx_{12} - TS)}{C_{p\,w} (T_{w\,cool\,out} - T_{w\,cool\,in})} \quad (26)$$

$$v_w = \frac{\dot{m}_{w\,cool\,max}}{\frac{\pi}{4} d^2 * \rho} \quad (27)$$

The supply air temperature with this worst scenario, is estimated with equation (25), giving a result of 20.17°C for both cases. Additionally, with equation (26) and (27) are calculated the water flow rates and water velocity for the two air flow rates.

In the case of 1.2 ACH, the water flow rate is 0.74056 kg/s, corresponding to a maximum volumetric flow rate of 2.666 m^3/h; assuming a water pipe of 1 ¼" (internal diameter of 36.6 mm) for the air to water heat exchanger, the resulting water velocity is 0.7039 m/s, which is in the range of 0.4 -1.5 m/s for avoiding turbulent flow.

Regarding the case of the 1.6 ACH, according to the same analysis, the water flow rate is 0.9875 kg/s, corresponding to a maximum volumetric flow rate of 3.555 m^3/h; considering the same dimension of the water pipe, the water velocity is 0.9386 m/s, still in the reference range.

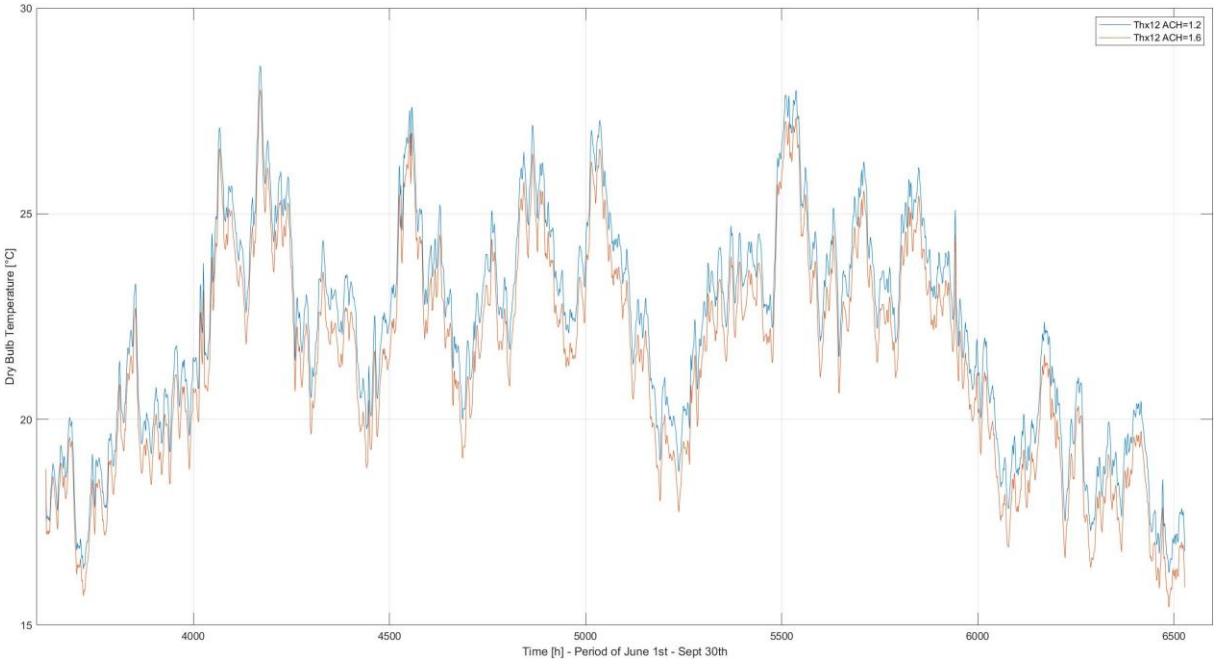

Figure 6.3. Inlet air temperature of process air into the cooling coil for the preliminary results. Thx12.

The control methodology for this component will be in function of the return temperature level (TR); According its value, the system can take different decisions that are summarized as follows:

- **Turn off** the cooling heat exchanger when one of the next two scenarios occurs:
  1. The indoor temperature condition is lower than temperature set point stablished of 24.5 °C.
  2. The indoor temperature condition is higher than 24.5 °C, but the inlet air temperature in the cooling coil (Thx12) is lower than the maximum supply temperature defined as 21°C.

  In both cases there is no water flow rate flowing in the cooling coil.

- **Turn on** the cooling coil when it is required to cool down the process air stream, adjusting the volumetric water flow rate for obtaining the minimum supply temperature of 18°C, taking care of not exceeding the maximum water flow rate previously defined. Cases where the required water flow rate is larger than the maximum one, it is settled to use the maximum flow rate on the component.

6.1.4. Humidifier.

The control of the humidifier will be just an ON-OFF decision according to the incoming indoor condition. When the return temperature exceeds the target set point of 24.5 °C, the component is turned ON, meaning that the evaporative cooling is necessary for lowering the output process air temperature at the heat recovery, the ON working condition is always at the nominal effectiveness of 0.8.

6.1.5. Rotary heat recovery.

Similarly, to the humidifier, the rotary heat recovery control is based on the return temperature level compared to the temperature set point. When the indoor temperature is lower than 21°C, the device is turned off by dropping to zero the rotational speed of the sensible heat exchanger. Additionally, the device is also deactivated when the inlet temperature of the regeneration air flow rate is higher than the inlet temperature of the process air flow rate (By-pass). On the contrary, conditions over the before indicated set point will enable the sensible heat exchange between regeneration air stream and process air flow rate at its nominal effectiveness of 0.8.

6.2. Application of the control strategy in the desiccant cooling system.

In this section, after implementing the previously descried control strategy in the desiccant cooling system, the main findings of the simulation for the cases of air changes per hour of 1.2 and 1.6 are presented and discussed to evaluate the performance of the system operating under different configuration and conditions.

In Figure 6.4 are illustrated the two temperature profiles of the resulting simulation, it can be observed that after few hours of operation, the internal residence temperatures reach values in the comfort dry bulb temperature interval. Additionally, it can be noted that for the initial (before June 15th) and final (after September 7th) periods of the conditioned hours, both volumetric flow rates are capable for maintaining the indoor temperature with values below 26 °C. This effect can be due to the low cooling demand on those periods. The difference becomes more noticeable in the intermediate period, when the return temperature for the ACH of 1.2 reaches values above the 27°C, which is the dry bulb limit for the ASHRAE comfort zone, in some hours, while the simulation with ACH of 1.6 hardly exceeds the 26°C during the whole conditioned

time interval. This reaffirms the greater capacity of the 1.6 ACH scenarios for managing the sensible heat demand.

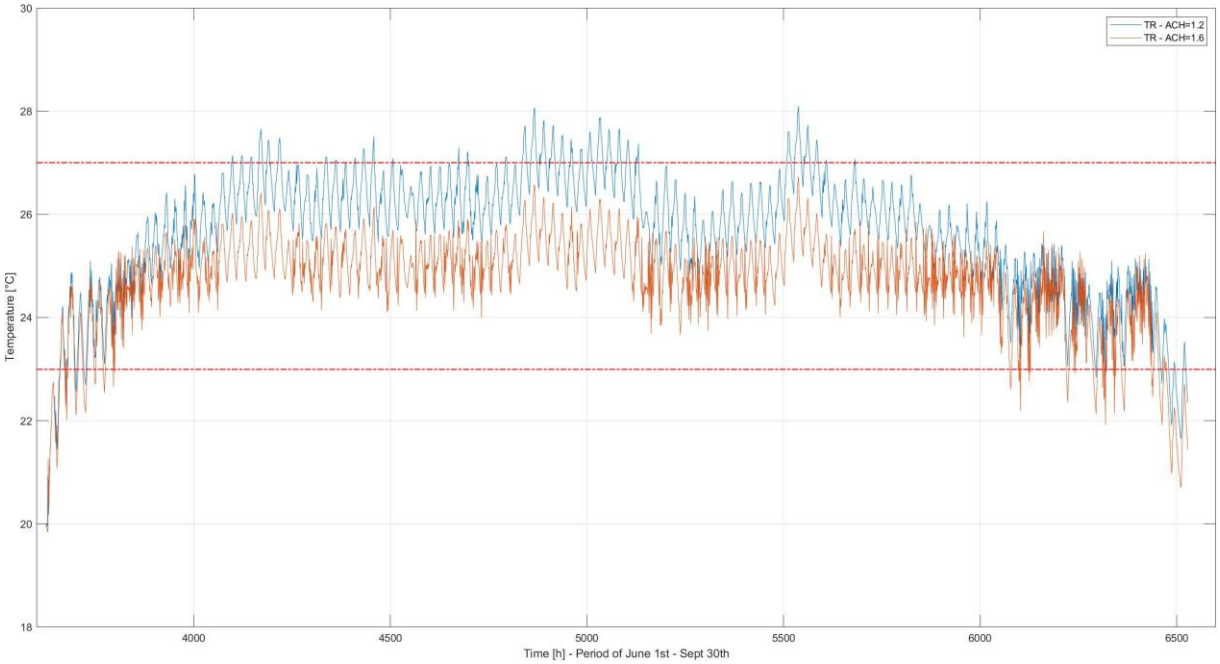

Figure 6.4. Return air temperature profiles for the two ACH in the final simulation with the control strategy.

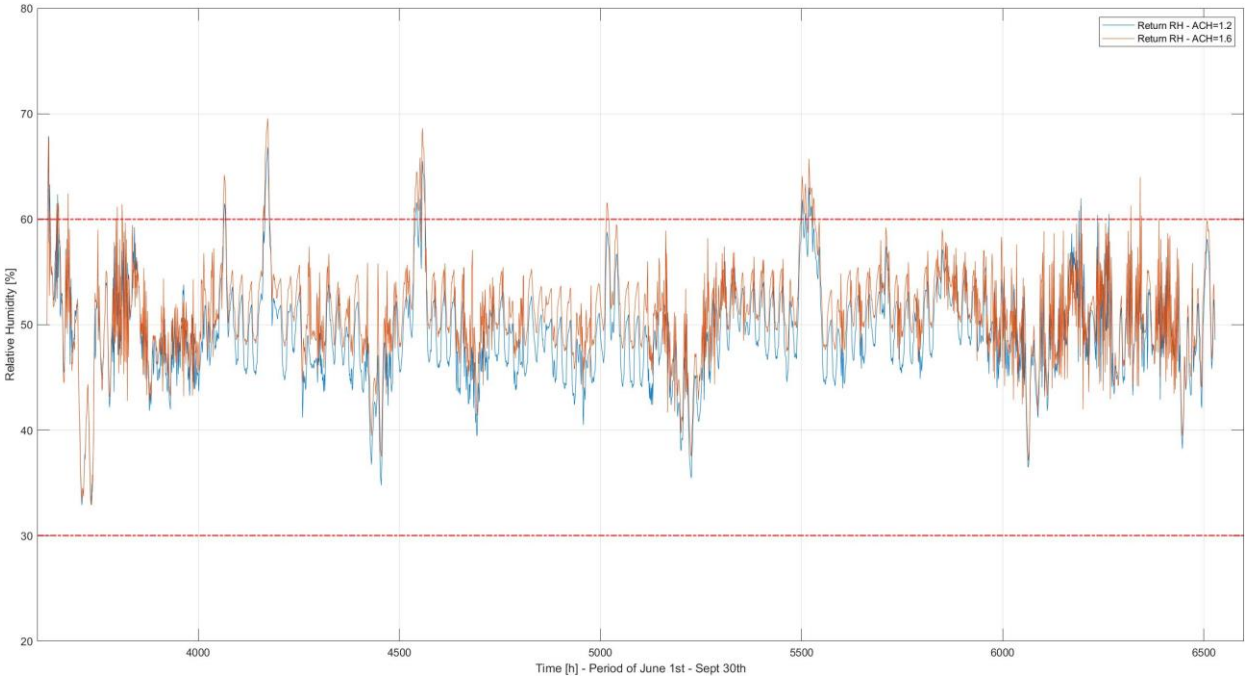

Figure 6.5. Return air relative humidity profiles for the two ACH in the final simulation with the control strategy.

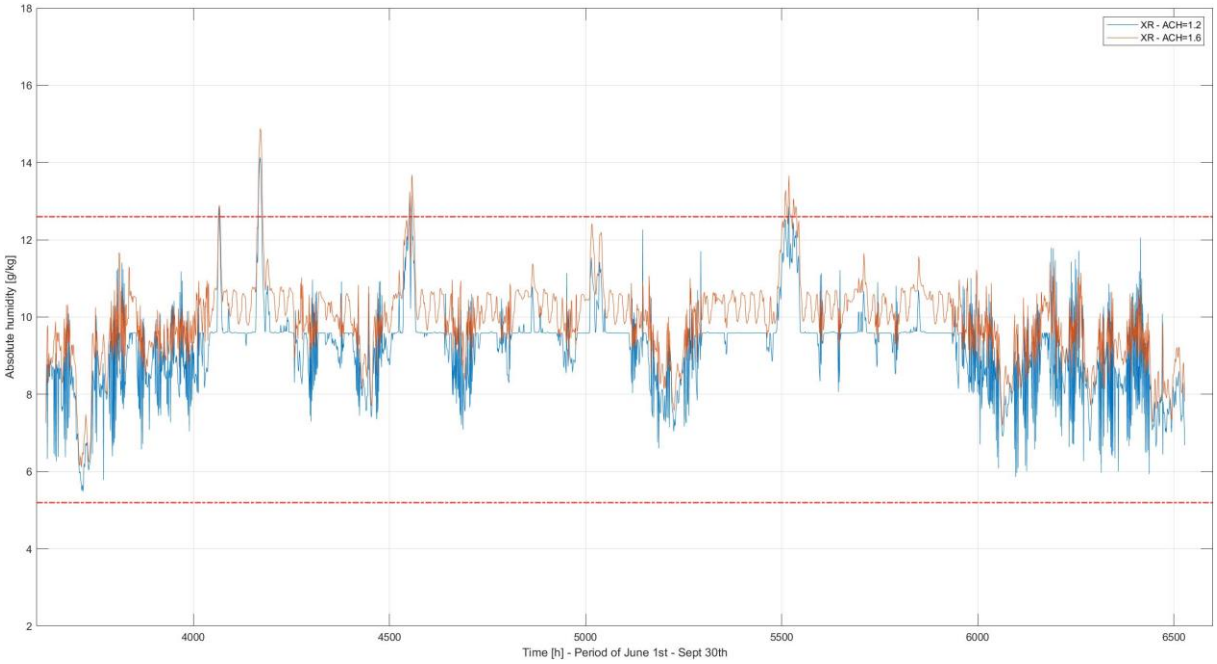

Figure 6.6. Return air absolute humidity profiles for the two ACH in the final simulation with the control strategy.

In contrast to the preliminary simulation, the majority of data points at the extremes of the Figure 5.1, that were below the acceptable temperature thresholds, have been rectified through the implementation of the control strategy as can be appreciated in Figure 6.4. This enhancement in the thermal indoor air quality is the combination effect of the system, that on those time intervals with low cooling the demand, regulates and/or turns off the humidifier, the rotary heat recovery, and the cooling coil for supplying air to the dwellings at a higher temperature.

Moving towards the humidity level behavior, Figure 6.5 and Figure 6.6 evidence the relative humidity profile and the absolute humidity profile of the findings, respectively. Both air flow rates provide an outstanding humidity control on the internal spaces limiting the indoor humidity ratio inside the boundaries for respecting the latent comfort zone. Just a slightly difference between the humidity ratios give a better result for the case ACH equals to 1.2. respect to the 1.6 ACH case.

Furthermore, in comparison to the preliminary results for humidity reported in Figure 5.2, where some indoor conditions experienced an absolute humidity that were below the minimum acceptable threshold of 5.2 g/kg of dry air; with the control strategy implemented on the desiccant wheel and regeneration coil, for managing the moisture content on the indoor air, these points were corrected. In fact, in Figure 6.5 there is no relative humidity under the 30%, meaning that the feeling of dryness is avoided and almost throughout the conditioned period, the relative humidity is maintained below the 60%, evading the humid air sensation in the skin.

The representation of the temperature and humidity ratio profile in the psychrometric diagram for both cases, enable to visually analyze where the majority return conditions

of the system are concentrated and whether they are located inside the delimited thermal comfort zone. In Figure 6.7 and **¡Error! No se encuentra el origen de la referencia.** are illustrated the common return conditions of the apartments for the case of ACH 1.2 and 1.6, respectively. It can be analyzed that in contrast to the preliminary case simulation, there is greater quantity of conditions which are within the comfort zone thanks to the integration of the control strategy to the desiccant cooling model. The larger portion of data points, which were located in the left side of the reference zone (requesting a reduction in the cooling capacity) and those below the 30% relative humidity line (requesting a reduction in the dehumidification capacity), are rectified.

The remaining points outside the boundaries, which are actually few, are not completely distant from the comfort zone, meaning that they are in a nearly thermal comfort condition.

In general, in the previous chapter, the simulation of 1.2 ACH, based on the common return conditions (mixed return air of all the apartments), presented 1581 hours inside the thermal comfort zone; considering the implementation of the control methodology, the comfort hours grow to 2502 hour of 2905 in the conditioned period. An improvement of 58.25% in the building's indoor air quality respect to the preliminary results. In comparison to reference case of natural ventilation, where the comfort hours represent on average the 23.42% of the summer period; with the optimized operation of the desiccant cooling system, the comfort hours depict 86.13% of the conditioned period, which signifies an important coverage of the latent and heating demand.

Doing the same analogy for the 1.6 ACH case, in the preceding chapter, the simulation revealed that the thermal comfort zone was achieved for 1654 hours during the conditioned period. Subsequently, with the introduced optimized operation, it results in an increase of the number of comfort hours to 2617 out of 2905 total conditioned hours. This represents a substantial enhancement of 58.22% in the indoor air quality of the building when compared to the initial findings. In contrast to the reference case employing natural ventilation, where the comfort hours accounted for an average of 23.42% of the summer period, the optimized operation of the desiccant cooling system yielded a notable increase in comfort hours, reaching 90.1% of the conditioned period. This signifies a substantial coverage of both latent and heating demand, indicating the effectiveness of the optimized system.

Despite the initial impression that the improvement between one hourly air exchange rate (ACH) and the other is not very significant, it should be noted that these percentages correspond to the mixed return condition of air from all the apartments. To closely examine the differences between the two ACH scenarios, it is needs to refer to Table 6.1 which provides a detailed breakdown of comfort hours for each apartment in the building.

For the case with an ACH of 1.2, the comfort hours in the apartments on the fourth floor, which experience the highest sensible and latent loads, are approximately 2000 hours, while for the case of 1.6 ACH, the hours remain around 2550 hours in the same apartments. Thus, it can be concluded that for the 1.6 ACH scenario, the comfort hours remain relatively consistent across different floors and orientations of the apartments, whereas for the 1.2 ACH scenario, the values fluctuate over a wider range, with higher values on the lower floors and lower values on the upper floors.

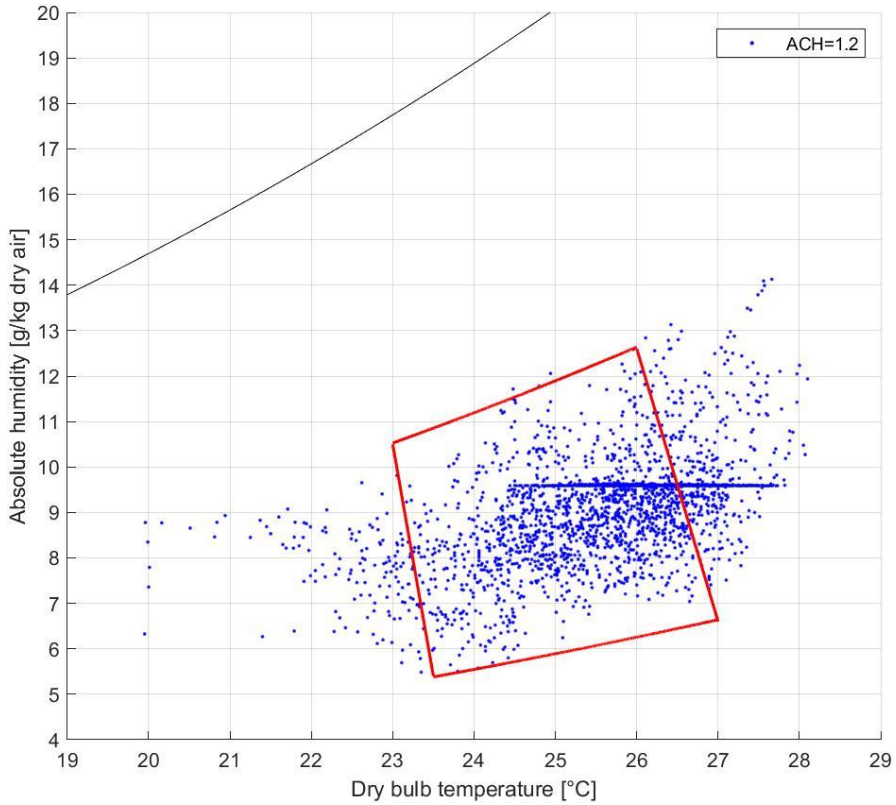

Figure 6.7. The results of the indoor residence conditions with the implementation of the control strategy. ACH Case 1.2

Table 6.1. Comfort hours by apartments for the two ACH cases with the implementation of the control strategy.

Apartments	**01_NE**	**01_E**	**01_SE**	**01_SO**	**01_O**	**01_NO**	**03_NE**	**03_E**	**03_SE**
ACH = 1.2	2582	2686	2637	2613	2573	2599	2694	2232	2256
ACH = 1.6	2440	2586	2595	2515	2553	2514	2596	2729	2721

Apartments	**03_SO**	**03_O**	**03_NO**	**04_NE**	**04_E**	**04_SE**	**04_SO**	**04_O**	**04_NO**
ACH = 1.2	2511	2118	2316	2483	2015	2019	2221	2011	2095
ACH = 1.6	2639	2678	2652	2542	2634	2635	2554	2483	2543

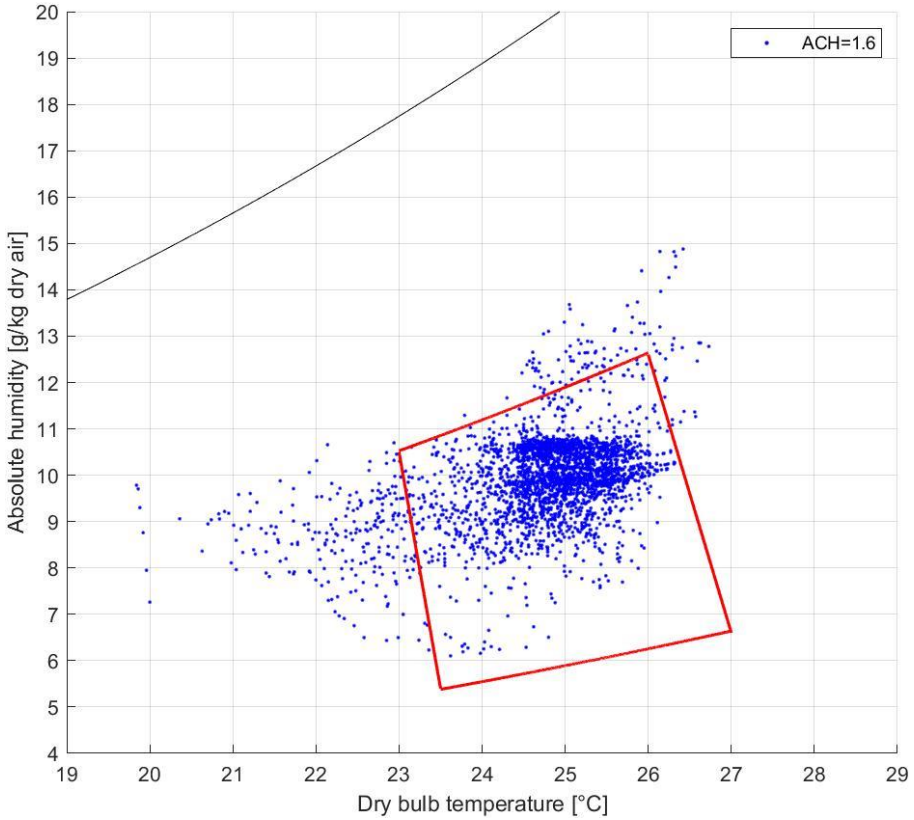

Figure 6.8. The results of the indoor residence conditions with the implementation of the control strategy. ACH Case 1.6

Continuing the analysis, the implementation of the control strategy not only results in an increase in thermal comfort hours but also, owing to the flexible operation of the system, facilitates cost savings during its operation. Savings are obtained by reducing the electrical consumption when the pumps responsible for water circulation in the regeneration and cooling heat exchangers are turned off. Furthermore, even more substantial savings are anticipated when the heating coil operates at partial load or is turned off, as these conditions favor the reduction in the hot water consumption procured from the district heating network. Figure 6.9 illustrates the behaviour of the volumetric flow rate within the heating coil, for the 1.6 ACH simulation, throughout the entire conditioning period.

Assuming the water flow rate constant during the current operation hour, for the case of 1.6 ACH the hot water consumption on the whole conditioned period will be 3141.6 m^3 whereas for the scenario with 1.2 ACH the consumption will be 2583.5 m^3 of hot water. If design engineers are looking for savings in the OPEX costs, they can reduce by 21.6% the hot water expenditure by selection the 1.2 air changes per hour instead of 1.6.

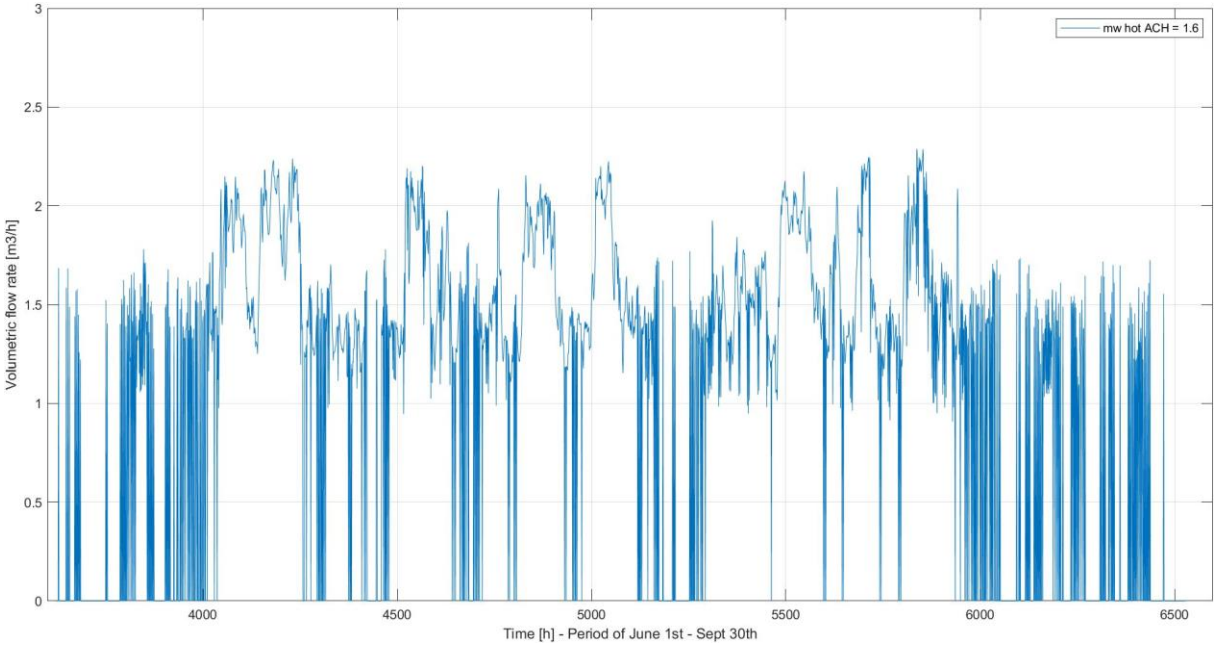

Figure 6.9. Hot water consumption in the regeneration heat exchanger with the implementation of the control strategy. Case 1.6 ACH

6.3. Analysis of coefficients of performance.

Only two alternatives for the nominal air flow rate have been considered to implement the control strategy, which are ACH 1.2 and ACH 1.6. As a first approach to compare the alternatives in terms of performance, the COP of the desiccant cycle is calculated, and it considers as desired output the supply air stream with the right temperature and humidity to reach comfort conditions in the conditioned spaces, starting from a non-controllable outdoor air stream. The COP is defined as follows:

$$COP_{cyc} = \frac{\dot{m}_{air} * (h_{OA} - h_S + Q_c)}{Q_h} \quad (28)$$

The trend of the COP of the desiccant cycle for both ACH 1.2 and ACH 1.6 is shown in Figure 6.10. Only the points when the system is in operating condition are considered in this graph. For both cases, the value of COP follows a similar trend during the entire cooling period considered. The instantaneous values of COP ranges between 0.2 and 1.2 approximately for both cases. The average COP in the case of ACH 1.6 is slightly higher than the average COP in the case of ACH 1.2, with a value of 0.7661 and 0.6998, respectively. By increasing the air flow rate from ACH 1.2 to ACH 1.6, an increase of 9.4% in the average COP of the cycle is obtained. Since this indicator does not show significant differences when changing the nominal air flow rate, an additional indicator has to be used.

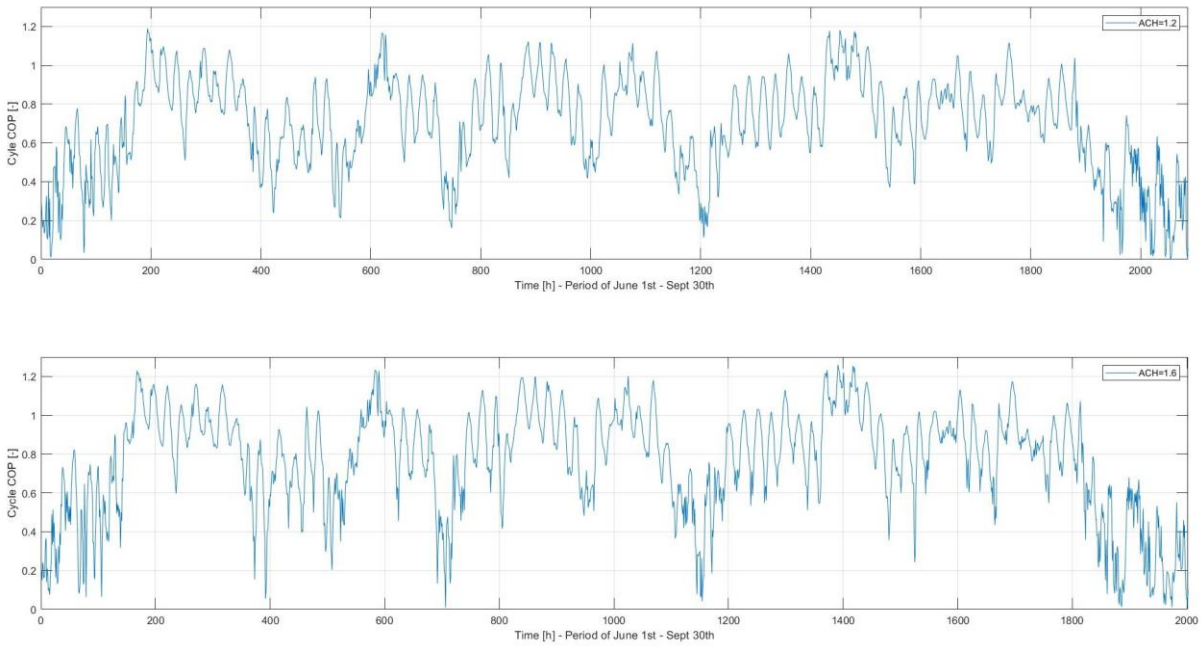

Figure 6.10. Trend of the desiccant cycle COP for ACH 1.2 and ACH 1.6 during the cooling season.

The thermal COP is then calculated considering a different perspective of the desired output effect. In this case, we do not focus on the state of the supplied air stream but on the objective of the system which is providing comfort conditions by controlling temperature and humidity inside the rooms. In this way, the expression for the thermal COP is written as follows:

$$COP_{th} = \frac{\dot{m}_{air} * (h_R - h_S)}{\dot{Q}_h} \quad (29)$$

The numerator represents the air enthalpy change due to the sensible and latent heat absorbed by the supply air when interacting with thermal and humidity loads inside the rooms. The denominator instead is the amount of heat required to perform the regeneration process in the desiccant wheel. The COP of ACH 1.2 is lower than the COP of ACH 1.6, but it is more stable during the entire cooling period considered compared to the one for ACH1.6, that presents higher variability as shown in Figure 6.11. This variation is introduced by the control system because a higher supply air flow tends to have a higher impact in the internal conditions of the room, adding complexity to the control strategy. The average thermal COP for ACH 1.2 and ACH 1.6 are 0.6119 and 0.6797, respectively. The increase in the air flow rate from ACH 1.2 to ACH 1.6 leads to an increase in average thermal COP around 11%.

However, analyzing the instantaneous values of thermal COP is possible to see that thermal COP of ACH 1.6 reaches higher values of COP respect to thermal COP of ACH 1.2, but it presents a higher variation during the studied cooling period. Thermal COP of ACH 1.2 presents less oscillations in the values obtained.

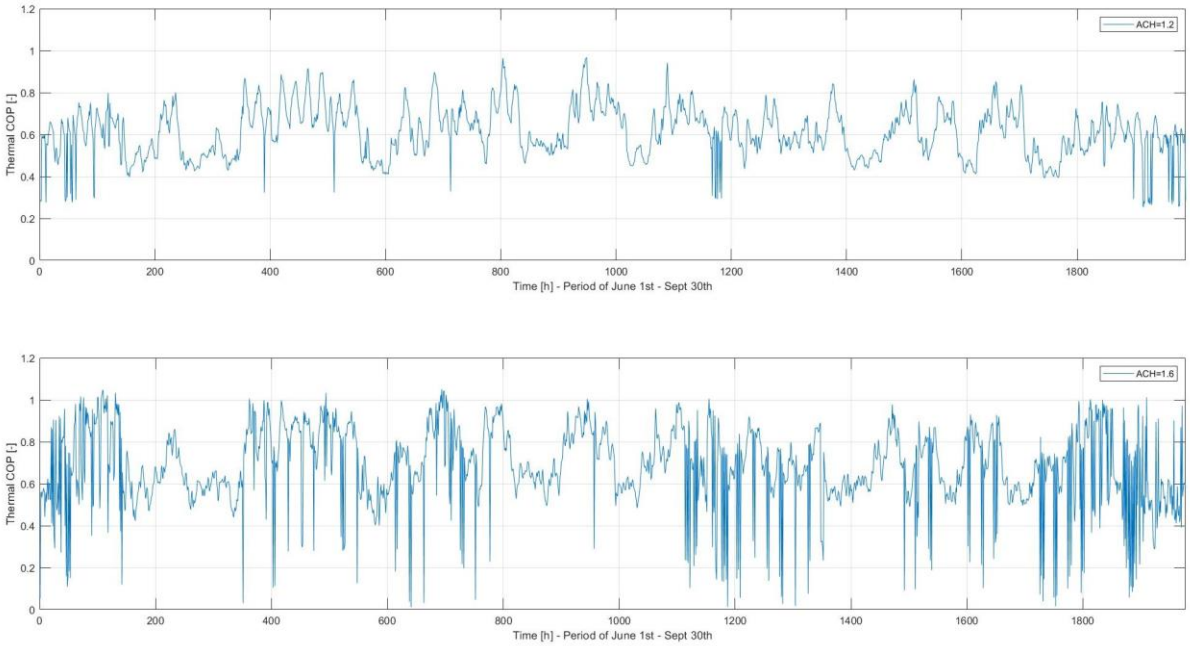

Figure 6.11. Trend of thermal COP for ACH 1.2 and ACH 1.6 during the cooling season.

As previously mentioned, since the coefficient of performance for the DC cycle (COPcyc) evidenced similar behaviour, as illustrated in Figure 6.10; and the thermal coefficient of performance evaluates just in terms of amount of heat exchanged; a third indicator of performance has been introduced for analysing the system in terms of electrical requirements. The electrical coefficient of performance (COPel) includes the electrical energy consumption needed to provide the desired cooling effect. The power needed for water pumping in the regeneration and cooling coil, and the one required to rotate the desiccant wheel are neglected due to their lower value in comparison with the fans power consumption [7]. Therefore, for the calculation of the electrical COP, it is considered only the fan power required to circulate the air streams that pass across the components involved in the cooling process. The electrical COP is calculated by using the equation (30).

$$COP_{el} = \frac{\dot{m}_a(h_R - h_S)}{\sum_1^{nfans} \dot{W}_{fan}} \quad (30)$$

The numerator corresponds to the enthalpy variation of the air produced by the interaction of the supply air with the sensible and latent loads inside the conditioned spaces. This definition allows to evaluate the performance of the system by focusing on the conditioning of the spaces as the desired effect and not only in the cycle performance. The power consumption of fans required to move the air streams through the different steps of the cycle is considered as the main input to provide the cooling effect in the conditioned spaces, thus it is present in the denominator of the equation.

Figure 6.12 shows the trend of the electrical COP for both ACH 1.2 and ACH 1.6 in the period between June 1st and September 30th. The values presented in the graph were filtered by excluding the non-operating points of the desiccant system. It is possible to notice that there is a significant difference between the COPs of each case specially when the cooling demand is higher. In the previous sections, we found that the implementation of the control strategy allows to reach acceptable results in terms of thermal comfort for both alternatives. ACH 1.6 case allows to have less variations in the thermal conditions of the single apartment than ACH 1.2 case, but looking the entire system they present similar behaviour. The power consumption needed to move the supply and return air streams is higher in the case of ACH 1.6 because of the higher air flow rate that has to pass across the DEC components.

All these aspects mentioned result in a higher electrical COP for the case ACH 1.2 that requires less electrical power consumption to provide the cooling effect needed to guarantee comfort conditions inside the apartments. The average electrical COP for ACH 1.2 and ACH 1.6 is 8.0445 and 6.4592, respectively. By changing the air flow rate form ACH 1.2 to ACH 1.6, it is obtained a reduction in the electrical COP by around 19.7 %.

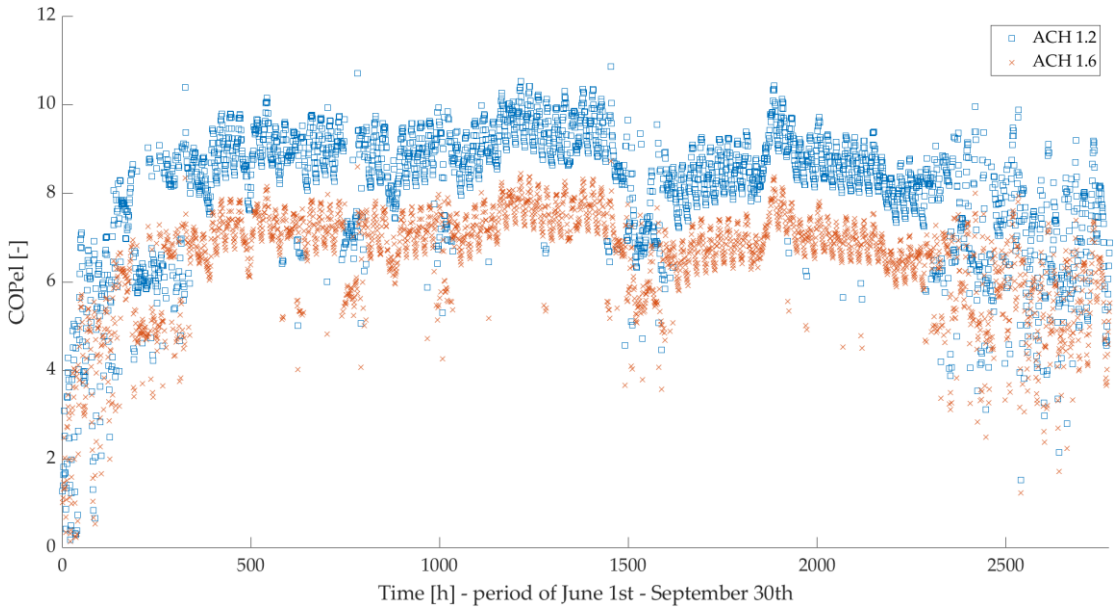

Figure 6.12. Electrical COP for both ACH 1.2 and ACH 1.6 during conditioned period.

Figure 6.13 shows an estimation of the fan power consumption for both cases considering the nominal parameters of a commercial exhaust centrifugal fan operating at the air flow rate indicated by each ACH value. Increasing the air flow rate from ACH 1.2 to ACH 1.6 results in an increase of the fan power consumption of 66.1%. Considering this fact, the selected nominal air flow rate of the system is a compromise between the thermal comfort reached inside the apartments and the electrical

consumption required to provide the desired effect. A higher flow rate allows to have a better control in the setpoints of temperature and humidity inside the rooms, but more electrical energy consumption is required, and also bigger machines have to be installed to move the air and to exchange the amount of heat needed in the regeneration coil and the cooling coil.

An increase in the thermal COP of 11% is not consistent with a reduction in the electrical COP of 19.7%. Therefore, it is not convenient to increase the air flow rate to ACH 1.6 because the benefit obtained in indoor thermal comfort is not supported by the increase in the electrical energy consumption. Additional air flow rates between ACH 1.2 and ACH 1.6 need to be analysed to obtain an optimal nominal air flow rate that result in a higher thermal COP with a reasonable increase in the electrical energy consumption.

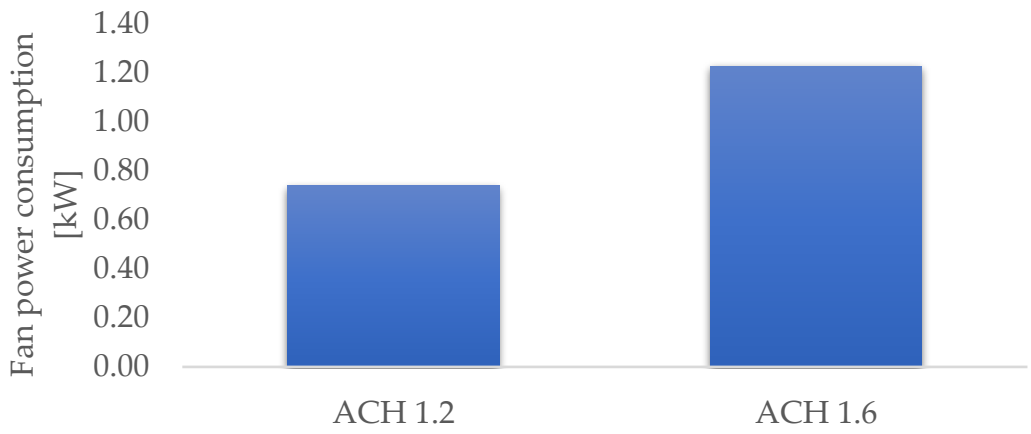

Figure 6.13. Fan power consumption considering a commercial exhaust centrifugal fan.

7 Conclusions and future developments.

The implementation of a desiccant cooling system integrated with a predictive control strategy, for managing both sensible and latent load in a building located in Milan, provides the following relevant findings:

- According to the defined framework of the building, it is needed an optimal range of the volumetric flow rate between 1.2 and 1.6 air volume changes per hour, which correspond to a flow rate of 4545 m^3/h and 6060 m^3/h. An air flow rate in this range can achieve a significant portion of indoor ambient conditions considered as thermal comfort for human occupancy. The percentage can vary from 86% up to 90%, depending on the ACH value chosen, respect to the natural ventilation as the only source for dealing with the thermal building load.
- The flexible operation of the internal system components, according to the internal condition, allows to optimize the indoor conditions for achieving better thermal comfort from the very beginning of the conditioned period to the lately final of it.
- The 1.6 ACH scenario demonstrate a superior management of sensible heat demand, specially maintain the number of comfort hours stable across the different apartment with distinct floors and orientation, with temperatures hardly exceeding 26°C throughout the entire conditioned period. In contrast, the 1.2 ACH scenario occasionally provides return temperatures above 27°C, leading to a reduced capacity for managing sensible heat demand. Moreover, both air flow rates effectively controlled indoor humidity levels within the boundaries of the latent comfort zone. The 1.2 ACH scenario demonstrated slightly better humidity control.
- The implementation of the predictive control methodology significantly improved the indoor air quality by increasing the thermal comfort hours by 58.2% for both cases, compared to the preliminary simulations, where the system operated always at nominal condition. This enhancement is attributed to the system's ability to regulate or turn off components like the desiccant wheel, the humidifier, rotary heat recovery, and cooling coil during periods of low thermal demand.
- So, it can be concluded that the control strategy successfully rectified indoor conditions that were out of the ASHRAE thermal comfort zone boundaries, in terms of temperature and humidity ratio.
- Increasing the nominal air flow rate allows to better manage the setpoints of temperature and humidity inside the rooms but it increases the electrical energy

consumption required to move the air through the system. By changing the air flow rate from ACH 1.2 to ACH 1.6 is obtained an increase in the thermal COP of 11% but with a reduction in the electrical COP of 19.7 %.

In general, this thesis work proved that a well-dimensioned desiccant cooling system in the ventilation mode configuration can successfully manage both the sensible and latent requirements of a residential buildings, composed by 24 apartments, under the weather conditions of Milan-Italy.

For the development of future investigations in this sector, it can be proposed a modification of the system configuration, which consists of integrating recirculation air stream of the return air flow rate. Meaning that a portion of the return flow rate, before entering into the humidifier, can be mixed with the process air stream before going into the cooling coil. This change allows to reduce the dimension of the desiccant structure and the heating coil. This modification will also reduce the electricity consumption by the regeneration fan.

Another possible improvement of the system configuration can be the integration of a heat pump for the cooling coil, replacing the air to water heat exchanger by an air to gas heat exchanger. This will help to reduce the dimension of the cooling coil and to enable the system to work not only in the summer period but also during the winter season.

Bibliography

[1] S. Solomon, G. K. Plattner, R. Knutti, and P. Friedlingstein, "Irreversible climate change due to carbon dioxide emissions," *Proc. Natl. Acad. Sci. U. S. A.*, vol. 106, no. 6, pp. 1704–1709, 2009, doi: 10.1073/pnas.0812721106.

[2] A. Wood and P. Du, "Dense Downtown vs. Suburban Dispersed: A Pilot Study on Urban Sustainability," *Int. J. High-Rise Build.*, vol. 6, no. 2, pp. 113–129, 2017, doi: 10.21022/ijhrb.2017.6.2.113.

[3] E. Union, M. State, and E. Union, "EUROSTAT 2021-05-12 Energy statistics - an overview," no. July, pp. 1–19, 2022.

[4] M. Maasoumy and A. Sangiovanni-Vincentelli, "Smart connected buildings design automation: Foundations and trends," *Found. Trends Electron. Des. Autom.*, vol. 10, no. 1–2, pp. 1–143, 2016, doi: 10.1561/1000000043.

[5] "C40 | Reinventing Cities."

[6] K. Daou, R. Z. Wang, and Z. Z. Xia, "Desiccant cooling air conditioning: A review," *Renew. Sustain. Energy Rev.*, vol. 10, no. 2, pp. 55–77, 2006, doi: 10.1016/j.rser.2004.09.010.

[7] M. Ryhl, W. Brix, L. Ove, D. Version, and L. Ove, "system with indirect evaporative cooling PhD Thesis," 2017.

[8] W. P. De Castro, "Analysis of Different Applications of," 2003.

[9] F. Bruno, "Testing of an Evaporative Cooling System That Supplies Air Near the Dew Point Temperature," pp. 1–8, 2016, doi: 10.18086/eurosun.2010.10.09.

[10] M. Mujahid Rafique, P. Gandhidasan, S. Rehman, and L. M. Al-Hadhrami, "A review on desiccant based evaporative cooling systems," *Renew. Sustain. Energy Rev.*, vol. 45, pp. 145–159, 2015, doi: 10.1016/j.rser.2015.01.051.

[11] Y. G. Akhlaghi, X. Ma, X. Zhao, S. Shittu, and J. Li, "A statistical model for dew point air cooler based on the multiple polynomial regression approach," *Energy*, vol. 181, pp. 868–881, 2019, doi: 10.1016/j.energy.2019.05.213.

[12] C. Zhan, Z. Duan, X. Zhao, S. Smith, H. Jin, and S. Riffat, "Comparative study of the performance of the M-cycle counter-flow and cross-flow heat exchangers for indirect evaporative cooling - Paving the path toward sustainable cooling of buildings," *Energy*, vol. 36, no. 12, pp. 6790–6805, 2011, doi:

10.1016/j.energy.2011.10.019.

[13] R. K. Kulkarni and S. P. S. Rajput, "Performance evaluation of two stage indirect / direct evaporative cooler with alternative shapes and cooling media in direct stage," *Int. J. Appl. Eng. Res.*, vol. 1, no. 4, pp. 800–812, 2011.

[14] S. D. Suryawanshi, T. M. Chordia, N. Nenwani, H. Bawaskar, and S. Yambal, "Efficient technique of air-conditioning," *Proc. World Congr. Eng. 2011, WCE 2011*, vol. 3, no. February 2016, pp. 2036–2041, 2011.

[15] S. Misha, S. Mat, M. H. Ruslan, and K. Sopian, "Review of solid / liquid desiccant in the drying applications and its regeneration methods," *Renew. Sustain. Energy Rev.*, vol. 16, no. 7, pp. 4686–4707, 2012, doi: 10.1016/j.rser.2012.04.041.

[16] M. M. Abd-Elhady, M. S. Salem, A. M. Hamed, and I. I. El-Sharkawy, "Solid desiccant-based dehumidification systems: A critical review on configurations, techniques, and current trends," *Int. J. Refrig.*, vol. 133, no. February 2021, pp. 337–352, 2022, doi: 10.1016/j.ijrefrig.2021.09.028.

[17] X. N. Wu, T. S. Ge, Y. J. Dai, and R. Z. Wang, "Review on substrate of solid desiccant dehumidification system," *Renew. Sustain. Energy Rev.*, vol. 82, no. July 2017, pp. 3236–3249, 2018, doi: 10.1016/j.rser.2017.10.021.

[18] M. M. Awad, A. Ramzy K, A. M. Hamed, and M. M. Bekheit, "Theoretical and experimental investigation on the radial flow desiccant dehumidification bed," *Appl. Therm. Eng.*, vol. 28, no. 1, pp. 75–85, 2008, doi: 10.1016/j.applthermaleng.2006.12.018.

[19] D. La, Y. J. Dai, Y. Li, R. Z. Wang, and T. S. Ge, "Technical development of rotary desiccant dehumidification and air conditioning: A review," *Renew. Sustain. Energy Rev.*, vol. 14, no. 1, pp. 130–147, 2010, doi: 10.1016/j.rser.2009.07.016.

[20] M. H. Ahmed, N. M. Kattab, and M. Fouad, "Evaluation and optimization of solar desiccant wheel performance," *Renew. Energy*, vol. 30, no. 3, pp. 305–325, 2005, doi: 10.1016/j.renene.2004.04.010.

[21] A. Kodama, N. Watanabe, T. Hirose, M. Goto, and H. Okano, "Performance of a Multipass Honeycomb Adsorber Regenerated by a Direct," pp. 603–608, 2005.

[22] M. M. Ra, P. Gandhidasan, and H. M. S. Bahaidarah, "Liquid desiccant materials and dehumidi fi ers – A review," vol. 56, pp. 179–195, 2016, doi: 10.1016/j.rser.2015.11.061.

[23] A. H. Abdel-Salam and C. J. Simonson, "State-of-the-art in liquid desiccant air conditioning equipment and systems," *Renew. Sustain. Energy Rev.*, vol. 58, pp. 1152–1183, 2016, doi: 10.1016/j.rser.2015.12.042.

[24] P. Bansal, S. Jain, and C. Moon, "Performance comparison of an adiabatic and an internally cooled structured packed-bed dehumidifier," *Appl. Therm. Eng.*,

vol. 31, no. 1, pp. 14–19, 2011, doi: 10.1016/j.applthermaleng.2010.06.026.

[25] Y. Gu and X. Zhang, "Performance investigation on the liquid desiccant regeneration using rotating packed bed," *Int. J. Refrig.*, vol. 109, pp. 45–54, 2020, doi: 10.1016/j.ijrefrig.2019.09.017.

[26] Y. Yin, J. Qian, and X. Zhang, "Recent advancements in liquid desiccant dehumidification technology," *Renew. Sustain. Energy Rev.*, vol. 31, pp. 38–52, 2014, doi: 10.1016/j.rser.2013.11.021.

[27] D. E. C. Systems and M. A. T. Erials, "C Oll I Er Sept Ember 1981 Submitted To the," 1981.

[28] M. Kanoğlu, M. Ö. Çarpinlioğlu, and M. Yildirim, "Energy and exergy analyses of an experimental open-cycle desiccant cooling system," *Appl. Therm. Eng.*, vol. 24, no. 5–6, pp. 919–932, 2004, doi: 10.1016/j.applthermaleng.2003.10.003.

[29] L. U. Bakmeedeniya, "Modelling Polygeneration with Desiccant Cooling System for Tropical (and Sub-Tropical) Climates," pp. 1–73, 2010.

[30] S. Jain, P. L. Dhar, and S. C. Kaushik, "Evaluation of solid-desiccant-based evaporative cooling cycles for typical hot and humid climates," *Int. J. Refrig.*, vol. 18, no. 5, pp. 287–296, 1995, doi: 10.1016/0140-7007(95)00016-5.

[31] R. Narayanan, E. Halawa, and S. Jain, "Performance characteristics of solid-desiccant evaporative cooling systems," *Energies*, vol. 11, no. 10, 2018, doi: 10.3390/en11102574.

[32] T. Katejanekarn and S. Kumar, "Performance of a solar-regenerated liquid desiccant ventilation pre-conditioning system," vol. 40, pp. 1252–1267, 2008, doi: 10.1016/j.enbuild.2007.11.005.

[33] "NRC Publications Archive Archives des publications du CNRC Desiccant-evaporative cooling system for residential buildings De sic c a nt -eva porat ive c ooling syst e m for re side nt ia l buildings," 2009.

[34] Parlamento italiano, "DPR n.412/93," vol. 412, 1993.

[35] Ministro dello sviluppo economico, "Decreto interministeriale n.192," pp. 1–8, 2015.

[36] V. Sannio, "Prestazioni energetiche degli edifici Parte 2 : Determinazione del fabbisogno di energia primaria e dei rendimenti per la climatizzazione invernale e per la produzione di acqua calda sanitaria UNI / TS 11300-2 Part 2 : Evaluation of primary energy need an," *Calcolo*, pp. 6–7, 2008.

[37] ASHRAE Standard 55, "Thermal Environmental Conditions for Human Occupancy 55-2004," *Am. Soc. Heating, Refrig. Air-Conditioning Eng. Inc.*, vol. 2004, no. ANSI/ASHRAE Standard 55-2004, pp. 1–34, 2004.

[38] A. Wicaksana and T. Rachman, "済無No Title No Title No Title," *Angew. Chemie*

Int. Ed. 6(11), 951–952., vol. 3, no. 1, pp. 10–27, 2018, [Online]. Available: https://medium.com/@arifwicaksanaa/pengertian-use-case-a7e576e1b6bf

[39] E. Politecnico, "Comfort termoigrometrico e condizioni interne di progetto negli impianti di climatizzazione," pp. 1–40.

[40] P. Stabat and D. Marchio, "Heat and mass transfer modeling in rotary desiccant dehumidifiers," *Appl. Energy*, vol. 86, no. 5, pp. 762–771, 2009, doi: 10.1016/j.apenergy.2007.06.018.

[41] T. Kasuda; and P. R. Achenboch, "The classified or limited status of this report applies to each page, unless otherwise marked. Separate page printouts MUST be nrked accordingly.," 1965.

[42] G. Levy, "Mathematical Reference," *Energy Power Risk*, vol. 4, pp. 291–295, 2018, doi: 10.1108/978-1-78743-527-820181015.

[43] A. Handbook, *2020 Heating , Ventilating , and SYSTEMS AND EQUIPMENT*. 2020.

[44] G. Serale, M. Fiorentini, A. Capozzoli, D. Bernardini, and A. Bemporad, "Model Predictive Control (MPC) for enhancing building and HVAC system energy efficiency: Problem formulation, applications and opportunities," *Energies*, vol. 11, no. 3, 2018, doi: 10.3390/en11030631.

[45] G. Panaras, E. Mathioulakis, and V. Belessiotis, "Proposal of a control strategy for desiccant air-conditioning systems," *Energy*, vol. 36, no. 9, pp. 5666–5676, 2011, doi: 10.1016/j.energy.2011.06.059.

List of Figures.

List of Tables.

List of symbols

Variable	Description	SI unit
u	solid displacement	m
u_f	fluid displacement	M
Qi	Volumetric air flow of apartment i	m3/h
Cd	Aperture coefficient of discharge	-
$Cd0i$	Logic signal to open or close the aperture	-
Ad,i	Geometrical opening area of the window i	m2
$\|\Delta P\|$	Pressure difference across the opening	Pa
ρ	Air density	Kg/m3
LT	TRNSYS logic operator (lower than)	-
TOA	Outdoor air temperature	°C
XOA	Outdoor air absolute humidity	g/Kg d.a.
$T12$	Process air temperature after the desiccant wheel	°C
$X12$	Process air absolute humidity after the desiccant wheel	g/Kg d.a.
$Thx12$	Process air temperature exiting the heat recovery	°C
TS	Supply temperature.	°C
XS	Supply absolute humidity	g/Kg d.a.
TR	Return Temperature	°C
XR	Return absolute humidity	g/Kg d.a.
Thu	Return temperature after the humidifier	°C
Xhu	Return absolute humidity after the humidifier	g/Kg d.a.
$Thx22$	Return air temperature exiting the heat recovery	°C
$Treg$	Regeneration temperature	°C
TE	Exhaust air temperature	°C
XE	Exhaust air absolute humidity	g/Kg d.a.
Tw_cool_in	Cooling coil water inlet temperature	°C
$T\ w\_hot\_in$	Heating coil water inlet temperature	°C
mw_cool_in	Cooling coil water inlet mass flow rate	Kg/s
mw_hot_in	Heating coil water inlet mass flow rate	
Tz,t	Soil temperature at depth z and time t	°C
$Tmean$	Mean surface temperature of the ground	°C

$Tamp$	Amplitude of surface temperature of the ground	°C
Z	Depth below the ground surface	M
αs	Thermal diffusivity of the ground	m2/s
$tnow$	Current day of the year	-
$tshift$	Day of the year corresponding to the minimum ground surface temperature	-
ks	Soil thermal conductivity	W/(m2.K)
ρs	Soil density	kg/m3
Cps	Soil specific heat capacity	kJ/(kg.K)
ACH	Air changes per hour	V/h
DCS	Desiccant Cooling System	-
DW	Desiccant Wheel	-
Ta	Ambient temperature	°C
h	Enthalpy	J/kg
$F1,i$	Potential function 1 of condition i	J/kg
$F2,i$	Potential function 2 of condition i	-
ε_1	Effectiveness 1 of the desiccant wheel	-
ε_2	Effectiveness 2 of the desiccant wheel	-
ε	Effectiveness of the heat exchanger	-
$\dot{m}_a$	Air mass flow rate	kg/s
d	Pipe diameter	m
Cpa	Air specific heat	kJ/(kg.K)
Cpw	Water specific heat	kJ/(kg.K)
COP_{cyc}	Coefficient of performance of the cycle	-
COP_{th}	Thermal coefficient of performance	-
COP_{el}	Electrical coefficient of performance	-

Acknowledgments

We would like to dedicate a few words for expressing our sincere gratitude to:

In the first instance, to God, for giving us the opportunity to conclude this stage in our lives with which we dreamed of in the past and today it has become a reality, thanks to a hard work of several years. For giving us strength and willingness to keep trying even when we felt tired and overwhelmed by every challenge that came our way.

We also want to thank our flatmates, who over this time, have become our family. Serri and Majo, thank you for making this experience as bearable as possible; without you both, it would not have been as special as it has been to share with you every moment of joy, triumph, personal growth, but also of sadness, loneliness, and discouragement. We are proud of every step of yours lives and we feel them as our own because we have seen how hard you have worked to achieve them.

To our respective work teams at our companies, for welcoming us and helping us to learn about the professional life, but also for supporting us and giving us the space to continue with this goal that we had pending.

We want to thank each other, because we only know how much we have fought to get this master's degree, with or without motivation they were many days of working a whole day and getting very tired home to continue working academically. Here is reflected the fruit of our effort and it serves to remind us that we are capable to achieve anything we propose in life.

Finalmente queremos dejar marcado en esta tesis, un profundo agradecimiento a nuestras familias, en nuestra lengua materna, ya que probablemente será el único párrafo que entiendan de este documento, pero lo que muy seguramente si entenderán es lo mucho que significa para nosotros lograr este paso. Gracias Howard, Ana, Pedro y Lucía, porque a pesar de la distancia que nos separa, un océano literalmente hablando, siempre han estado muy presentes durante cada momento de esta experiencia, sobre todo en los momentos más difíciles, ustedes se encargaron de llenarnos de esperanza y recordarnos lo mucho que hemos luchado para llegar aquí. Gracias por siempre creer en nosotros a pesar de que en algunas circunstancias nosotros llegáramos a dudarlo, somos los que somos gracias a su amor, esfuerzo y sacrificio.